PLANETARY SCIENCE INSTITUTE

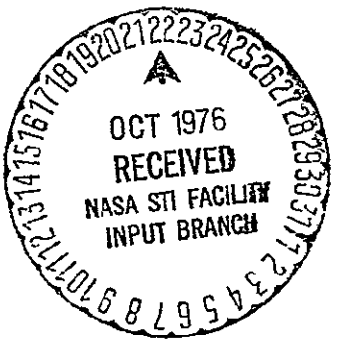

NASW 2718

ASTEROIDAL AND PLANETARY ANALYSIS

Final Report
11 August 1975

Submitted by:

Planetary Science Institute
252 W. Ina Road, Suite D
Tucson, Arizona 85704

William K. Hartmann
Manager

TASK 1: ASTEROID SPECTROPHOTOMETRY AND INTERPRETATION
(Principal Investigator: Clark R. Chapman)

A. INTRODUCTION

The asteroid research program during 1974/5 has three major goals: (1) continued spectrophotometric reconnaissance of the asteroid belt to define compositional types; (2) detailed spectrophotometric observations of particular asteroids, especially to determine variations with rotational phase, if any; and (3) synthesis of these data with other physical studies of asteroids and interpretation of the implications of physical studies of the asteroids for meteoritics and solar system history.

The program has been an especially fruitful one, yielding fundamental new insights to the nature of the asteroids and the implications for the early development of the terrestrial planets. In particular, it is believed that the level of understanding of the asteroids has been reached, and sufficiently fundamental questions raised about their nature, that serious consideration should be given to possible future spacecraft missions directed to study a sample of asteroids at close range. Anders (1971) has argued that serious consideration of asteroid missions should be postponed until ground-based techniques for studying asteroids had been sufficiently exploited so that we could intelligently select appropriate asteroids for spacecraft targeting. It is clear that that point has been reached, and now that relatively inexpensive fly-by missions have been discovered to be possible by utilizing Venus and Earth gravity assists (Bender and Friedlander, 1975), serious planning for such missions ought to begin.

This final report will not repeat the numerous results already presented in the first three Quarterly Reports. Reference is made to those reports and to papers that have been published or are in press that are based on this work. We begin with a brief description of the work conducted in the fourth quarter, and conclude with a summary of the entire year's effort.

B. FOURTH QUARTERLY REPORT

During the fourth quarter, progress was made in several areas including further data reduction and preparation of manuscripts for publication. In addition, preparations were conducted for a major spectrophotometric observing program at the Mauna Kea Observatory that will be underway during the final days of the quarter.

Reduction of February Data

Although the spectrophotometric asteroid measurements made in February were reduced in a preliminary fashion during the previous quarter, final reduction was completed during the present quarter. The qualitative results are unchanged, however. Numerous C-type (carbonaceous) objects were observed, plus a few of very distinctive composition. It is intended that a manuscript will

TASK 1: ASTEROID SPECTROPHOTOMETRY AND INTERPRETATION
(Principal Investigator: Clark R. Chapman)

A. INTRODUCTION

The asteroid research program during 1974/5 has three major goals: (1) continued spectrophotometric reconnaissance of the asteroid belt to define compositional types; (2) detailed spectrophotometric observations of particular asteroids, especially to determine variations with rotational phase, if any; and (3) synthesis of these data with other physical studies of asteroids and interpretation of the implications of physical studies of the asteroids for meteoritics and solar system history.

The program has been an especially fruitful one, yielding fundamental new insights to the nature of the asteroids and the implications for the early development of the terrestrial planets. In particular, it is believed that the level of understanding of the asteroids has been reached, and sufficiently fundamental questions raised about their nature, that serious consideration should be given to possible future spacecraft missions directed to study a sample of asteroids at close range. Anders (1971) has argued that serious consideration of asteroid missions should be postponed until ground-based techniques for studying asteroids had been sufficiently exploited so that we could intelligently select appropriate asteroids for spacecraft targeting. It is clear that that point has been reached, and now that relatively inexpensive fly-by missions have been discovered to be possible by utilizing Venus and Earth gravity assists (Bender and Friedlander, 1975), serious planning for such missions ought to begin.

This final report will not repeat the numerous results already presented in the first three Quarterly Reports. Reference is made to those reports and to papers that have been published or are in press that are based on this work. We begin with a brief description of the work conducted in the fourth quarter, and conclude with a summary of the entire year's effort.

B. FOURTH QUARTERLY REPORT

During the fourth quarter, progress was made in several areas including further data reduction and preparation of manuscripts for publication. In addition, preparations were conducted for a major spectrophotometric observing program at the Mauna Kea Observatory that will be underway during the final days of the quarter.

Reduction of February Data

Although the spectrophotometric asteroid measurements made in February were reduced in a preliminary fashion during the previous quarter, final reduction was completed during the present quarter. The qualitative results are unchanged, however. Numerous C-type (carbonaceous) objects were observed, plus a few of very distinctive composition. It is intended that a manuscript will

be prepared by McCord and Chapman (to be the third part of the series published earlier this year in the Astrophysical Journal (McCord and Chapman, 1975a,b), based on the data obtained last summer, in February 1975, May 1975, and the present observing run in Hawaii.

433 Eros Campaign

Chapman concluded final reduction of Eros spectrophotometry obtained on 13 February at Kitt Peak National Observatory (replacing the preliminary reduction reported in the previous Quarterly Report). Chapman worked jointly with C. Pieters, M. Gaffey, and T. McCord (MIT) in developing an interpretation of these data combined with similar data obtained by Pieters at Cerro Tololo. A paper has been written and submitted to Icarus (see Appendix A). The fundamental conclusion is that Eros seems to be composed of an assemblage of moderately high temperature minerals (including iron, olivine, and pyroxene) such as the H or L-type ordinary chondrites. However, detailed interpretation of the spectrum reveals that the particle size of the iron on Eros' surface must be much finer than that produced by hand-crushing of a meteorite sample in the laboratory. In the absence of appropriate laboratory work it would be premature to assert categorically that Eros is an ordinary chondrite, but it does seem probable. No major compositional variations with rotation were detected on Eros.

March Radiometry

Chapman assisted D. Morrison (U. of Hawaii) on an observing run during mid-March during which 10 micron measurements were obtained of 22 asteroids. During the present quarter, Morrison and Chapman prepared a manuscript (submitted to the Astrophysical Journal, see Appendix B) summarizing the results. The first small main-belt asteroids to be measured radiometrically were sampled during this run. Chapman will present a joint paper on these data at the San Diego meeting of the American Astronomical Society.

March JHKL Spectrophotometry

During the final night of the Morrison/Chapman observing run in March, near infrared photometric measurements were made of eleven asteroids (plus two satellites of Saturn) in the J, H, K, and (for 2 asteroids) L standard filters. Although this portion of the reflection spectrum (1 to 3 microns) contains a number of diagnostic absorption bands, detailed spectra have been measured so far for only 2 asteroids (4 Vesta, Larson and Fink, 1975, and 433 Eros, Larson et al, 1975). While broadband data are less diagnostic of composition, they do have some interpretive value as shown by Johnson et al (1975).

Preliminary reduction has been completed of our own photometry, although the calibration is subject to change. As shown in Fig. 1-1, color ratios indicate a moderate spread in asteroid colors over the K/J vs K/H plane, implying compositional differences that do not show a straightforward correlation with the C and S compositional types described by Chapman et al (1975). Both

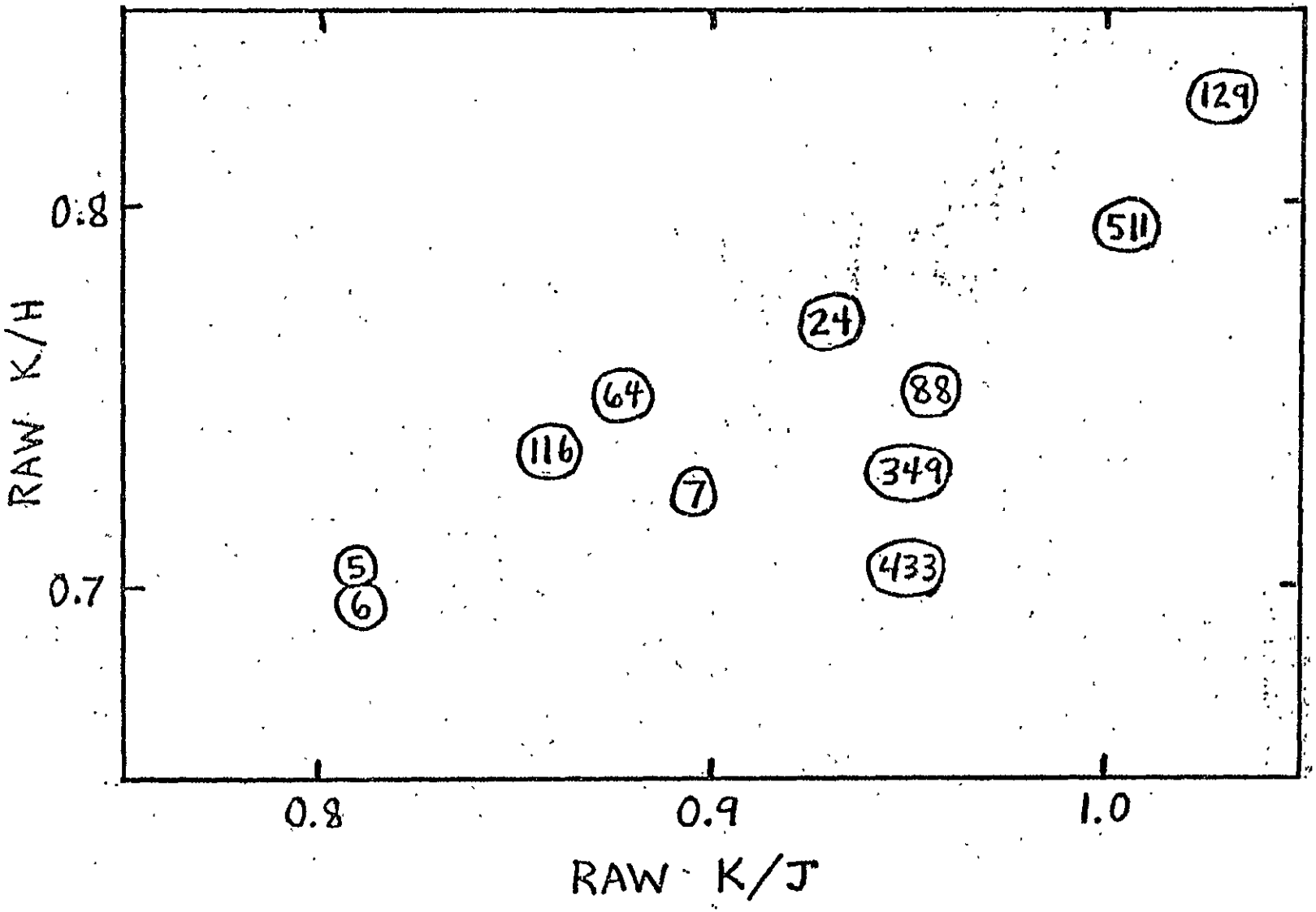

Fig. 1-1

129 Antigone and 6 Hebe, at opposite ends of this plot, seem otherwise to be typical S objects.

Detailed intrepretation at this time is premature, but study of the spectral behavior of asteroids in this mid-infrared region is important because of the bearing it has on the metallicity of the S-type asteroids. Chapman and Morrison will be preparing a paper on this topic.

May Spectrophotometry

The spectrophotometry reported in the previous Quarterly Report has now been reduced for most asteroids observed. Some representative spectral reflectance curves are illustrated in Fig. 1-2.

The most significant discovery is that a second large asteroid in the main belt (471 Papagena) seems to have the composition of a metamorphosed ordinary chondrite. It possesses a wide, deep absorption feature near 0.9 microns. The fact that both asteroids so identified (the other is 349 Dembowska, McCord and Chapman, 1975b) are located near 2.9 A.U., in the midst of the region already recognized by Chapman et al (1975) as having an unusual distribution of compositions, raises questions about how ordinary chondrites are "produced" preferentially in this zone that otherwise seems dominated by the effects of two nearby Kirkwood gap commensurabilities. Perhaps the proximity of these asteroids to the gaps has some bearing on the fact that chondrites are so plentiful in terrestrial meteorite collections, since another Kirkwood gap (at the 2:1 commensurability) has been proposed by Zimmerman and Wetherill (1973) as a source for many meteorites but is located where nearly all asteroids are of carbonaceous composition.

I will now briefly summarize the spectral characteristics of some of the asteroids measured in May.

110 Lydia shows a moderately reddish spectrum, with little curvature, and a possible 0.9 micron band. It is a somewhat anomalous S-type object, in the Chapman et al (1975) terminology.

558 Carmen is a small member of the Hirayama family that also includes ordinary chondrite-like 349 Dembowska. Morrison and Chapman found an intermediate geometric albedo for Carmen (0.08). Its spectrum also seems somewhat intermediate, but more like that of a carbonaceous object than a silicaceous object. It is relatively bright in the near infrared.

153 Hilda, a major member of the Hilda-grouping at the 2:3 commensurability beyond the main belt (4.0 A.U.), seems to be a carbonaceous body. It is also relatively bright in the infrared.

57 Mnemosyne shows a typical S-type curving, reddish spectrum. There is probably a 0.9 micron absorption feature.

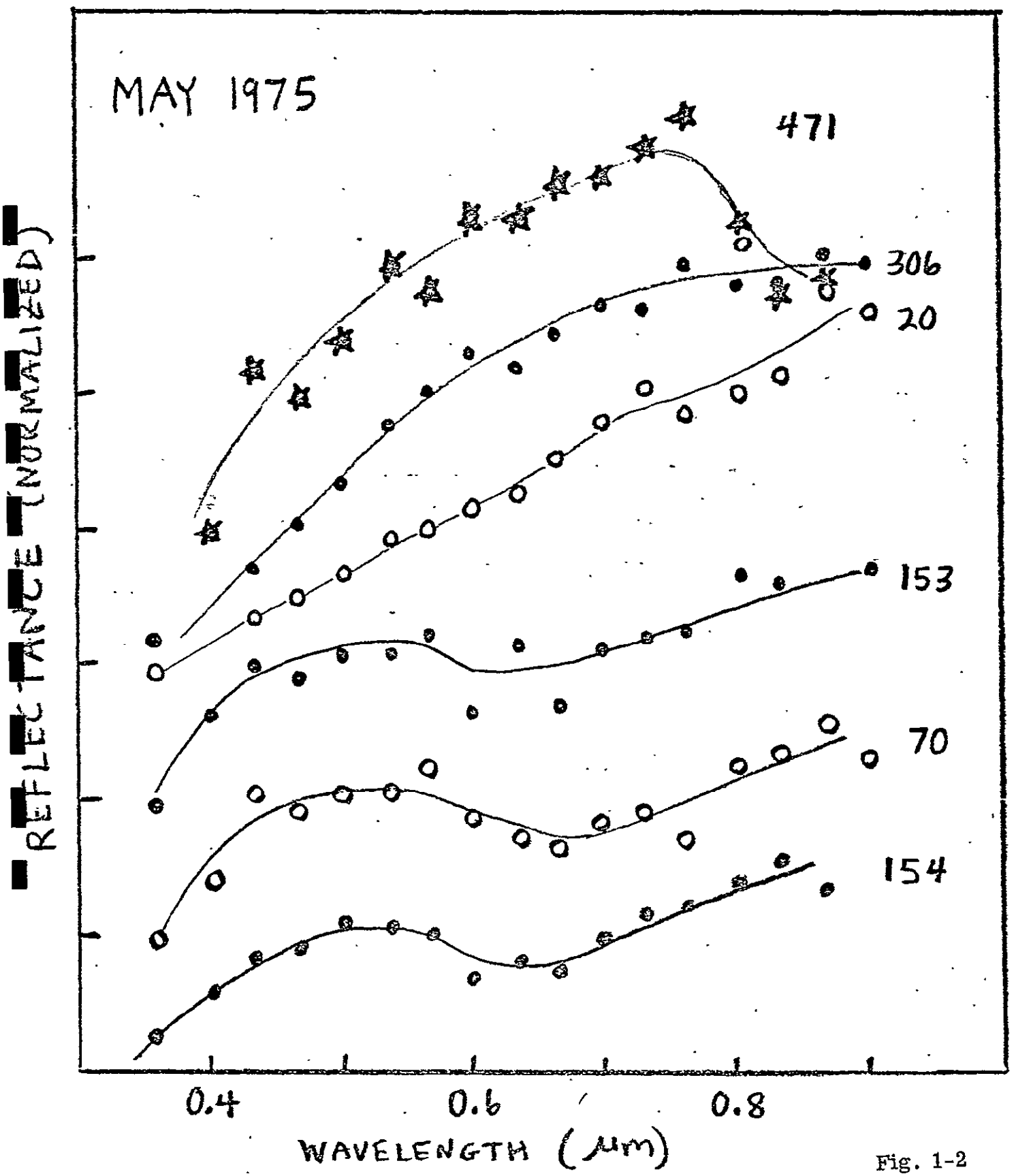
MAY 1975
471
306
20
153
70
154
REFLECTANCE (NORMALIZED)
0.4
0.6
0.8
WAVELENGTH (μm)

Fig. 1-2

154 Bertha shows a typical C-type spectrum, similar to C2 type carbonaceous meteorites.

31 Euphrosyne is also a C-type asteroid as is 70 Panopaea.

20 Massalia shows an unusual reddish spectrum distinctly unlike S-type asteroids. The spectrum lacks any curvature, and in that sense is similar to 16 Psyche and other "M" type asteroids. The reddening is quite extreme, although not so red as the unique object 170 Maria. Although Chapman et al (1975) had classified Massalia as an S-type object, its albedo is brighter than any other asteroid so classified. Further study of this large, unusual asteroid would be important.

344 Desiderata has a nearly flat, C-type spectrum.

306 Unitas shows a typical, curving, S-type spectrum.

August Hawaii Observing Run

Six nights have been assigned to Chapman and McCord on the 88-inch telescope at Mauna Kea, August 9-14. In order to maximize the chances of success during this opportunity for studying faint asteroids, the equipment was tested in complete detail during practise observing sessions at the MIT Observatory during the first week of July.

Through the cooperation of Paul Herget (Cincinnati Observatory) who provided accurate ephemerides for several dozen asteroids, we have prepared finding charts for a variety of important faint asteroids available in August.

C. FINAL REPORT - SUMMARY OF 1974/5 WORK

The asteroid research consisted of several major activities: spectrophotometric observations conducted at the Kitt Peak National Observatory, reduction and publication of the spectral data, and interpretation of these and related data for their implications for the nature and evolution of the asteroids. In addition, several other activities related to asteroid research were carried out to support the main program. The major results have been presented at meetings and colloquia, especially in two papers before the Division for Planetary Sciences of the American Astronomical Society. Nine papers emanating from this program have been published or prepared during this year. In addition, Chapman on his own time has incorporated the results of some of the current investigations in some popular articles so that the general public may become aware of the advances made in asteroid research (an article appeared in the January 1975 issue of Scientific American, and a review has been prepared for the McGraw-Hill Encyclopedia of Science and Technology, to be published next year).

Asteroid Observing Programs

During the past year major spectrophotometric observing runs were carried out in February and May on the 1.3m telescope of Kitt Peak National Observatory. Spectral data (0.3 to 1.1 microns) were obtained for 27 asteroids. An additional observing run is currently underway at the Mauna Kea Observatory. Also, mid-infrared JHKL spectrophotometry was carried out on about a dozen asteroids in March, in cooperation with D. Morrison, at KPNO.

Chapman also assisted several other asteroid observing programs, including observations of 433 Eros by Wisniewski (University of Arizona) and radiometry of 22 asteroids by Morrison (University of Hawaii).

Data Reduction

Preliminary reductions have been done for data obtained in August 1974 and for the March 1975 JHKL photometry. Complete reductions are now finished for asteroids observed in February and May 1975. Data previously reduced were published during the present year by McCord and Chapman.

Interpretation

Major progress was made in interpreting asteroid compositions and the origin and nature of these bodies. The surface composition of 433 Eros has been determined on the basis of observations obtained during its close passage to Earth early in 1975. The compositional variability of asteroids with semi-major axis is now understood in terms of condensation processes in the solar nebula, combined with selective subsequent melting, followed by differential effects of asteroidal collisions. Indeed, examination of the collisional behavior of asteroids having bulk compositions similar to surface compositions inferred from spectrophotometry shows that the present asteroid belt is probably only a small remnant of an initially much more massive population of bodies.

A major review of modern spectrophotometric, polarimetric, and radiometric astronomical observations was completed early in the present contract period by Chapman in collaboration with Morrison (University of Hawaii) and Zellner (University of Arizona). The overwhelming predominance of carbonaceous asteroids in the belt was convincingly demonstrated in that paper, which has recently appeared in Icarus (May 1975 issue). Furthermore, unusual distributional properties of the remaining S-type asteroids (of probable stony-iron composition) and unusual types have important implications for the thermal evolution of the asteroids and the relationships between asteroids and meteorites. The latter topic (the asteroids as meteorite parent-bodies) has been reviewed by Chapman in a major paper submitted a month ago to Geochimica et Cosmochimica Acta (see Appendix C).

Miscellaneous

An effort was made by Chapman to inform the public in New England of the unusual occultation of Kappa Geminorum by asteroid 433 Eros that occurred in January. Through publicity by a press release, it was hoped that an accurate diameter could be obtained by observations of the disappearance of this 3rd magnitude star by the general public. Unfortunately, the event occurred across a path near cities whose newspapers failed to carry the press release in a prominent fashion.

Papers Published and/or Written During 1974/5 Contract Period

McCord, T.B. and Chapman, C.R. (1975a) Asteroids: spectral reflectance and color characteristics. Astrophys. J. 195, 553.

McCord, T.B. and Chapman, C.R. (1975b) Asteroids: spectral reflectance and color characteristics II. Astrophys. J. 197, 781.

Chapman, C.R., Morrision, D. and Zellner, B. (1975) Surface properties of asteroids: a synthesis of polarimetry, radiometry, and spectrophotometry. Icarus 25, 104.

Chapman, C.R. (1974) Asteroid size distribution: implications for the origin of stony-iron and iron meteorites. Geophys. Res. Lett. 1, 341.

Chapman, C.R. and Davis, D.R. (1975) Asteroid collisional evolution: evidence for a much larger early population. Science, in press.

Chapman, C.R. (1975) Asteroids as meteorite parent-bodies: the astronomical perspective. Submitted to Geochim. Cosmochim. Acta. (Appendix)

Hartmann, W.K., Chapman, C.R. and Williams, J. (1976) Asteroids -- a review. To be submitted to Rev. Geoph.

Pieters, C., Gaffey, M.J., Chapman, C.R. and McCord, T.B. (1975) Spectrophotometry (0.33 to 1.07 μm) of 433 Eros and compositional implications. Submitted to Icarus. (Appendix)

Morrison, D. and Chapman, C.R. (1975) Radiometric diameters for an additional 22 asteroids. Submitted to Astrophys. J. (Appendix)

Conclusion

The new view of the asteroids that has emerged this year has important implications not only for the development of these small bodies but for the larger questions involving the origin and early history of the solar system itself. As illustrated in Fig. 1-3, the asteroids are the last remaining remnants of the planetesimals that went into forming the planets -- except no planet formed in the asteroid zone. In this one zone in the solar system, the planetesimals proceeded only part way through the accretionary phase until interrupted by augmented velocities giving rise to net fragmentation. The subsequent history

ROLE OF ASTEROIDS IN SOLAR SYSTEM STUDIES

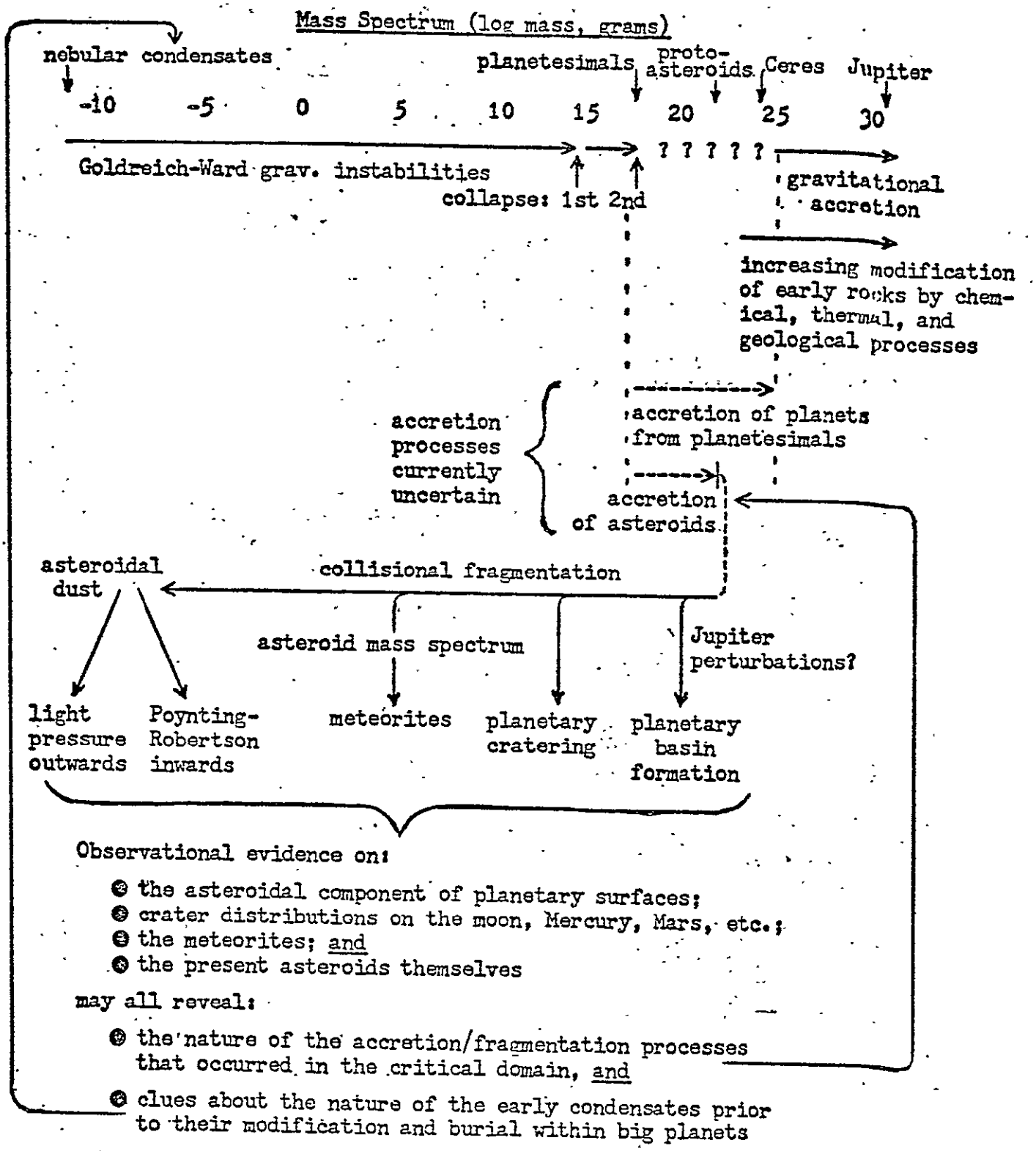

Fig. 1-3

of the asteroids has been determined by fragmentational and erosional processes which have persisted over the age of the solar system. Because of the prolonged timescale for fragmentation (determined by the fragmentation process itself) the asteroids have spread their debris around the solar system (either by dynamical scattering processes leading to cratering, or by radiation processes acting on asteroidal dust). Thus asteroids may have contributed a disproportionate share to the outer surfaces of planets during the final stages of accretion, continuing to the present day. Thus the craters we see on the surfaces of most planets, and perhaps a major fraction of surface materials, are due to the asteroids. Since the asteroids are too small to have been substantially altered by thermally induced geological processes active on most (or all) planets and the moon, their material, part of which we have already sampled in meteorite collections, may represent relatively unaltered samples from these important early phases of solar system history. The study of the asteroids may ultimately shed much light on questions of the accretion process, the processes that heated the planets in the first 10^8 years of the solar system, and the formation of the outer surfaces of the terrestrial planets.

REFERENCES

Anders, E. (1971) In NASA SP-267, p.479.

Bender, D. and Friedlander, A. (1975) Am. Astronaut Soc. Paper 75-086.

Chapman, C. R., Morrison, D. and Zellner, B. (1975) Icarus 25, p. 104.

Johnson, T.V., Matson, D.L., Veeder, G.J. and Loer, S. J. (1975) Astrophys. J. 197, p. 527.

Larson, H. P. and Fink, U. (1975) Submitted to Icarus.

Larson, H.P., Fink, U., Treffers, R.T., and Gautier, T.N. (1975) Submitted to Icarus.

McCord, T. B. and Chapman, C.R. (1975a) Astrophys. J. 195, p. 553.

McCord, T.B. and Chapman, C.R. (1975b) Astrophys. J. 197, p. 781.

Zimmerman, P.D. and Wetherill, G. W. (1973) Science 182, p. 51.

TASK 2: THE URANUS ATMOSPHERE: INVESTIGATION OF ITS PHYSICAL STRUCTURE UTILIZING RADIAL INTENSITY PROFILES OF THE PLANETARY DISK
(Principal Investigator: Michael J. Price)

The major objectives of the Uranus project have been (1) to determine the vertical location of the cloud deck in the Uranus atmosphere and (2) to determine the degree of clarity of the gas above the cloud deck. Specific questions include the fraction of cloud cover and the question of evidence for aerosol particles scattering and extinction. In the first quarter models for theoretical work were selected and considerable effort was expended to anticipate observational and interpretational problems expected to arise during later quarters.

During the second quarter theoretical programs concerning the geometrical albedo and limb profile for the Uranus atmosphere were programmed on the PSI Hewlett-Packard 9820A computer and debugging was completed. The third quarter was a dormant period, waiting until Uranus was accessible for observational work.

During the final quarter successful observations were achieved on the six nights in May and June at Lowell Observatory by Otto Franz. Slit and pinhole observations were made. Preliminary results indicate the basic validity of Belton/Price Uranus atmospheric model. In every observational case, limb-brightening was observed as predicted. Because the data have just been obtained analysis will continue in the future.

TASK 3: FURTHER DEVELOPMENT OF SATURN RING MODELS
(Principal Investigator: Michael J. Price)

This task dealt with thermal and photographic properties of the rings of Saturn. During the first quarter intrepretation of the thermal radiation characteristics was begun and contacts were made at Lowell Observatory preparatory to observation of the rings with Dr. Otto Franz.

During the second quarter the theoretical modelling was greatly extended. A "Model I" viewed the ring particles as being in isolated thermal equilibrium with incoming solar flux. A "Model II" viewed the thermometric temperature as resulting from thermal equilibrium of the entire ring. Results of the two models were compared and found to be mutually reinforcing. Meanwhile, early observational runs were thwarted by poor observing weather during the second quarter.

During the third quarter a paper on the theoretical models was drafted. Scans across the rings were obtained in the UBV photometric system by Dr. Otto Franz at Lowell Observatory at the 72-inch aperture Perkins reflector. The investigator has analysed these observations and found systematic

differences in brightness occurring between the individual quadrants of the ring. The observed southern face is symmetrically brightess in the northeast and southwest quadrants and faintest in the other two quadrants. Brightness differences amount to a few percent. Analyses of these data are still in progress. The front-back asymmetry appears to result from indirect illumination of the ring by the ball of Saturn.

During the fourth quarter a report on the theoretical modelling of Saturn's rings has been completed and internally reviewed at PSI and submitted to Icarus. This report is appended as part of this final report on the contract (Appendix D).

TASK 4: UTILIZATION OF GROUND-BASED MARS OBSERVATIONS: LONG-TERM COMPARISON WITH MARINER 9 RESULTS
(Principal Investigator: William K. Hartmann)

The principal goal of this project has been to review old photographic observations of transient phenomena on Mars, in particular blue and red clouds, and correlate them if possible with phenomena observed in the Mariner 9 photographic survey of the planet. This goal has been achieved and positive correlations found. The principal product of this study was planned to be a research paper describing the results; such a paper is nearly ready for publication and completed sections are appended to this final report (Appendix E).

Two working visits to the Lowell Observatory Planetary Data Center, each about one week long, were made to review photographic materials and their analyses at Lowell. Lowell Observatory staff members Leonard Martin, Charles Capin, and William Baum had already prepared both published and unpublished surveys of cloud phenomena on Mars, but only with the classical albedo features used as a background or base map. In the current study, Lowell staff members kindly provided much of the original material used in their work. This included measurements on photographs dating to the first few years of this century.

Perhaps the most interesting statistical result was that about half of all the blue clouds observed during this long period fell precisely on the summits or flanks of seven major volcanic mountains on Mars; another quarter of the clouds are located on steeply sloping ground or contacts between cratered uplands and smooth plains. These data support the pre-Mariner and post-Mariner indications that the blue clouds are orographic condensation clouds.

Red clouds, generally thought to be dust storms, have a more complex distribution and behavior. One of the simpler behavioral trends relates the dust activity to large basins. Of three major "core areas" or "spawning grounds" for dust storms, one is the Hellas Basin and another the Isidus Basin. Also, dust storms seem to show some correlation with the Argyre Basin, the chaotic and canyon complex, and other depressed areas that appear to be reservoirs of dust, based on Mariner 9 photographs. In other words, there is some suggestion that the largest ancient impact basins and other depressed regions have become sinks or traps for large deposits of mobile dust. However, a third major "core area" for dust storms, the nearly featureless plains near Solis Lacus, being at high altitude, do not fit this simple description. Further understanding of dust storm sources probably will require meteorological wind modelling of the type recently attempted by Sagan and Gierasch. Further discussion is given in the appended drafts of the research report which will be a product of this study.

In addition to direct analysis of clouds and related variations observed during the 66-year period represented in the Lowell plate collection, analysis of topography was included in the study, in order to establish histograms of altitude distributions of the true surface of Mars, that could be compared with the altitude distributions of blue clouds, red clouds, and other variable features. This was made possible with a June 1975 synthesis map of topography, prepared by the U.S.G.S., which could be compared with earlier topographic maps of other observers. It was found that a bi-modal elevation distribution is present on Mars, consistent with other Mariner 9 maps, and my own early analysis (Icarus 19, 550, 1973). Low plains define a lobe lying at about -0.4 km; the upper unit, mostly of cratered plains and volcanics, peaks near +3.4 km. The median elevation for the entire surface is +2.4 km.

The median elevation for blue clouds was found to be +4.5 km, significantly above the global median. This supports the conclusion that blue clouds are a high-level phenomenon, presumably condensation clouds. A median elevation of red clouds was found to be +1.9 km, significantly below the global median. They appear to be associated with the lower featureless plains, supporting the view that dust has collected in those areas.

Preliminary results of this study were presented at the February 1975 meeting of the Division of Planetary Sciences, American Astronomical Society, in Columbia, Maryland.

APPENDIX A

SPECTROPHOTOMETRY (0.33 to 1.07 μm) OF 433 EROS AND COMPOSITIONAL IMPLICATIONS

Carle Pieters[1,3]

Michael J. Gaffey[1]

Clark R. Chapman[2,3]

Thomas B. McCord[1,3]

[1]Remote Sensing Laboratory
Department of Earth and Planetary Sciences
Massachusetts Institute of Technology
Cambridge, Massachusetts 02139

[2]Planetary Science Institute
252 W. Ina Rd.
Tucson, Arizona 85704

[3]Visiting Astronomers at the Cerro-Tololo Inter-American Observatory and Kitt Peak National Observatory, which are operated by the Association of Universities for Research in Astronomy, Inc., under contract with the National Science Foundation.

MITRSL Publication #142

Planetary Science Inst. Contribution No. 52

Submitted to ICARUS, 31 July 1975

No. Copies: 4
No. Pages: 30
No. Figs: 4 (Fig. 4 in 3 parts)
No. Tables: 1

ABSTRACT

The spectral reflectance (0.33-1.07 μm) for the asteroid 433 Eros was determined as a function of rotational phase during January 28-30, and February 15, 1975. Interpreation of spectral features suggests Eros is composed of an undifferentiated assemblage of moderate to high temperature minerals (iron, pyroxene, and olivine, but no carbon). H-type ordinary chondrites are such assemblages but it would be premature to conclude that Eros is an H chondrite until we understand possible physical differences between laboratory powders and asteroid regoliths for metal-rich assemblages. There are no major compositional variations on the different sides of Eros.

Running Title: Spectrophotometry of Eros

Address Correspondence to: C. R. Chapman
Planetary Science Institute
252 W. Ina Road
Tucson, Arizona 85704

I. INTRODUCTION

Since Eros is the largest asteroid in an Earth-approaching orbit, it is a prime potential source for meteorites. Therefore, determination of its composition and comparison with common meteorite types provides an important application of remote-sensing techniques. The reflection spectrum from 0.3 to about 3 μm is especially diagnostic of mineralogy. We have made spectrophotometric measurements from 0.33 to 1.07 μm on several nights in late January and early February 1975 during the close approach of Eros to Earth. These supplement noisier spectra of McCord and Chapman (1975a), obtained during a much less favorable opposition in 1972, and complement spectra obtained from about 1 μm to 2.2 μm by Larson et al (1975).

We first present the new spectral data and discuss the data reduction. We then interpret the probable surface mineralogy of Eros, first from our data alone and secondly from all relevant data that are available. Finally we consider the compositional implications of our analysis of Eros for other asteroids and for meteorites.

II. OBSERVATIONS AND DATA

Spectrophotometric measurements were made of Eros on three consecutive nights, January 28, 29, and 30, 1975 UT, using a two-beam chopping filter photometer on the 0.9m telescope of the Cerro Tololo Inter-American Observatory in Chile. Similar independent

measurements were made on February 13, 1975, using the 1.3m telescope of Kitt Peak National Observatory. Twenty-five narrow-band interference filters were used covering the range from 0.33 to 1.07 μm, each with a bandpass of ~300Å. An S-1 photomultiplier was used as a detector in the pulse-counting mode. A Ga-As photomultiplier was also used for a single run during the February observations. A "run" consists of a complete sequence of measurements with the 25 filters taking about two minutes.

In January, 12 Eros runs were obtained on the first night, 30 on the second, and 41 on the third. Although skies were hazy at sunset on the first and second nights, extinction coefficient measurements of γ Geminorum (one hour RA from Eros) indicate the sky was stable to better than 1%. On the third night, scattered cirrus was present during measurements of γ Gem causing small errors (~ 1½%) in the extinction measurements for two filters (0.93, 0.96 μm). An extinction-corrected lightcurve for Eros was obtained for the January observations using the 0.57 μm filter, using γ Gem as the standard (Figure 1). The measurements for each night are plotted so as to maintain the proper rotational phase relationship, assuming a rotation period of 5h 16m. The data were divided into seven groups according to position on the lightcurve in order to study different sides of the rotating asteroid. In Figure 1, group 1 data are superimposed nine periods later in reduced size on group 6 data.

A different but similar set of 25 filters was used during the February observations. One Ga-As run and 12 S-1 runs were spaced over a 5h period on a single night of somewhat marginal photometric quality. The data system permitted us to obtain similar counting statistics in each filter, so the UV and IR observations are no noisier than visible data. Extinction was measured in each filter using our two photometric standards, η Hydrae and θ Crateris.

Inasmuch as there are some inconsistencies between our spectra and data in an overlapping spectral range of Larson et al (1975; see below), we now explain our calibration procedure in some detail.

Reflectance spectra for Eros were derived using the spectral flux ratios for γ Gem/Sun (January, see Figure 2) and η Hya/Sun (February, see Figure 3) listed in Table 1. The calibration of γ Gem was derived in two parts:

$$\gamma \text{ Gem/Sun} = (\alpha \text{ Lyrae/Sun}) \cdot (\gamma \text{ Gem}/\alpha \text{ Lyrae}) \quad (1)$$

First, α Lyr/Sun flux ratios were determined for the filters used in the manner of Elias (1972) which incorporates solar and stellar photometry, theoretical models for stellar spectra, and measured characteristics of the filters and photometer systems. The errors in resulting flux ratios are due primarily to our imperfect knowledge of the α Lyr and solar fluxes. Absolute errors are expected to be less than 5% although errors as large as 8% could occur from 0.3 to 0.4 μm (Balmer feature) and 6% at 0.87 μm (Paschen feature). As a check

we have also derived α Lyr/Sun ratios using returned lunar soils (eg. from the Apollo 16 site) as a calibration:

$$\frac{\alpha \text{ Lyr}}{\text{Sun}} = \left(\frac{\alpha \text{ Lyr}}{\text{Apollo 16}}\right)_{\text{telescope}} \cdot \left(\frac{\text{Apollo 16}}{\text{MgO}}\right)_{\text{laboratory}} \cdot \left(\frac{\text{MgO}}{\text{Sun}}\right) \quad (2)$$

(Since MgO is a white standard, the MgO/Sun ratio is very close to unity.) This work is still in progress (Nygard, 1975) but preliminary results indicate that the absolute errors of the adopted α Lyr/Sun flux ratios are not greater than 5% and that the relative accuracy of adjacent filters is likely to be better than 1%. These preliminary lunar calibrations also indicate that the weak feature seen at 0.6 μm in many asteroid spectra is at least in part due to systematic calibration errors.

The second ratio in eq. (1), γ Gem/α Lyr, was measured at the telescope for each filter (with about 2% precision) in August 1974 as part of a larger calibration project (Pieters et al., in preparation). These flux ratios were compared with those of Hayes (1970) in regions of overlap. For regions where the differences between the two ratios were greater than 2% a best estimate of the flux ratio was made according to trends in flux ratios for similar stars (Pieters, in preparation). The γ Gem/α Lyr flux ratio trend beyond 1.0 μm is unclear; we have adopted values near the upper limit of the estimated error. The values may in reality trend smoothly from 1.0 μm to numbers smaller by 4% at 1.1 μm which would only exacerbate our discrepancy with Larson et al (1975).

The reflectance spectra for the groups of data shown in Figures 2 and 3 have been scaled to unity at 0.57 μm. The average reflectance spectrum from the seven groups of January data is shown in Figure 4. The standard errors of the means are generally smaller than the plotted data points and are not shown. The error bars plotted in Figure 4 are estimated errors in stellar calibration. The scale in Figure 4a is wavelength and in Figure 4b is energy. To examine the absorption features in greater detail a continuum (linear in energy) was estimated from the slope between 0.4 and 0.7 μm and removed in Figure 4c.

The standard stars used during the February observations have not yet been recalibrated. Therefore the spectral reflectance average shown in Figure 3 has been derived using Elias' (1972) interpolations for our filter set in the calibrations of η Hya by Hayes (1970). The errors (not shown)determined from the internal consistency between runs are somewhat larger than the plotted symbols; calibration errors are similar to those shown in Figure 4a.

McCord and Chapman (1975a,b) have defined and tabulated spectral parameters for other asteroids. The spectrum in Figure 4 yields the following values for 433 Eros: R/B = 1.69; Bend = 0.15, IR = -0.07, and IR Band Depth = 0.90.

III. ROTATIONAL VARIATIONS

All spectra in Figures 2 and 3 are remarkably similar indicating no major spectral variation with rotational phase. The same is true of the separate runs (not shown) that are averaged in Figure 3. This implies the surface composition of Eros is basically homogeneous.

There are small, consistent, and possibly significant spectral variations, although they are of similar magnitude to the error bars in Figure 2. For instance, Group 1 and Group 6 are roughly in the same position on the lightcurve (Figure 1); of the seven groups these two have the widest infrared absorption feature. This difference, if confirmed, would indicate a higher olivine/pyroxene ratio (see Section IV) implying some minor difference in concentration of minerals on different sides of the asteroid. Our error bars do not exclude other minor spectral variations of a couple percent or less.

IV. INTERPRETATION OF SPECTRUM

Several diagnostic spectral features are identified in the mean Eros spectrum (Figure 4). A broad, shallow absorption feature occurs between 0.9 and 1.0 μm. The UV portion of the data falls below the linear continuum fitted through the visible portion of the spectrum. The overall spectrum has a reddish slope, and the spectral region between 0.75 and 1.1 μm is significantly brighter than that expected for a primarily silicate assemblage. Although still more definitive

interpretations are possible for asteroid spectra having deeper absorption bands, these spectral features imply a specific series of mineralogical characteristics for the surface material of Eros.

A. Absorption Feature

The absorption feature near 0.9 μm arises from a crystal field electronic transition in an Fe^{2+} cation residing in the M2 coordination site in a pyroxene structure (White and Keester, 1967; Burns,1970a; Adams, 1974). The breadth of the feature, relative to that of an isolated pyroxene, implies the presence of a second absorbing mineral phase, olivine, which has a broad, weak (relative to pyroxene) feature centered near 1.0 μm arising from the presence of Fe^{2+} cations in the M1 and M2 coordination sites of this mineral (Burns, 1970a, b; Runciman et al., 1973). Such a broad asymmetric absorption band is characteristic of spectra of mineral assemblages, such as ordinary chondrites, that contain roughly equal abundances of pyroxene and olivine (Gaffey, 1974, 1975a,b).

This absorption feature is shallow (Band Depth = 0.9) compared with features exhibited by clean, homogeneous mixtures containing pyroxene and olivine (e.g., ordinary chondrites: Band Depth = 0.7-0.8). To decrease the effective absorption of a mineral phase, it is necessary to decrease the mean path length of light through the absorbing material. Several mechanisms can accomplish this in a mixture of mineral phases:

(1) The mean path length of the light can be shortened by the inclusion of a diffuse metal (Ni-Fe) component that absorbs or reflects photons before they traverse through many silicate grains. Such metal is a relatively good reflector in the IR and thus tends to lower the spectral contrast of absorption features while increasing the IR reflectance, thereby maintaining overall spectral contrast (reddening) (Gaffey, 1975b; Gaffey and McCord, 1975).

(2) The mixture may contain other opaque or strongly absorbing phases, so that photons are likely to be totally absorbed after traversing a short distance (Johnson and Fanale, 1973). Meteoritic mineral assemblages such as the carbonaceous chondrites, which contain variable amounts of opaque material, tend to have weak features, low overall spectral contrast, and low albedos. The relative reddness of the spectrum of 433 Eros would argue against this mechanism for explaining the shallowness of the absorption band.

(3) If the mean particle size of the phase giving rise to the color and absorption features is very large ($\sim$1000 μm) or very small ($\sim$20 μm), spectral contrasts are reduced (Pieters, 1972). In the former case, many optical depths are reached before photons of any wavelength intersect a surface so as to be reflected back to the observer, so they are nearly totally absorbed. In the latter case, photons

of all wavelengths suffer numerous surface reflections before they can traverse significantly through the absorbing phase, so the observed light is nearly totally the specularly reflected component. The strong spectral features in asteroids such as 4 Vesta and 349 Dembowska suggest that their surfaces have particle size distributions on the same order as meteoritic grain sizes; lunar soils set a lower bound of ~ 70 μm. If we were to account for the weak feature in the spectrum of Eros using a particle size mechanism, we would have to explain why the particle size distribution in the surface material of this object is so atypical. There is an additional test of this mechanism: a distribution of large particles has a low albedo and small particles have a high albedo (Adams and Filice, 1967). But the albedo of Eros is neither unusually low nor high (see next section).

(4) The proportion of pyroxene and olivine in the total assemblage could be low; that is, the mixture could consist mostly of a material lacking transition metal cations (Fe^{2+}, Ti^{3+}, etc.), such as meteoritic enstatite (Fs_0) or pure quartz (SiO_2). Such material would behave as a neutral carrier, with no absorption features in the spectral region 0.35 to 1.1 μm. Other neutral carriers are materials,

such as plagioclase feldspar (Bell and Mao, 1973), that contain only large coordination sites; the crystal field splitting for Fe^{2+} is low so the absorptions occur in the infrared beyond 1.1 μm. Of common meteoritic or lunar materials, the only neutral carriers are Fs_0 enstatite and feldspar. The coexistence of reduced and non-reduced fractions of such mafic minerals is cosmically unlikely, however, except for assemblages composed of a physical mixture of materials of different origins. Though a system could be reduced sufficiently ($Fs_{0.1-1.0\%}$) to decrease the absorption contrast, the observed olivine absorption would require that the Mg/Si ratio in the parent region of the solar nebula be ~ 1.5-2.0, rather than the more typical value of ~1.0. Also both enstatite and feldspar have relatively high albedos (~0.30), inconsistent with that of Eros. Furthermore the presence of a large modal abundance of feldspar, resulting from differentiation of the Eros parent-body, would require a strong absorption near 1.3 μm, which is apparently lacking in the spectra of Larson et al. (1975).

Briefly, the broad absorption feature in the spectrum of 433 Eros indicates the presence of a silicate assemblage containing pyroxene and olivine. The weakness of the absorption feature indicates

the additional presence of a spectral blocking phase, most probably Ni-Fe metal.

B. UV Drop-off

The negative departure (drop-off) of the UV spectrum from a linear continuum in the visible (Figure 4c) is characteristic of mineral assemblages containing transition metal silicates which cause increasingly efficient charge transfer absorption toward shorter wavelengths (Gaffey, 1975a,b). Such drop-offs are observed in spectra of mineral mixtures consisting primarily of clean, well-equilibrated silicates (e.g. high metamorphic grade ordinary chondrites, eucrites, howardites, and diogenites). The spectrum of 4 Vesta, for example, exhibits just such a UV drop-off (Gaffey and McCord, 1975). But no drop-off is observed for materials consisting primarily of metallic iron or nickel-iron. Intermediate drop-offs, such as seen in the spectrum of Eros, are observed in three types of meteoritic material: (1) clean mixtures of metal and silicates, (2) low grade ordinary chondritic assemblages, and (3) shock-blackened chondritic materials. The latter two cases have a weak drop-off due to spectral blocking phases which also cause a relatively low albedo.

In a metal-silicate mix, there is a coupling between the magnitude of the UV drop-off and the strength of the infrared absorption bands. Both the bands and the drop-off become shallower with increasing metal content. For large particle-sizes of both silicate and metal fractions, the reflectance spectrum is a simple

geometrical average, weighted by relative surface area, of the silicate spectrum, which contains the spectral features, and the metal spectrum, which does not. The spectra of stony-iron meteorites can be modeled using just this principle (Gaffey, 1975b), in which the material is effectively a checkerboard such that a photon is likely to interact with one phase, or the other, but not both.

If finely divided metallic particles are intermixed with silicate particles, a relatively small volume fraction of them can effectively shorten the path length of photons interacting with the silicates, and weaken the spectral features (see Part A above). But for typical regolith particle sizes ($\sim$100 μm), this effect is much more pronounced for the crystal field band than for the ultraviolet charge-transfer band, due to the much stronger absorption coefficient in the latter and the corresponding shorter absorption pathlengths. Unless the particle sizes were even finer than found in regoliths, photons having wavelengths in the wings of the charge-transfer band interact with the assemblage like a checkerboard while those of longer wavelengths are blocked from interacting with the crystal-field band by the intermixed metallic grains.

The spectrum of 3 Juno has an infrared absorption band similar in depth to that of Eros, but lacks a significant UV drop-off. It can be modeled (cf. McCord and Gaffey, 1974) as a checkerboard (i.e. particle sizes $\geq$ 500 μm) of roughly equal parts metal and silicate. The similar absorption band depths but stronger UV

drop-off for Eros suggests Eros has a metal-silicate mixture involving a smaller proportion of metal but of correspondingly finer size. If the particle size is~ 100 μm, then the percentage of metal is about 10-30%.

C. Infrared Brightness

The strongly reddened spectrum of 433 Eros is relatively bright between 0.75 and 1.1 μm ($R \equiv R_{0.57-1.1}/R_{0.56} = 1.07-1.19$). This is significantly higher than for a primarily silicate assemblage, $R \sim 0.7-1.0$, but is consistent with an assemblage having a significant metallic Ni-Fe component, $R = 1.10-1.30$. Still higher reflectances beyond 1.1 μm (see Section V) further support the existence of a spectral contribution from Ni-Fe metal.

In summary, our spectra alone suggest that the surface material of 433 Eros most probably consists of a pyroxene-olivine assemblage with a significant fraction of finely divided Ni-Fe metal. The olivine and pyroxene are approximately equally abundant. If the metal is in fact finely divided (e.g. by fragmentation during hypervelocity impact, see next sections), its total abundance must be in the range of only 10-30% (~ L or H type chondrites).

V. COMPOSITION OF EROS: A SYNTHESIS

Data other than the 0.3 to 1.1 μm spectra further constrain the probable composition of Eros. As just described, the critical question of metal content on Eros can be answered confidently by comparison of the 2 μm brightness of Eros with the visible brightness. JHK infrared photometry of Eros by Morrison and Chapman (1975), Rieke (1975), and Johnson, Matson, and Veeder (1975), as well as the infrared spectrum of Eros of Larson et al. (1975), all show that the spectral reflectance of Eros near 2 μm is roughly 1.5, relative to unit reflectance at 0.56 μm. That is, the straight, reddish component of the visible spectrum continues to be evident into the mid-infrared. Such behavior is not known for any common silicates or silicate assemblages, all of which have 2 μm reflectances < 1.3, and seems to require the presence of a metallic phase like iron.

It is difficult to specify the required amount of metal or its form. Lunar soils, for instance, show an even redder slope, due to a combination of lunar regolith glasses and agglutinates which contain abundant iron and titanium ions and small amounts of extremely fine, reduced metal particles. Development of a similar mature regolith on Eros is unlikely, however, and agglutinate formation should be markedly reduced due to the low surface gravity on Eros and the lower mean impact velocities at larger heliocentric distances. It seems more likely that the metal component responsible

for the reddish slope is the small amount (10-30%) of particulated iron suggested in the previous section. The iron content could not be as high as the 50% values typical of the mesosiderite class of stony-iron meteorites because the reddening is not very great. Eros shows distinctly less infrared reddening than the several larger "S-type" asteroids (a compositional class, e.g. Juno, defined by Chapman et al. 1975) that have been measured to have high 2 μm reflectances approaching 2.0 (T.V. Johnson, personal communication). The S asteroids are inferred on both spectral grounds (McCord and Gaffey, 1974) and on the basis of size-frequency distribution (Chapman, 1974) to be stony-iron assemblages. Since an increased nickel content in the metal phase could also reduce the infrared spectral reddening to the value exhibited by Eros while maintaining a high metal content, the argument for lower metal content of Eros compared with other S-type asteroids is more firmly grounded in our interpretation of the UV drop-off (Section IV B).

Preliminary reports of thermal infrared measurements of Eros by Rieke (1975) and Morrison (1975) and of radar observations by Jurgens and Goldstein (1975) favor relatively low values for the thermal inertia and radar reflectivity of Eros, both of which rule out the presence of metal in quantities sufficient to be electrically conducting, as in the stony-iron meteorites. These results strengthen our inference of a relatively small amount of finely particulated iron (10 - 30%) based on the UV drop-off (see also discussion of UBV colors below) and 0.95 μm band depth.

Geometric albedos inferred for Eros from both the radiometric technique (Morrison, 1975) and the polarimetric technique (Zellner and Gradie, 1975) are in the range of 0.15 to 0.2. They are more reliable than albedos derived from radar (because of the low signal-to-noise ratio near the "limb" of Eros) or from the occultation of Kappa Geminorum (due to the poor coverage near the western limits of the occultation zone; cf. O'Leary et al. 1975). Such an albedo is brighter than most asteroids in the brighter "S" class, though less bright than a few unusual objects (4 Vesta, 44 Nysa, and 349 Dembowska). Thus the surface material of Eros is relatively free of absorbers and non-metallic opaques (carbon) that might otherwise explain the shallowness of Eros' absorption band. The relatively high albedo is consistent with a significant metal content, but it alone does not exclude a composition similar to low metamorphic grade ordinary chondrites.

Further information on composition is contained in the mid-infrared spectrum of Larson et al. (1975). The presence of a weak pyroxene absorption feature near 0.95 μm in our data requires that there be an associated weak band near 2 μm. Such a band is readily apparent in the spectrum of Larson et al. although its short wavelength side and center are obscured by terrestrial atmospheric absorptions. In principle, measurements of the center positions of both the 0.95 and 2 μm bands can specify the Mg/Fe/Ca content of the pyroxene as well as the approximate amount of olivine contained

in the mineral assemblage (Adams, 1974). But it appears that data on both bands are insufficiently precise, mainly because of the shallowness of the bands, to specify these compositional parameters with precision. We note that if the 1.95 μm band center position assigned by Larson et al is correct, it is consistent with laboratory spectra of a wide variety of meteorites, including howardites and H, L, and LL chondrites (Gaffey, 1975a).

If the range of possible centers for the short pyroxene band is compared to the possible range for the long band, the short band of our data appears to be centered at slightly longer wavelengths than would be predicted for a pure pyroxene assemblage. This indicates olivine may be present (Adams, 1974; Gaffey, 1975a,b).

A more definitive indication of olivine in our data is the asymmetry of the 0.95 μm band and the relatively low reflectances in the range of 1.0 - 1.07 μm. However, all these characteristics of our spectrum that are so strongly diagnostic of olivine are in conflict with the ratio spectrum below 1.0 μm of Larson et al. The discrepancy between the two data sets is almost certainly due to a calibration or other processing error in one or both of the data sets -- no real differences in phase angle, part of Eros observed, etc. can explain the difference. On the basis of our review of our own calibration procedures (Section II) we feel obliged to stand by the essential validity of our own results.

In summary, we infer the following compositional properties for the surface of Eros: It contains abundant silicates, including pyroxene that is probably admixed with olivine in the ratio of pyx:ol = 1:1 to 1:2. Other silicates that lack strong absorptions in accessible portions of the spectrum (e.g. plagioclase) may or may not be present in considerable quantities. Also present is an opaque phase, almost certainly metal rather than an absorber such as carbon. The metallic phase is probably iron or nickel-iron and comprises an uncertain percentage of the surface material, probably well under 50% -- perhaps 10% to 30%. Such a metallic phase must be reasonably well dispersed in fine grains, probably finer than the metallic grains in ordinary chondritic meteorites.

VI. RELATIONSHIP TO METEORITES AND IMPLICATIONS FOR OTHER ASTEROIDS

Although the mineralogical assemblage just described as most likely for Eros is similar to that of many meteorites, especially the ordinary chondrites, no measured meteorite (e.g. by Gaffey, 1974) shows a reflection spectrum like that of Eros. Yet Eros passes sufficiently close to the Earth and has a sufficiently large collisional cross-section that it is likely to be the source-body for at least a few meteorites in terrestrial collections.

It is at least possible that H or even L chondrites, converted into a regolith by impact, might be modified to appear similar to Eros. Although H chondrites contain up to 20% metallic iron,

laboratory spectra of these meteorites show only slight effect of the spectral signature of iron. This is because the iron in chondrites is present in reasonably large pieces (e.g. up to a millimeter) and is very difficult (impossible) to grind. The laboratory preparation of powders of such meteorites greatly increases the surface area of the silicates but not of the iron. But in impacts exceeding 1 km/sec, it is possible that the iron can be shattered and finely disseminated, resulting in a more enhanced iron signature in the infrared portions of the reflectance spectrum of the resulting thin regolith. Before we can confidently conclude that an asteroid of H chondritic composition might appear spectrally similar to Eros, impact experiments must be conducted on such meteoritic material.

Not is it clear that Eros can retain a regolith environment adequate for fragmenting the iron particles. In the past, various authors have doubted that impact processes on asteroid regoliths could significantly affect the spectral characteristics of the materials (e.g. Chapman and Salisbury,1973; Gaffey, 1974, 1975a; Chapman, 1975). This conclusion is probably still generally valid, but our suggestion of a possible exception impels us to review the earlier conclusion (Chapman, 1971) that it is impossible for small-to-moderate sized asteroids to retain regoliths; new impact data by Gault et al. (1975) suggest that the cut-off size in regolith formation is at asteroid diameters similar to, or smaller than, the

diameter of Eros. Secondly, it had been argued that the nearly perfect spectral matches between Vesta and basaltic achondrites on the one hand (McCord et al. 1970) and between Dembowska and LL6 chondrites on the other (McCord and Chapman, 1975b), showed that modification processes were not occurring in the asteroid belt. However, basaltic achondrites and LL chondrites contain very small amounts of metal, so their spectral properties would be expected to be very similar to specimens processed in the laboratory. We still do not expect appreciable vitrification or chemical modification of asteroid surfaces such as occur on the moon (e.g. Adams, Charette, and Rhodes, 1975). Vesta, for instance, has a mineralogical composition very similar to that of the moon, but has an unmodified basaltic spectrum. Based on the earlier spectrum, McCord and Chapman (1975a) had classified Eros as an "S-type" object, similar to Juno and 192 Nausikaa. The new Eros spectrum largely falls within the error bars of the older data, though the UV drop-off is more extreme than previously recognized. The question arises, however, whether other S-type asteroids that have previously been likened to stony-iron meteorites might also be H or L chondrites modified in the manner we have hypothesized for Eros. On the plot of B-V vs. U-B color of numerous asteroids by Zellner et al. (1975), Eros falls on or beyond the upper-right boundary of the domain occupied by S-type asteroid. Its UBV color, reflecting the UV drop-off, is close to that for the LL6 chondrite-like asteroid 349 Dembowska.

Several other observations imply that the larger S-type asteroids really are distinct from Eros and are more related to stony-iron meteorites. First, while the UV drop-offs differ between Eros and the S-type asteroids, the absorption band depths are similar, suggesting a particle-size difference in the metal, with the metal being coarser in the case of the typical S-type asteroids (Section IV). Further, the relatively narrow absorption bands in spectra of many S-type asteroids (e.g. 8 Flora, 89 Julia, and 192 Nausikaa) imply a very low abundance of olivine in those asteroids, which would be characteristic of mesosiderites but not ordinary chondrites. Other S-type asteroids (e.g. 7 Iris, 15 Eunomia, and 68 Leto) appear to have olivine, but no pyroxene, similar to pallasite meteorites but also unlike ordinary chondrites. Thus in most cases, we still prefer non-chondritic stony-iron assemblages for the S-type asteroids. If Eros is indeed an H or L chondrite, it is one of the very few that have been measured in UBV colors, since few other asteroids have such colors.

In conclusion, the Earth-approaching asteroid Eros appears to be composed of an undifferentiated assemblage of moderate to high temperature minerals (iron, pyroxene, and olivine, but no carbon). Its surface composition is homogeneous, although moderate variations in pyroxene/olivine ratio may be present near the noise level in our data. If, as we suggest, the impact processes encountered at the surface of Eros can reduce the particle size distribution of

metal grains as well as the silicate grains and if this material is retained, then the spectral properties of Eros indicate a composition that corresponds to H or L type chondritic meteorites. Eros is distinctly atypical of most main-belt asteroids, which are chiefly of carbonaceous composition, and probably also different from the minority of main belt asteroids with differentiated stony-iron assemblages. Although Eros is spectrally different from all other asteroids measured to date, it is most similar in inferred composition to other Earth-approaching asteroids such as 1685 Toro (Chapman et al. 1973).

ACKNOWLEDGEMENTS

The research reported here has been carried out under NASA grant NGR-22-009-583 to MIT and NASA contract NASW-2718 to PSI. We thank the organizers and participants at the Eros meeting in Tucson for useful discussions. H. Larson has been especially helpful. This is MIT Remote Sensing Lab Publication 142 and Planetary Science Institute Contribution 52.

REFERENCES

Adams, J.B. (1974). Visible and near-infrared diffuse reflectance spectra of pyroxenes as applied to remote sensing of solid objects in the solar system. J. Geophys. Res. 79, 4829-4836.

Adams, J.B., Charette, M.P., and Rhodes, J.M. (1975). Chemical fractionation of the lunar regolith by impact melting. Science, in press.

Adams, J.B. and Filice, A.L. (1967). Spectral reflectance 0.4 μm to 2.0 μm of silicate rock powder, J. Geophys. Res. 72, 5705-5715.

Bell, P.M. and Mao, H.K. (1973). Optical and chemical analysis of iron in Luna 20 plagioclase, Geochim. Cosmochim. Acta 37, 755-759.

Burns, R.G. (1970a). Mineralogical Applications of Crystal Field Theory. Cambridge University Press, Cambridge, England.

Burns, R. G. (1970b). Crystal field spectra and evidence of cation ordering in olivine minerals. Am. Min. 55, 1608-1632.

Chapman, C. R. (1971). Surface properties of asteroids. Doctoral dissertation, Mass. Inst. of Technology, Cambridge, Mass.

Chapman, C.R. (1974). Asteroid size distribution: implications for the origin of stony-iron and iron meteorites. Geophys. Res. Lett. 1. 341-344.

Chapman, C.R. (1975). Asteroids as meteorite parent-bodies: the astronomical perspective. Geochim. Cosmochim. Acta, submitted.

Chapman, C.R., McCord, T.B., and Pieters, C. (1973). Minor planets and related objects. X. Spectrophotometric study of the composition of (1685) Toro. Astron. J. 78, 502-505.

Chapman, C.R., Morrison, D., and Zellner, B. (1975). Surface properties of asteroids: a synthesis of polarimetry, radiometry, and spectrophotometry. Icarus 25, 104-130.

Chapman, C.R. and Salisbury, J.W. (1973). Comparison of meteorite and asteroid spectral reflectivities. Icarus 19, 507-522.

Dunlap, J.L. (1975). Lightcurves and the axis of rotation of 433 Eros. Icarus, submitted.

Elias, J.E. (1972). Calibration of standard stars for planetary reflectivity studies. Master's dissertation, Mass. Inst. of Technology, Cambridge, Mass.

Gaffey, M.J. (1974). A systematic study of the spectral reflectivity characteristics of the meteorite classes with applications to the interpretation of asteroid spectra for mineralogical and petrological information, Ph.D. Thesis, Mass. Inst. of Tech., Cambridge, Mass.

Gaffey, M.J. (1975a) Spectral reflectance characteristics of the meteorite classes. J. Geophys. Res., in press.

Gaffey, M.J. (1975b). Quantification of spectral reflectance parameters for meteoritic mineral assemblages. In preparation.

Gaffey, M.J. and McCord, T.B. (1975). Asteroid surface materials. In preparation.

Gault, D.E., Hörz, F., Brownlee, D.E., and Hartung, J.B. (1975). Mixing of the lunar regolith. Proc. Fifth Lunar Sci. Conf. (Supp. 5, Geochim. Cosmochim. Acta) 3, 2365-2386.

Hayes, D.S. (1970). An absolute spectrophotometric calibration of the energy distribution of twelve standard stars. Astrophys. J. 159, 165-176.

Johnson, T.V. and F. P. Fanale (1973). Optical properties of carbonaceous chondrites and their relationship to asteroids. J. Geophys. Res. 78, 8507 8518.

Johnson, T.V., Matson, D., and Veeder, G.(1975). In preparation.

Jurgens, R. and Goldstein, R.(1975). In preparation.

Larson, H.P., Fink, U., Treffers, R.T., and Gautier, T.N. (1975). The infrared spectrum of asteroid 433 Eros. Icarus, submitted.

McCord, T.B., Adams, J.B., and Johnson, T.V. (1970). Asteroid Vesta: spectral reflectivity and compositional implications. Science 168, 1445-1447.

McCord, T.B. and Chapman, C.R. (1975a) Asteroids: spectral reflectance and color characteristics. Astrophys. J. 195, 553-562.

McCord, T.B., and Chapman, C.R. (1975b). Asteroids: spectral reflectance and color characteristics II. Astrophys. J. 197, 781-790.

Morrison, D.(1975). The diameter and thermal inertia of 433 Eros. Icarus, submitted.

Morrison, D. and Chapman, C.R. (1975). Infrared JHKL photometry of eleven asteroids, in preparation.

Nygard, S.(1975). Calibration of stars for use in planetary astronomy: results for three techniques. Masters thesis, Mass. Inst. of Tech., Cambridge, Mass.

O'Leary, B., Marsden, B.G., Dragon, R., Hauser, E., McGrath, M., Backus, P., and Robkoff, H.(1975). The occultation of $\varkappa$ Geminorum by Eros. Icarus, submitted.

Pieters, C.E. (1972). Wavelength dependence of the polarization of light reflected from a particulate surface in the spectral region of a transition metal absorption band. Masters thesis, Mass. Inst. of Tech., Cambridge, Mass.

Rieke, G.(1975). In preparation.

Runciman, W.A., Sengupta, D. and Marshall, M.(1973). The polarized spectra of iron in silicates: II. Olivine. Am. Min. 58, 451-456.

Scaltriti, F. and Zappala, V.(1975). Photometric lightcurves and pole determination of 433 Eros. Icarus, submitted.

White, W.B., and Keester, K.L. (1967). Selection rules and assignments for the spectra of ferrous iron in pyroxene. Am. Min.58,1508.

Zellner, B. and Gradie, J.(1975). Polarization of the reflected light of asteroid 433 Eros. Icarus, submitted.

Zellner, B., Wisniewski, W., Andersson, L., and Bowell, E.(1975). Minor planets and related objects. UBV photometry and surface composition. Astron. J., submitted.

TABLE 1: STAR/SUN RATIOS

Filter (μm)	γ Gem/Sun	η Hya/Sun
.33	1.625	7.175
.35	1.606	6.349
.37	(2.287)	5.126
.40	2.552	3.080
.43	2.138	2.238
.47	1.567	1.648
.50	1.329	1.388
.53	1.154	1.166
.57	1.000	1:000
.60	.858	.832
.63	.790	.725
.67	.687	.626
.70	.670	.593
.73	.630	.555
.77	.602	.518
.80	.570	.484
.83	.556	.455
.87	(.555)	.442*
.90	.552	.427
.93	.549	.402*
.97	.542	.382
1.00	.501	.350
1.03	.504	.339
1.07	.493	.312
1.10	.443	.325

* tentative

Figure Captions

Figure 1 Lightcurve of Eros/γ Gem during January 28, 29, and 30, UT 1975, for the wavelength 0.57 μm. The data are plotted to maintain the proper phase relationship assuming a period of 5h 16m. The epoch of primary maximum (as defined by Dunlap, 1975) is 5:15 UT on 29 Jan. (see Scaltriti and Zappala, 1975). The data are divided into seven groups for purposes of determining the seven spectra in Figure 2.

Figure 2 Spectral reflectance values of Eros scaled to unity at λ = 0.57 μm for the seven January data groups. Two filters were used centered at 0.87 μm. Error bars show standard errors of the means.

Figure 3 Mean spectral reflectance values of Eros scaled to unity at λ = 0.57 μm for the February data. The open circles indicate reduction using the tentatively improved calibrations shown with asterisks in Table 1.

Figure 4 Spectral reflectance of Eros (average of runs from Fig. 2) scaled to unity at λ = 0.57 μm: (a) spectral scale is wavelength (μm); (b) spectral scale is energy (cm^{-1}); (c) residue of (b) after removal of a continuum.

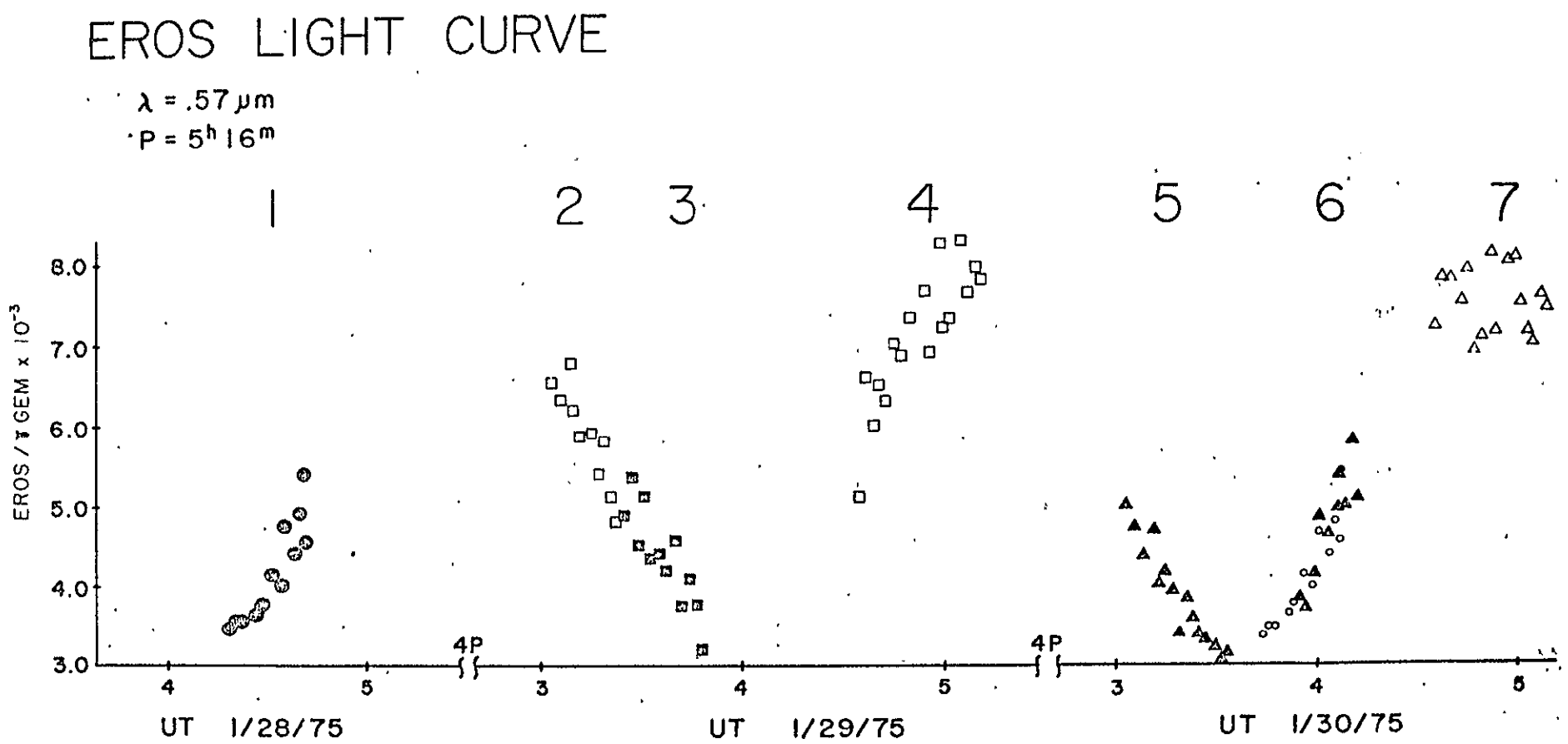

Figure 1

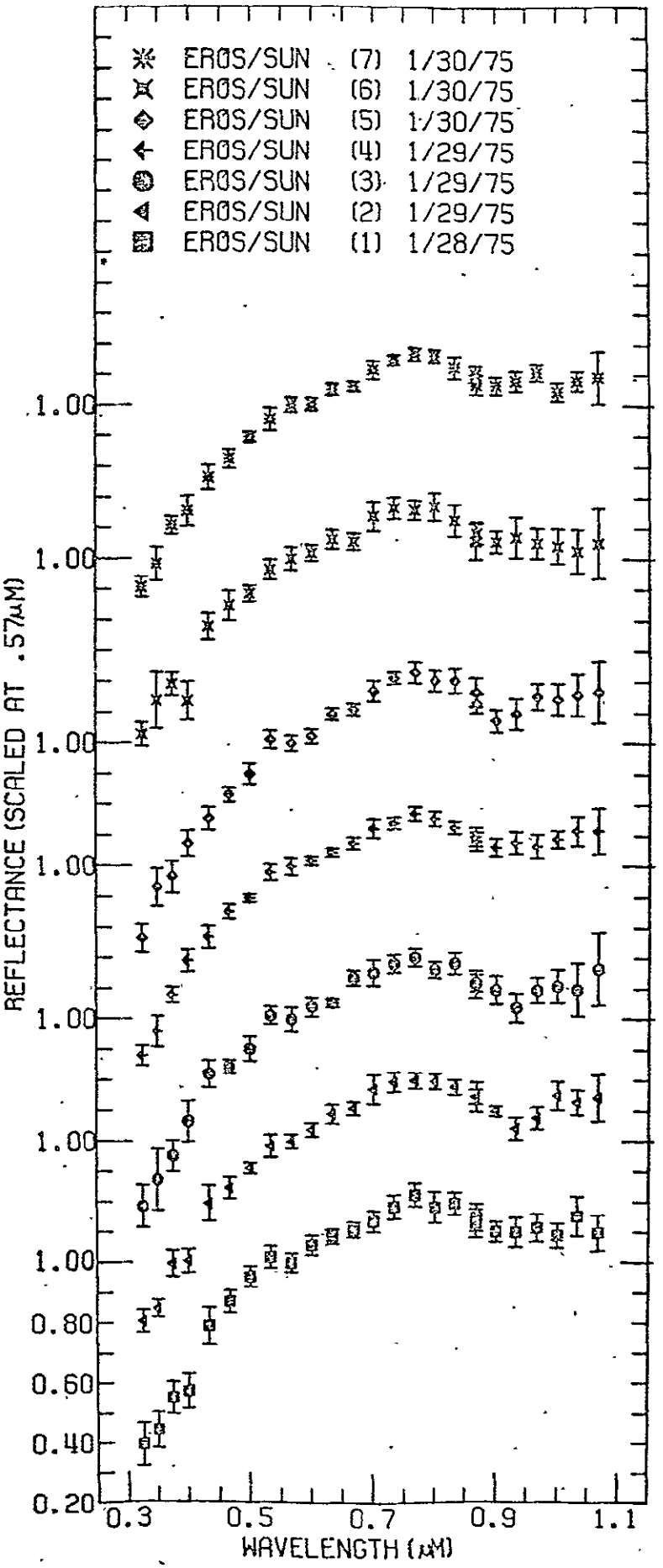
EROS/SUN (7) 1/30/75
EROS/SUN (6) 1/30/75
EROS/SUN (5) 1/30/75
EROS/SUN (4) 1/29/75
EROS/SUN (3) 1/29/75
EROS/SUN (2) 1/29/75
EROS/SUN (1) 1/28/75
REFLECTANCE (SCALED AT .57μM)
1.00
1.00
1.00
1.00
1.00
1.00
0.80
0.60
0.40
0.20
0.3
0.5
0.7
0.9
1.1
WAVELENGTH (μM)

Figure 2

Figure 3

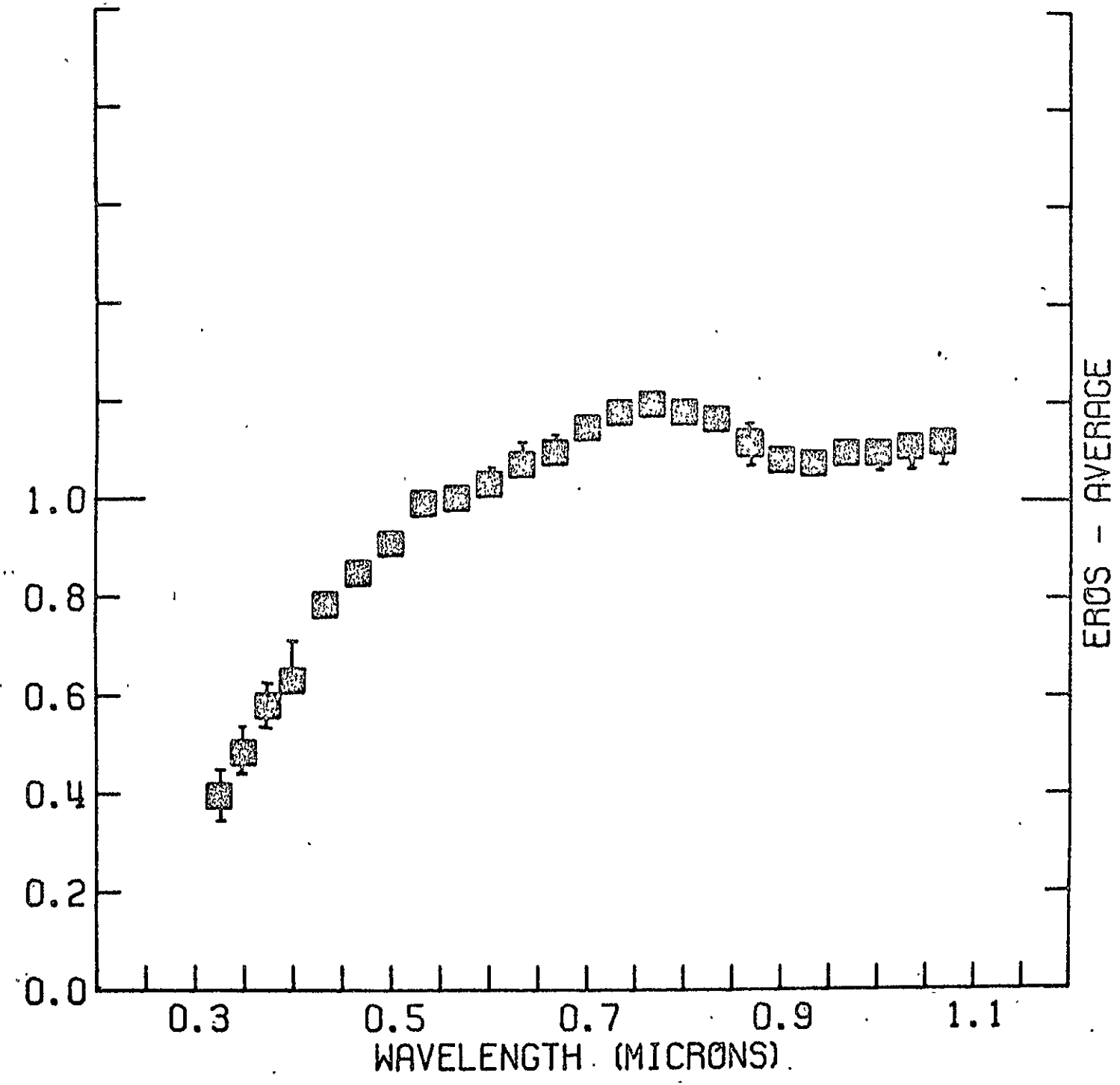
1.0
0.8
0.6
0.4
0.2
0.0
0.3
0.5
0.7
0.9
1.1
WAVELENGTH (MICRONS)
EROS - AVERAGE

Figure 4 (a)

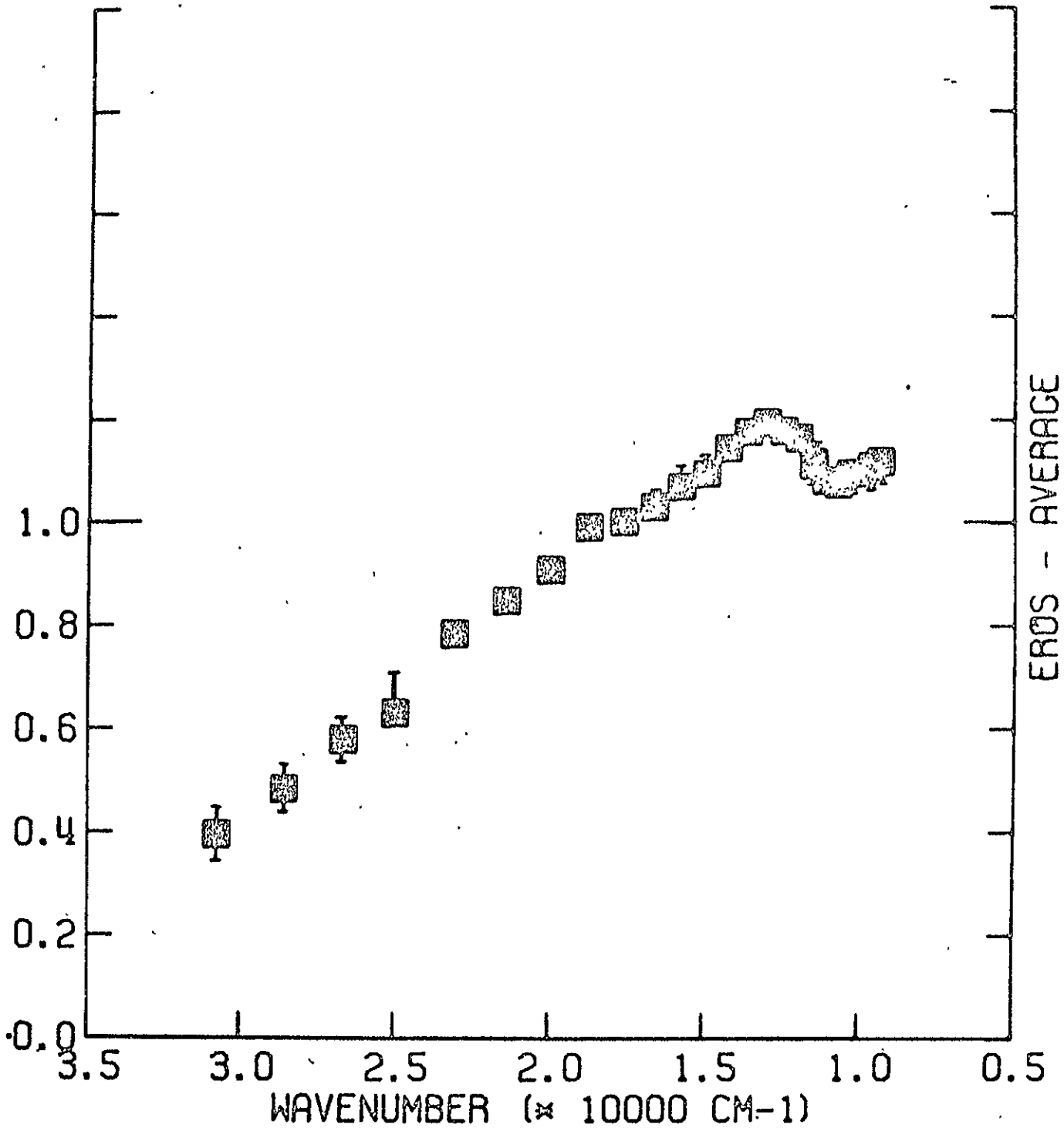
1.0
0.8
0.6
0.4
0.2
0.0
3.5
3.0
2.5
2.0
1.5
1.0
0.5
WAVENUMBER (× 10000 CM-1)
EROS - AVERAGE

Figure 4 (b)

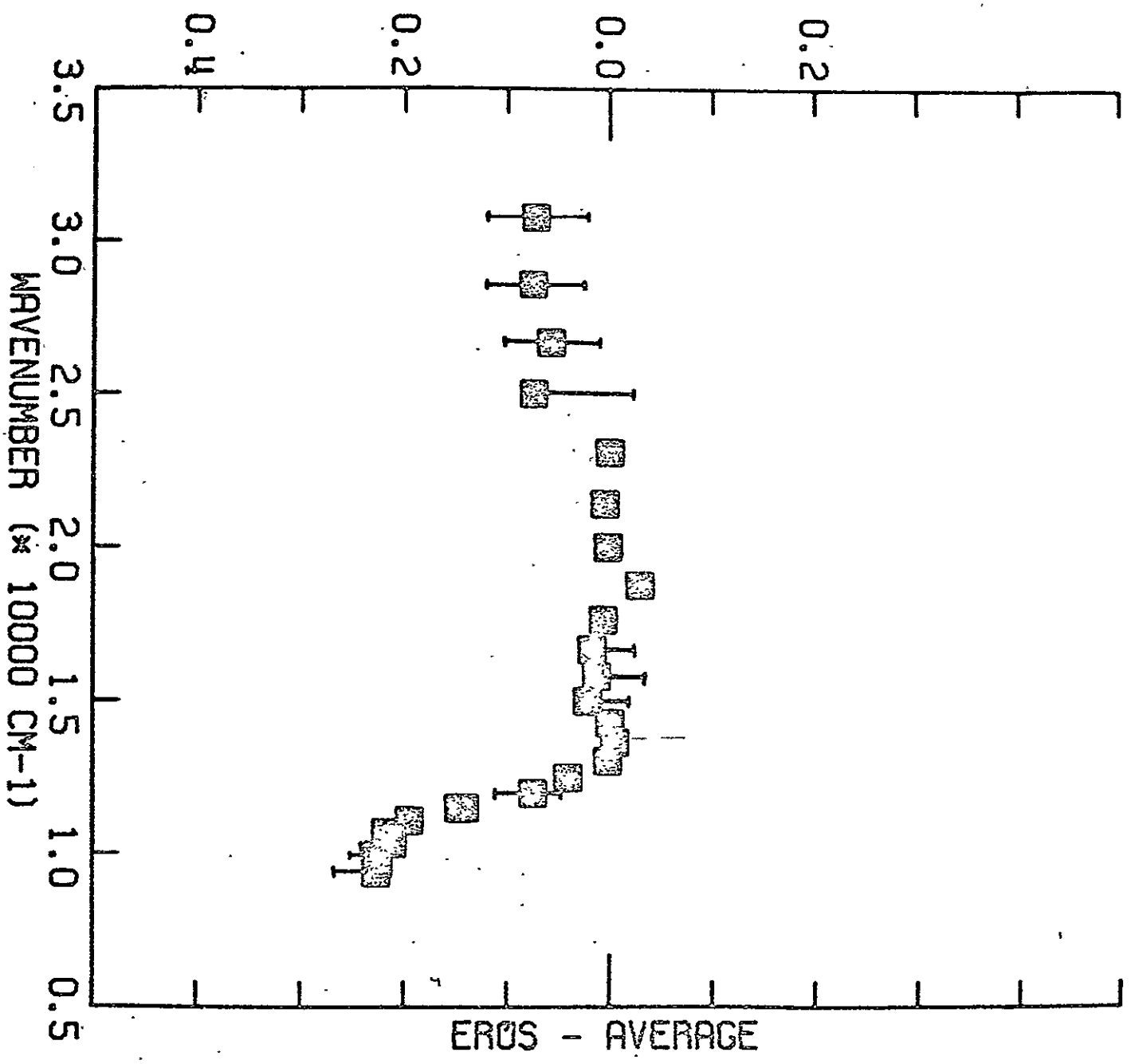

Figure 4 (c)

APPENDIX B

RADIOMETRIC DIAMETERS FOR AN ADDITIONAL 22 ASTEROIDS

DAVID MORRISON*
Institute for Astronomy
2680 Woodlawn Drive
University of Hawaii
Honolulu, HI 96822

CLARK R. CHAPMAN*
Planetary Science Institute
252 W. Ina Road
Tucson, AZ 85704

Submitted to: Astrophysical Journal

Submitted:

Received: _____

* Visiting Astronomer, Kitt Peak National Observatory, which is operated by the Association of Universities for Research in Astronomy, Inc., under contract with the National Science Foundation.

ABSTRACT

New 10-μ radiometry is presented for 24 asteroids, 22 of which have not previously had their diameters and albedos determined. Half are dark objects($0.025 < p_V < 0.06$), apparently of the C (or carbonaceous) type, which appears to be the predominant class of minor planets. One of these, 65 Cybele, is one of the ten largest asteroids. Unusually high albedos ($p_V \geq 0.25$) are found for asteroids 64, 349, and 863. The high albedo for 349 Dembowska reinforces the conclusion from spectrophotometry that it is a metamorphosed ordinary chondrite. 64 Angelina may be an aubrite. The fainter objects in our sample are the smallest main-belt asteroids to have measured diameters and albedos.

Subject headings: Asteroids--infrared--meteorites, meteors

I. INTRODUCTION

Recent intensive studies of asteroids by photometry, spectrophotometry, polarimetry, and infrared radiometry have greatly increased the available physical information on these objects and have spurred interest in their origin, evolution, and relationships to meteorites. In a comprehensive review written in mid-1974, Chapman, Morrison, and Zellner (1975; hereafter CMZ) summarized physical data on more than 100 asteroids, most of which had been observed spectrophotometrically (0.3 to 1.1 μ) and about half of which had measured diameters based on either polarimetric or radiometric data. This sample primarily represented brighter asteroids, so that it favored objects of high albedo and included very few objects with diameters less than 100 km. Indeed, at that time the only objects with measured diameters of less than 80 km were five Earth-approaching asteroids (433, 887, 1566, 1620, 1685). We therefore undertook the present observations primarily to provide diameters and albedos for an initial sample of small objects ($D < 100$ km) in the main asteroid belt. In two nights of observing, we obtained 10-μ radiometry of 22 asteroids, including 13 smaller than 100 km.

The technique and its calibration have been discussed recently by Morrison (1973, 1975, 1976), Jones and Morrison (1974), and CMZ. To obtain the full power of the method, one requires essentially simultaneous measurements of both the reflected and thermally emitted radiation in order to define the instantaneous heat budget of the asteroid and hence its albedo and diameter. In practice, however, with the exception of the recent work of Hansen (1975),

radiometric data have been reduced using standard tabulated visible magnitudes that represent, at best, an average value that does not necessarily correspond to the visible magnitude at the time of the infrared measurement. Particularly in the case of faint asteroids, which in general have not been observed photoelectrically, the uncertainties in the standard B or V magnitudes can easily be as great as half a magnitude (cf. Zellner et al., 1975). In such cases the radiometric observations define the diameter (or more properly the cross-section, for an irregular object) reasonably well but do not allow a good albedo determination. In the extreme (and unrealized) case for which no photometric observations exist whatever, the radiometry still defines the probable diameter to within about 50%, since all measured asteroids have values of(one-minus-albedo) with a spread of less than a factor of 2. In contrast, the spread in albedo itself exceeds a factor of 10, so that photometry without radiometry is a very poor measure of size. In the worst real case, the standard photometry may be uncertain by $\pm$ 0.5 mag. at at the time of the radiometric observations; here the calculated albedo is still uncertain by roughly a factor of 2, but if the radiometry is good, the diameter is determined to within better than 10%. Thus the primary physical datum derived for each asteroid in this study(and in previous work by Morrison and colleagues) is a diameter, defined as the diameter of a sphere of cross-section equal to that of the asteroid at the time the observations were made. Geometric albedos can also be derived, but they are only as certain as the V magnitudes.

II. OBSERVATIONS

The observations were made on 16, 17, and 18 March 1975 with the Kitt Peak 1.3-meter telescope and a Cu:Ge bolometer. The photometer aperture was 13 arcsec in diameter and the cassegrain secondary oscillated at 10 Hz in a square wave of amplitude 18 arcsec. All observations were made with a standard broad-band 10-μ filter that closely approximates the N-magnitude system. The standard stars and their adopted magnitudes were: β Gem (-1.30), α Leo (+1.55), α Boo (-3.20), and α Lyr (-0.05). At least one of these standards was observed each hour, and their magnitudes were in all cases reproducible to within 0.05 magnitude. All magnitudes were reduced to their zenith values with a nominal extinction coefficient of 0.1 mag/air mass, although in practice the extinction corrections were never larger than the observational uncertainties.

An abbreviated log of the observations is given in Table I. A total of 24 asteroids was measured: 22 for the first time and two (324 Bamberga and 511 Davida) that have been studied previously (Cruikshank and Morrison, 1973; Morrison, 1974). Not listed in the table are data obtained on these same nights on 433 Eros, which will be reported in a separate paper (Morrison, 1976). Except for the faintest asteroids (208, 558, 782, 863, and 1178), the infrared signal was peaked before each observation to ensure proper centering in the aperture, and in several cases for the five faintest objects readings were taken with several different centerings to eliminate any chance of serious errors due to pointing. Possibly there is one further uncertainty for 1178 Irmela which, with a visual magnitude of about 15, was difficult to

see in the eyepiece and could be centered only by averted vision. We note that in spite of the visual faintness of several of these asteroids, the presence of an infrared signal from each eliminated any doubt as to their correct identification in the star field. The magnitudes in Table I are rounded to the nearest 0.05 mag.

Asteroids only a few tens of kilometers in diameter might be expected to be irregular objects with cross-sections that vary substantially with rotation. Most small Earth-approaching asteroids that have been measured have large-amplitude lightcurves, and for both 433 Eros and 1620 Geographos the ratio of major to minor diameters exceeds 2:1. We might therefore expect substantial variations in both infrared and visible brightness of several of our smaller asteroids over the course of our observations. Unfortunately, there exists no extended photoelectric photometry of most of the objects we observed by which to check this possibility. On the basis of our observations alone, however, we have some evidence for large-amplitude variations. In Table I multiple entries are given for each night's observation of an asteroid and for each case of apparently significant variations during one night. Variations appear to have been detected for 36 Atalante, 80 Sappho, 107 Camilla, and 129 Antigone. In addition, 782 Montefiore seemed to change in visual brightness in the guiding eyepiece, but the signal-to-noise ratio in the radiometry was insufficient to establish a change in the infrared magnitude. For none of these five asteroids can we estimate either the amplitude or the period of the variations. Taylor (1971) lists a visual amplitude of 0.3 to 0.4 mag. for 349 Dembowska, but our limited observations do not show any significant variations.

In order to derive diameters and albedos we require the monochromatic radiometric magnitude reduced to zero phase angle and unit distance from Earth. (Since one does not know how such magnitudes scale with distance from the sun, we cannot reduce them to unit distance as is commonly done with photometry). To convert broad-band 10-μ observations to monochromatic magnitudes at 10 μ (m_{10}), we add 0.1 mag for objects at temperatures appropriate to the asteroid belt (Morrison, 1973). The dependence of infrared magnitude on phase angle is poorly known, and for this study we adopt a nominal phase coefficient of 0.01 mag/deg (Matson, 1972; Morrison, 1974) and note the additional uncertainty introduced by this phase dependence for the reduced values of m_{10} derived from observations at large α. Where variations were seen in the radiometric brightness, we adopt an average flux value for our calculations. The resulting average monochromatic magnitudes (m_{10}) at $\Delta = 1$ and $\alpha = 0$, rounded to nearest 0.05 mag, are listed in the sixth column of Table II, which summarizes the calculation of diameter and albedo for the 22 asteroids observed.

Values of the visual magnitude are also required in order to derive the basic parameter, $V-m_{10}$ (at $\alpha = 0$ and distance from the sun R), used to calculate diameter and albedo. For our asteroids, we are dependent on tabulated magnitudes derived from isolated photoelectric or photographic photometry. For seven asteroids we adopt the recent photoelectric values of V(1,0) given by Zellner et al. (1974, 1975), as indicated in the footnotes to Table II. For the others, we use the values of B(1,0) given in the listing of magnitudes for all numbered asteroids by Gehrels (1970) and derive from

them approximate values of V(1,0) by assuming values of (B-V) derived either from spectrophotometry (McCord and Chapman 1975a,b) or from the average relationship between color and albedo derived in CMZ. Values of the ratio of bolometric to visual geometric albedo (p/p_V), a parameter required to compute the energy balance of the surface, were also computed either from known colors or from the color-albedo relationship. We assume that for all asteroids the phase integral q = 0.6, but the results are not sensitive to departures from this value except for the asteroids with highest albedos (Jones and Morrison, 1974).

The final columns of Table II give the calculated diameters and albedos. We have carried out the computations for two values of the model parameter T_0, defined as the subsolar infrared brightness temperature of a non-rotating black sphere at 1 AU from the sun (Jones and Morrison, 1974). As discussed most recently by Morrison (1975), the best value of T_0 derived from data on several satellites, the Moon, and the two largest asteroids, is $T_0 = 408$ K, with an uncertainty of ~ 6 K. The values of D and p_V calculated with $T_0 = 408$ are our best estimates for the results of this study. However, Zellner (private communication, 1975) informs us that even with $T_0 = 408$ there is still a systematic discrepancy between polarimetric and radiometric albedos for asteroids (cf. discussion in CMZ), in the sense that the radiometric albedos are a few percent too low. This discrepancy is largely eliminated if $T_0 = 412$ K, and so in order to provide results that can be compared directly with those obtained from polarimetry, we also list diameters and albedos calculated with

$T_0 = 412$. We expect that future work will resolve this apparent discrepancy between the polarimetric and radiometric calibrations.

No estimates of the uncertainties in the calculated diameters and albedos are given in Table II. Although none of our data are extensive enough to exclude possible large amplitude variations, the calculated diameters should be correct to $\pm$ 10% for cases of well determined m_{10}. The largest uncertainties are probably associated with the three highest-albedo objects, 64 Angelina, 349 Dembowska, and 863 Benkoela, since for these objects errors in either V(1,0) or the assumed phase integral (q = 0.6) lead to the largest errors in diameter. In contrast, the diameters of the darkest objects are insensitive to either V(1,0) or q. The computed albedos are at best uncertain by $\sim$ 20%, and if the V magnitudes are greatly in error, the errors in p_V could be substantially larger than 20%.

III. DISCUSSION

The 22 asteroids studied in this investigation were selected according to a variety of criteria. First, of course, were their availability for observation in March 1975 and their not having been previously studied radiometrically. Two (129 Antigone and 349 Dembowska) are among the approximately 30 asteroids with $B(1,0) < 8.0$. Many others were selected in order to provide a sample of objects fainter than had been observed previously ($B > 13$), at a variety of semi-major axes. A few were included because they had been observed either spectrophotometrically or polarimetrically. We next discuss a few individual objects of particular interest and then examine the contribution of all of these new data to the overall picture of the asteroids, particularly

in the context of the broad compositional classifications developed previously in CMZ.

64 Angelina has the highest albedo ($p_V = 0.28$) of any in this simple and is the first asteroid to be found with a radiometric albedo probably higher than that of the unique asteroid 4 Vesta ($p_V = 0.25$). Its UBV colors show that it is only slightly redder than the sun, very different from the reddish, S-type asteroids and closer in color to the very dark C-type objects (Zellner et al., 1975). Spectrophotometry from 0.3 to 1.1 μ (McCord and Chapman, 1976) indicates a slightly reddish surface without any diagnostic absorption bands such as that of Vesta; the spectrum and the high albedo may be consistent with an enstatite composition. It is tempting to identify 64 Angelina as a less extreme (in both color and albedo) version of the remarkably blue and high-albedo objects 44 Nysa, which Zellner (1975) suggests is an aubrite; i.e., a highly iron-depleted enstatite achondrite.

349 Dembowska is remarkable for its unique spectral reflectivity, which shows a 0.95-μ absorption band as deep as, and wider than, that of 4 Vesta, but a visible reflectivity curve that is dramatically different from that of Vesta (McCord and Chapman, 1975b). The spectral reflectance is very similar to that of some ordinary chondrites, with a high olivine content and a pyroxene/olivine proportion similar to that of type LL 6 chondrites. The high albedo ($p_V = 0.24$) found in this work is entirely consistent with the identification of this asteroid with the metamorphosed ordinary chondrites. In the CMZ system of asteroid classification, Dembowska is a U (unclassified).

Its diameter of 140 km makes Dembowska one of the hundred largest asteroids, although this diameter is substantially smaller than might have been guessed from its visible brightness alone.

558 Carmen has an albedo ($p_V = 0.08$) derived in this study near the crossover between the C and S classifications. In the absence of other data, we cannot assign it even tentatively to either group. But it is distinctly unlike its unusual family member 349 Dembowska.

80 Sappho was measured radiometrically by Matson (1972), who derived an approximate diameter of 100 km, as compared with D = 80 km found here. The larger diameter implied an albedo near the border between C- and S-type asteroids (CMZ), but it now seems distinctly in the S-range. Sappho's spectrum (McCord and Chapman, 1975b) is unusual for an S-object, resembling laboratory spectra (Chapman and Salisbury, 1973) of the unusual Lancé meteorite (type C3O). The higher albedo we derive for Sappho ($p_V = 0.12$) is similar to that of Lancé, but the composition for Sappho cannot be inferred uniquely. Its spectrum and albedo are, in fact, also similar to that of the S-type Apollo asteroid 887 Alinda.

65 Cybele, with its diameter of more than 300 km, is the largest asteroid in the present sample, probably the sixth largest in the belt, and is probably one of the last of the dozen largest asteroids to be recognized as such. In spite of its large size, its low albedo and location far out in the asteroid belt result in a mean opposition B magnitude of only 12.4, and no photoelectric photometric or spectrophotometric observations exist of it. Still, on the basis of its low albedo ($p_V = 0.03$) Cybele is clearly in the C-class.

88 Thisbe and 93 Minerva were both classified as C? by CMZ on the basis of their spectrophotometry. The low albedos (both 0.04) derived in this study confirm the classification for both asteroids. Thisbe, along with 107 Camilla, is the second largest (D = 209) asteroid in the present sample.

36 Atalante appears from our observations to have an appreciable lightcurve amplitude and a mean diameter of $\sim$ 100 km. Both its low albedo ($p_V \cong 0.03$) and its spectral reflectance (McCord and Chapman, 1976) indicate that it is a C object. It is spectrally similar to 1 Ceres and 13 Egeria, and it resembles its family members 145 Adeona and 166 Rhodope.

116 Sirona has both an albedo ($p_V = 0.18$) and a spectral reflectance (McCord and Chapman, 1976) consistent with its identification as a standard S asteroid.

415 Palatia has one of the lowest radiometric albedos ($p_V = 0.026$) of any asteroid ever observed. Spectrophotometrically, however, this asteroid has a somewhat reddish slope without absorption bands (McCord and Chapman, 1976) suggestive of metallic or metal-rich enstatite composition, which seems inconsistent with the albedo. But Zellner et al (1975) have also classified this asteroid as a C object, apparently on the basis of polarimetry. More work on this asteroid would be useful.

782 Montefiore is the smallest (D = 15 km) main-belt asteroid with a measured diameter, and is even smaller than the Mars-crossing asteroid 433 Eros. Its moderately high albedo of 0.15 is perhaps not surprising in view of its location on the extreme inner edge of the belt and the tendency of small Mars-crossing asteroids to have such albedos.

107 Camilla has the largest semi-major axis (3.49 AU) of any non-Trojan asteroid with a measured diameter. It appears on the basis of its low albedo ($p_V = 0.04$) to be a C object, as might be expected at such a large distance from the sun.

863 Benkoela has an albedo as high as that of 4 Vesta and 349 Dembowska, which suggests that it is not a typical S object. This asteroid should be considered as a candidate for other physical studies, especially since it is a potential source for meteorites.

1178 Irmela is the smallest (D = 19 km) C asteroid ever observed and was the faintest object visually in this study. Since there are apparently few C asteroids near the inner edge of the belt, it is probable that the only way small members of this class will be measured is by taking advantage of perihelic oppositions of faint asteroids from further out, as we did with Irmela.

The total range in size of these 22 asteroids is from 14 to 300 km, and in albedo is from 0.024 to 0.28. Tentatively, we classify them as follows: ten C (36, 65, 70, 88, 93, 107, 381, 790, 1178, 1567); seven S (80, 116, 129, 131, 208, 441, 782); three U (64, 349, 863), and two unknown (415, 558). These classifications also appear in the final column of Table II. The average semi-major axis for the C's is 3.03 AU and for the S's is 2.61 AU, consistent with the previously noted tendency for the C objects to predominate in the outer part of the belt.

Figure 1 illustrates the position of the objects discussed in this paper in the (diameter-albedo) plane. Also shown, as filled circles, are the 56 asteroids with measured diameters listed in CMZ. The results derived here for 80 Sappho have been substituted for the CMZ values, and also added to the sample is the new polarimetric result for 44 Nysa (Zellner 1975). In this figure, ten of the new asteroids cluster near albedo 0.03 and diameter 100-200 km, in a region previously occupied by only seven asteroids but where CMZ predicted many objects would be identified upon sampling fainter than $V \simeq 12$. Five of the new S asteroids have diameters of 80 km or smaller and thus fall into an area of the albedo-diameter plane previously not occupied by main-belt asteroids. Although not inconsistent with the CMZ conclusion that S asteroids preferentially have diameters of 100-200 km, the new data suggest that there are substantial numbers of S asteroids with $D < 100$ km in the inner part of the belt.

The most remarkable change in Figure 1 from that presented in CMZ is the addition of high-albedo objects; there are now five asteroids known to have $p_V \gtrsim 0.25$, whereas the only one identified a few months ago was 4 Vesta.

When the many other asteroids observed polarimetrically and radiometrically during 1974 and 1975 have been added to the sample with known diameters and albedos, we anticipate that the statistical conclusions reached in CMZ should be re-evaluated, but it is still premature to do so now on the basis of only 22 new measurements. Even the present data are sufficient, however, to verify the great predominance of C asteroids in the outer belt and

to demonstrate the existence of perhaps several new classes of asteroids of high albedo and unusual composition whose largest members have diameters of less than 200 km.

We thank S. G. Kleinman, R.W. Capps, and S. E. Strom for instruction and assistance with the KPNO infrared photometer and B. Zellner for useful discussions and communication of his UBV photometry in advance of publication. P. Herget kindly provided ephemerides used for finding the asteroids. This research was supported in part by NASA grant NGL 12-001-057 to the University of Hawaii and NASA contract NASW-2718 to the Planetary Science Institute. This is Planetary Science Institute Contribution No. 51.

TABLE I
LOG OF OBSERVATIONS

Asteroid	UT Date March 1975	n	Magnitude
36 Atalante	18.08	1	1.50±.10
	18.13	2	1.45±.05
	18.25	1	1.30±.10
64 Angelina	16.21	3	2.35±.05
	18.20	2	2.30±.05
65 Cybele	18.35	3	0.85±.05
70 Panopaea	18.46	3	0.85±.05
80 Sappho	16.44	2	2.50±.05
	18.42	2	2.35±.05
88 Thisbe	17.27	2	1.60±.15
	18.13	2	1.45±.10
93 Minerva	17.29	2	1.50±.10
	18.16	2	1.40±.05
107 Camilla	18.29	1	1.80±.10
	18.35	2	1.40±.05
	18.39	2	1.80±.10
116 Sirona	18.40	3	1.50±.10
129 Antigone	16.14	1	2.35±.10
	16.19	2	2.80±.10
131 Vala	16.33	3	2.95±.10
208 Lacrimosa	16.35	2	4.00±.15
324 Bamberga	18.10	3	0.50±.05
349 Dembowska	16.46	2	2.80±.10
	18.45	1	2.80±.10
381 Myrrha	16.40	3	2.10±.10
415 Palatia	16.16	2	1.45±.10
441 Bathilda	16.26	2	2.80±.10
511 Davida	18.11	4	-0.35±.05
558 Carmen	16.46	2	3.40±.15
	18.46	2	3.30±.10
782 Montefiore	16.31	6	4.20±.15
	18.25	4	4.25±.15
790 Pretoria	18.23	3	2.85±.10
863 Benkoela	16.38	4	5.35±.25
	18.38	2	5.35±.25
1178 Irmela	18.35	6	3.70±.15
1567 1941 HN	18.25	6	3.20±.10

TABLE II.
SUMMARY OF RESULTS

Asteroid	V(1,0)	p/p_V	α	R	m_{10}*	V-m_{10}	D(408)	D(412)	P_V(408)	P_V(412)
36 Atalante	9.16a	1.0	+21	2.48	-0.10±.20	11.19	118	115	.026	.028
64 Angelina	8.01a	1.1	+12	2.38	1.50±.10	8.38	61	60	.284	.297
65 Cybele	7.17c	1.0	+ 3	3.44	-1.00±.10	10.85	304	294	.025	.027
70 Panopaea	8.45c	1.0	-12	2.65	-0.40±.10	10.97	150	146	.032	.033
80 Sappho	8.28d	1.1	-13	2.70	1.05±.10	9.39	83	81	.120	.127
88 Thisbe	7.54b	1.0	+11	3.19	-0.45±.15	10.50	209	202	.038	.040
93 Minerva	8.06b	1.0	+12	2.96	-0.25±.10	10.66	168	163	.036	.039
107 Camilla	7.46c	1.0	+ 2	3.37	-0.25±.20	10.34	209	203	.041	.043
116 Sirona	7.97c	1.1	- 3	2.41	0.85±.10	8.69	79	77	.178	.187
129 Antigone	7.21a	1.1	+16	2.94	0.75±.25	8.79	114	111	.174	.183
131 Vala	10.20c	1.1	- 7	2.29	2.40±.10	9.59	34	34	.118	.124
208 Lacrimosa	9.72c	1.1	- 1	2.86	2.75±.15	9.25	42	41	.126	.133
324 Bamberga	7.41	1.0	+19	2.81	-1.35±.10	11.00	255	248	.029	.030
349 Dembowska	6.33b	1.1	-16	3.15	0.60±.15	8.22	144	141	.244	.257
381 Myrrha	8.88c	1.0	- 6	3.07	0.50±.15	10.82	126	122	.030	.032
415 Palatia	9.70a	1.0	+22	2.32	0.20±.20	11.32	93	90	.026	.027
441 Bathilda	8.97c	1.0	+ 8	2.70	1.60±.10	9.52	64	62	.109	.115
511 Davida	6.46	1.0	+16	2.83	-2.00±.10	10.71	350	340	.037	.039
558 Carmen	9.30c	1.0	- 9	2.91	1.85±.10	9.77	63	61	.081	.086
782 Montefiore	11.72c	1.1	+10	2.09	3.95±.20	9.37	15	14	.153	.160
790 Pretoria	8.42c	1.0	+ 9	3.77	0.55±.10	10.75	175	169	.024	.025
863 Benkoela	9.37c	1.1	+10	3.07	3.65±.20	8.16	34	33	.263	.276
1178 Irmela	12.23c	1.0	- 2	2.19	3.40±.20	10.53	19	19	.056	.059
1567 1941 HN	10.30c	1.0	+11	2.96	1.60±.15	11.04	71	69	.025	.027

* Monochromatic magnitude reduced to $\Delta = 1$, $R = R$, $\alpha = 0$.

a. Zellner et al. 1975. b. Zellner et al. 1974. c. Gehrels 1970, and assumed (B-V). d. Gehrels 1970 and McCord and Chapman 1974b.

REFERENCES

Chapman, C.R., Morrison, D., and Zellner, B. 1975, Icarus 25, 104.

Chapman, C.R., and Salisbury, J.W. 1973, Icarus 19, 507.

Cruikshank, D.P., and Morrison, D., 1973, Icarus 20, 477.

Jones, T. J., and Morrison, D.1974, A.J. 79, 892.

Gehrels, T. 1970, in Surfaces and Interiors of Planets and Satellites, ed. A. Dollfus (Academic Press, London and New York), p. 319.

Hansen, O.L. 1975, submitted to Astron. J.

Matson, D.L. 1972, Ph.D. thesis, California Institute of Technology

McCord, T.B., and Chapman, C.R. 1975a, Ap.J. 195, 553.

McCord, T.B., and Chapman, C.R. 1975b, Ap.J. 197, 781.

McCord, T.B., and Chapman, C.R. 1976, in preparation.

Morrison, D. 1973, Icarus 19, 1.

Morrison, D. 1975, in Planetary Satellites, ed. J.A. Burns (U. Arizona Press, Tucson), in press.

Morrison, D. 1976, submitted to Icarus.

Taylor, R.C. 1971, in Physical Studies of Minor Planets, ed. T. Gehrels (NASA SP-267), p. 117.

Zellner, B. 1975, Ap.J. (Lett.) 198, L45.

Zellner, B., Gehrels, T., and Gradie, J. 1974, A.J. 79, 1100.

Zellner, B., Wisniewski, W.,Andersson, L., and Bowell, E. 1975, A.J., in press.

FIGURE CAPTION

Fig. 1. Distribution of the 22 asteroids in this study in log diameter and log albedo. Filled circles are the 54 asteroids larger than 4 km with previously measured diameters as listed by Chapman et al. (1975), plus 44 Nysa (Zellner, 1975); identifying numbers are given for a few unusual asteroids from this list. The division in albedo between the C and S classes is at approximately 0.09.

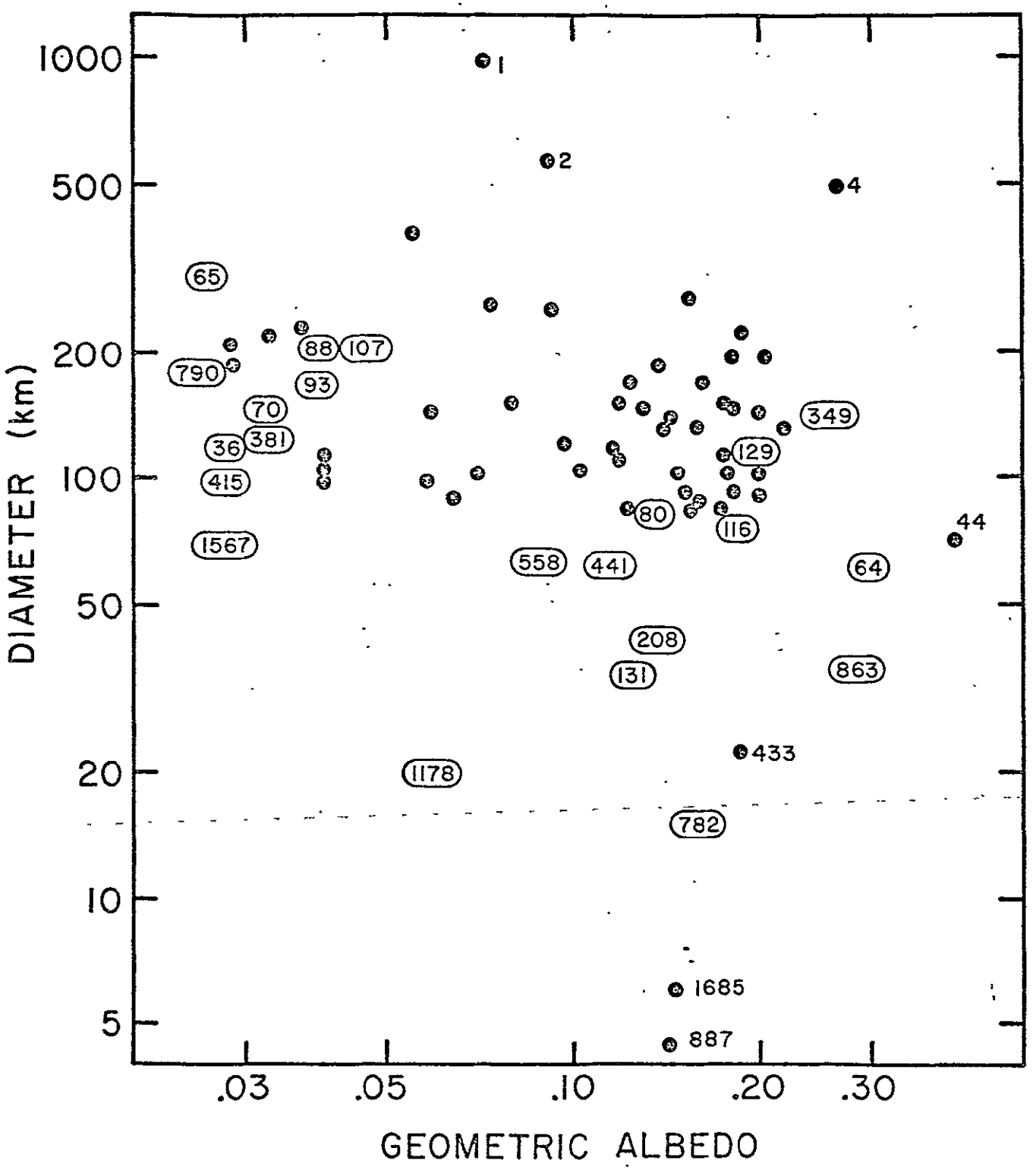
1000
500
200
100
50
20
10
5
DIAMETER (km)
.03
.05
.10
.20
.30
GEOMETRIC ALBEDO
1
2
4
65
88
107
790
93
70
36
381
415
1567
349
129
80
116
44
558
441
64
208
131
863
433
1178
782
1685
887

APPENDIX C

ASTEROIDS AS METEORITE PARENT-BODIES: THE ASTRONOMICAL PERSPECTIVE

Clark R. Chapman
Planetary Science Institute
252 W. Ina Road
Tucson, Arizona 85704

Submitted To:

Geochim. Cosmochim. Acta

30 June 1975

ASTEROIDS AS METEORITE PARENT-BODIES: THE ASTRONOMICAL PERSPECTIVE

Clark R. Chapman
Planetary Science Institute
252 W. Ina Road
Tucson, Arizona 85704

ABSTRACT

A review of astronomical evidence suggests that asteroids are the parent-bodies for most meteorites. Most asteroids are like carbonaceous chondrites while a significant minority are of stony-iron composition. Other meteorite types are recognized in the belt but are rare. Plausible dynamical processes are known that can deliver meteorites from the main belt to Earth. Asteroid compositions vary roughly with solar distance, suggesting that the boundary between ordinary and carbonaceous chondritic nebular condensates was near the inner edge of the present belt. The size distribution of stony-iron asteroids implies they are remnant cores of ~ 100 differentiated bodies subjected to collisional fragmentation by carbonaceous objects initially ~ 300 times more numerous than now. Incomplete evidence on parent-body collisions exists in data on Hirayama families, asteroid lightcurves, and the compositional homogeniety of individual asteroids. Modern-day asteroid regoliths are thin and cannot have been environments for formation of most brecciated, gas-rich meteorites; such meteorites formed during early accretion of the asteroids. A scenario for the origin and evolution of meteorite parent-bodies is presented which involves: (1) interruption of planet-formation and possibly heating of parent-bodies by Jupiter-scattered planetesimals; (2) substantial asteroidal collisions during the first 0.5 b.y.; and (3) formation of most meteorite types within the differentiated bodies.

ASTEROIDS AS METEORITE PARENT-BODIES: THE ASTRONOMICAL PERSPECTIVE

Clark R. Chapman

I. INTRODUCTION

During the past five years, astronomical observations of asteroids have provided data of great potential importance for understanding the relationship between meteorites and asteroids. Asteroid reflection spectra have been measured in visible and near infrared wave-lengths (McCord et al 1970, Chapman et al 1971, Chapman et al 1973a, Chapman et al 1973b, McCord and Chapman 1975a, and McCord and Chapman 1975b). The spectral curves have been augmented by absolute reflectivity (or albedo) measurements of asteroids by the radiometric technique (Allen, 1970; Allen, 1971; Matson, 1972; Cruikshank and Morrison, 1973; Morrison, 1974; Morrison and Chapman, 1975; Hansen, 1975) and the polarimetric technique (Veverka and Noland, 1973; Bowell and Zellner, 1974; and Zellner et al, 1974).

Spectral absorption features may be interpreted using crystal-field theory and identified with particular electronic transitions within crystal lattices of particular minerals. Asteroid spectra also may be interpreted by comparison with a library of laboratory spectra of various mineral assemblages; including meteorites. Initial attempts to interpret asteroid surface mineralogy and relate it to meteorites were by Chapman and Salisbury (1973), Johnson and Fanale (1973), Egan et al (1973), McCord and Gaffey (1974), Gaffey (1973), and Gaffey and McCord (1975). A comprehensive synthesis of the astronomical data, viewed in the light of the laboratory meteoritical measurements, has been published by Chapman et al (1975).

In this article I elaborate on possible implications for meteorite parent-bodies that emerge from astronomical studies of asteroids. I argue that the meteorites indeed are asteroidal fragments, an idea that has been discussed since the time of Olbers (1805) but in the last decade was seriously disputed. I consider: (1) the possible associations between meteorite parent-bodies and various asteroids; (2) the likely modes of deriving meteorites from the asteroid belt; (3) the distribution of mineralogical assemblages in the belt (as a function of distance from the sun, orbital inclination, size and state of fragmentation, and so on); (4) inferred processes of thermal evolution and geochemical differentiation of asteroids; (5) collisional fragmentation history of asteroids and meteorite parent-bodies; and (6) the origin of gas-rich and brecciated meteorites.

Many previous authors (e.g. Anders, 1964; Wood, 1968; and Wasson, 1972) have attempted to interpret and synthesize meteoritical data in order to devise a consistent scenario of early solar system processes and plausible models for meteorite parent-bodies in order to account for the abundant meteoritical data. Such syntheses, and more limited interpretations that accompany most articles on meteoritics published in this journal, attempt with varying degrees of success to account for the available meteoritical data. But such models and scenarios have been generally unconstrained by astronomical evidence on the physical nature of the asteroids -- the supposed meteorite parent-bodies. Of course, there has been a virtual lack of such data until the last few years.

In this article I will adopt the astronomical data as the major framework of constraints in accounting for the evolution of meteorite parent-bodies.

In doing so, I wish to bring a fresh viewpoint to these problems. Perhaps I may be excused if I gloss over some meteoritical details in my attempt to fashion a sensible scenario from the astronomical data, which are the data that I am better able to judge. This article is intended to serve two major functions: (a) to review the astronomical work for the benefit of meteoriticists and cosmochemists and (b) to extend the interpretation of the data beyond the preliminary stages presented in my previous articles on asteroids.

II. COMPARISONS OF METEORITE AND ASTEROID SPECTRA

A comprehensive library of laboratory spectral albedo curves for meteorites now exists. The first, but smaller, study was by Salisbury and Hunt (1975), presented in a more relevant context by Chapman and Salisbury (1973): 41 meteorite powders were measured, with emphasis on the ordinary chondrites. Johnson and Fanale (1973) measured 9 carbonaceous chondrites. Gaffey (1973; see also McCord and Gaffey, 1974; Gaffey and McCord, 1975) measured more than 150 meteorite powders representing (usually with several individual examples) all major classes of meteorites, including each of the chondrite classes of Van Schmus and Wood (1967). Several other researchers have measured a few meteorites, but the three studies just described, especially that of Gaffey, form the foundation of meteorite laboratory comparisons. Only the irons and stony-irons have been relatively neglected because of problems of sample preparation, but it is relatively easy to model the likely reflectance spectra of such metal-silicate mixtures. The laboratory measurements are highly reliable, although terrestrial weathering of meteorites is noticeable

in some spectra (Salisbury and Hunt, 1974). The particle-size distribution in the prepared meteorite powders can appreciably affect the absolute reflectivity (albedo) but spectral properties are not greatly altered, so comparisons with asteroid surfaces, which are probably dusty or particulated, are reasonable.

In Fig. 1 spectral reflectance data for nine asteroids are matched with spectral curves of similar meteorites. Albedos are not known for all of the asteroids, but in cases where they are known they agree approximately with the albedos of the meteorites with which they are compared. It can be seen that the matches are reasonably good in these cases, generally within the errors of the astronomical observations. In most cases, the spectral characteristics are dominated by one or a very few optically-important minerals, generally pyroxenes for the brighter spectra and opaques (carbon) for the darker spectra. With respect to such optically-important minerals,* the similarity of the meteorite and asteroid spectra shown in Fig. 1 bespeak similar compositions.

I will now give a brief overview of the probable mineralogy of asteroids and relationships to meteorites, assuming spectral similarity imply compositional similarity. This approach is a fruitful one if carefully applied but ignores the strict question of uniqueness (cf. Adams, 1974). For instance 349 Dembowska (McCord and Chapman, 1975b) can be interpreted as having

---

* Optically-important minerals are not necessarily the dominant minerals by weight since some, such as plagioclase, exert a minor affect on spectra unless present in overwhelming quantities -- cf. Adams and McCord (1972) and Nash and Conel (1974).

roughly the same mix of orthopyroxenes, olivine, and opaques as LL (or maybe L) chondrites of petrologic type 6 (or maybe 5). Very plausibly its surface is indeed composed of LL6 chondrites. But a rock composed of the same minerals although completely lacking in chondrules would be spectrally indistinguishable from an LL6 chondrite, and the reflection spectrum obviously says nothing about trace elements and other characteristics important in meteorite classification.

Figure 2 shows spectral albedo curves for the 46 asteroids for which both spectral reflectances and geometric albedos have been measured (Chapman, Morrison, and Zellner, 1975). For comparison, Figure 3 shows the mean spectral albedo curves for various meteorite classes, taken from Gaffey's work. The shapes of the spectra are more significant for comparisons than the absolute albedo levels, except for albedo differences exceeding a factor of ~ 2. This is because differences in sample particle size as well as real differences (such as state of shock) between meteorites of the same classification have an important effect on albedos, though minimal effect on spectral shape.

Asteroid spectra span roughly the same range of albedos (from very dark to moderate) that pertain to meteorites. However the distribution of asteroid spectral types is numerically non-representative of meteorites. The most common meteorites -- the metamorphosed ordinary chondrites -- are represented by at most two of the 98 asteroids so far observed.(349 Dembowska is not plotted in Fig. 3 since its albedo is not well-determined, although preliminary reduction of radiometry by Morrison and Chapman (1975) suggest it is in the range 0.25 to 0.3, consistent with ordinary chondrites.) Nevertheless most asteroids have plausible, or at least possible, meteorite analogs (see summary by Hartmann et al, 1975).

Vesta, the brightest asteroid, has a unique spectrum diagnostic of a basaltic achondritic composition with dominant pigeonite pyroxene (but once again, as a final caution, if Vesta's surface material were formed of round "chondrules" of this mineralogy, we would never know it). This important compositional inference (first made by McCord et al 1970) stands regardless of more detailed analyses of Vesta's spectrum that might distinguish between eucrites and howardites (see Chapman, 1971; Gaffey, 1973; Larson and Fink, 1975; Veeder, Johnson, and Matson, 1975).

The darkest asteroids in Figure 2 are almost certainly of carbonaceous composition, and spectrally most closely resemble C2 meteorites (there are inadequate data on C1's because of the paucity of samples). This is the most common composition of main-belt asteroid surfaces sampled so far. Related spectra, which I call C^* type, are shown by dashed lines in Fig. 2. They are flat throughout the visible, show a pronounced ultraviolet fall-off, and have albedos higher than C2 types. Although it has been suggested (Johnson and Fanale, 1973) that these objects are ultraprimitive carbonaceous material, Chapman et al (1975) argue that they more likely are metamorphosed C-type material such as the C4 meteorite Karoonda. The C^* objects are among the largest asteroids in the belt (e.g. 1 Ceres, 2 Pallas, 10 Hygiea, and 511 Davida). The possibility that they are opaque-rich basalts (cf. Ross et al, 1969) cannot be excluded, but seems inconsistent with Ceres' low density of ~ 2.6 gm cm^{-3}. Figure 4, a histogram of asteroid colors from spectrophotometry shows as many neutral-colored asteroids (most of which show the C2-type spectrum) as reddish asteroids (which are predominant in the smaller sample shown in Figure 2). When corrections are made for sampling bias

favoring bright objects, C-type objects are found to comprise > 80% of asteroids larger than 60 km diameter (Chapman et al, 1975).

Reddish spectra are common among the brighter asteroids. They show relatively weak infrared absorption features, mostly due to orthopyroxenes or calcic pyroxenes, but some due to olivine, and some perhaps due to mixtures of pyroxenes and olivines. More precise mineralogical inferences await better infrared photometry. Gaffey and McCord (1975, also McCord and Gaffey, 1974) have argued persuasively that the overall reddish color of these asteroids is due to an admixture of nickel-iron, in abundances exceeding those found in ordinary chondrites. Very possibly these asteroid surfaces resemble pallasites, mesosiderites, or other plausible stony-iron compositions. The spectra are most consistent with nickel-poor iron mixed with silicates in the ratio of 1:2 to 4:1.

The group of stony-iron (S) asteroids has unusual distributional properties, discussed later in this paper, which support the hypothesis that they have the strength of stony-iron meteorites. Since I will base much of my interpretation of parent-body evolution on the identification of S-asteroids with stony-iron meteorites, a note of caution is in order. The Mars-crossing asteroid 433 Eros shows many, but not all, of the spectral characteristics of S-asteroids, leading both Pieters et al (1975) and Larson et al (1975) to suggest that it might be a stony-iron assemblage. But preliminary reduction of radar observations of Eros (Jurgens and Goldstein, 1975) are inconsistent with a metallic matrix. Chapman (1973), Anders (personal communication, 1975), and others have suggested alternatives to the stony-iron interpretation of S-type spectra. But

no known assemblage of meteoritic minerals seems capable of reproducing S-type spectra. Suggestions that ordinary chondritic assemblages might be modified to S-type in impact regolith environments (e.g. by impact shock and vitrification or compositional sorting) are deemed unlikely (Chapman and Salisbury, 1973). Such alterations are especially difficult to reconcile with the fact that several asteroids in similar environments (e.g. 4 Vesta and 349 Dembowska) exhibit normal achondritic or chondritic spectral signatures.

A couple of asteroids have straight, gently-sloping, reddish spectra (albedo about 10%) which are not diagnostic but match laboratory spectra of enstatite chondrites, especially those containing abundant metal (e.g. Abee). An alternative interpretation —— that these "E-type" asteroids are of pure iron —— cannot be ruled out until we have better understanding of the probable physical state of an iron asteroid surface subject to space bombardment.

Several other spectral types are represented in Fig. 2, including a few resembling C3 meteorites and one resembling an ordinary chondrite of low petrological type. Zellner (1975) suggests that another asteroid, 44 Nysa, may be similar to aubrites. A few asteroids (e.g. the Trojans) appear to have compositions different from known meteorites. Unfortunately, in most cases their spectra lack prominent absorption bands so the dominant mineralogy cannot be characterized uniquely. There are also many meteorite classes -- the majority, in fact -- that have reflection spectra clearly not yet represented in the sample of 98 asteroid spectra measured. They include

several types of ordinary chondrites (especially H types), angrites, diogenites, nakhlites, and chassignites; the ureilites and C1 chondrites have not yet been recognized but improved laboratory spectra of these meteorites are required to be sure.

In summary, then, it can be said that the ranges of asteroidal and meteorite mineralogies appear similar. There is a preponderance of apparently carbonaceous asteroids in the main belt, with a lesser number of objects perhaps of stony-iron composition. Achondrites and ordinary chondrites are represented in the asteroid belt but are rare.

III. THE ASTEROIDS AS SOURCES FOR METEORITES

The first asteroids were discovered shortly after the acceptance by the scientific community of the extraterrestrial origin of meteorites. Since then it has been widely assumed that meteorites are asteroidal fragments (e.g. Anders, 1964). But the consensus was severely challenged a decade ago, chiefly by Öpik (1965) and Wetherill (1969) who demonstrated the difficulty of getting asteroidal fragments into appropriate earth-crossing orbits. Certainly the normal collisional and fragmentation events in the belt cannot directly get fragments to Earth because the required accelerations are so severe that rocky materials would be pulverized.

Anders (1964, 1971) proposed that "high-velocity" asteroids that closely approach the orbit of Mars might be sources for meteorites since relatively small collisional accelerations would place fragments in regions where perturbations by Mars could convert their orbits into Earth-crossing orbits. The details of how this process might yield stony meteorites have never been

worked out, but other specialists doubt that stony meteorites can be derived in this fashion. It is more likely, though, that iron and stony-iron meteorites can be derived in such a manner since they have exposure ages of the requisite duration (Arnold, 1965; Wetherill, 1974) and S-type asteroids predominate in Mars-approaching orbits.

Recently, two mechanisms have been proposed to deliver fragments from certain main belt asteroids into Earth-crossing orbits (Zimmerman and Wetherill, 1973; Williams, 1973). In both models, fragments are knocked off certain asteroids at low velocities into nearby resonances (the "secular resonances" or the 2:1 Kirkwood gap). Under some circumstances, fragments are then rapidly perturbed into orbits which frequently intersect the Earth. Approximate terrestrial meteorite yields have been calculated for one of these modes and are significant. It is not yet known, however, exactly which asteroids ought to be the dominant souces of meteorites. Clearly, proximity to a resonance is important. Also larger asteroids have greater collisional cross-sections and will contribute more fragments except possibly the largest ones with appreciable gravity. The trade-off in effective yield between size and proximity to resonances is not yet known (Wetherill, 1974). Nor do we know how representative the sampling is of candidate sources, given the occasional and random occurrence of impacts sufficiently large to contribute to the meteorite yield. It is quite possible that the time-scale for clearing a resonance of fragments from a major collision is short compared with the duration between such collisions, in which case the candidate bodies will be sampled non-representatively.

There are some observational tests of the two hypothesized modes for delivering asteroidal fragments to Earth which have been investigated by McCord and Chapman (1975b). First, consistent with the hypotheses, no prominent candidate asteroid has been observed to have spectral reflectance characteristics that cannot be ascribed to some known meteorite. Secondly, the spectra of candidate source asteroids have been compared for resemblance to the suite of meteorite spectra. The relative representation of different types among terrestrial meteorite falls and the hypothesized asteroid sources differs appreciably, partly explicable by factors affecting the survival and recovery of meteorites on Earth. But we must await more complete sampling of asteroids before defining the degree to which the meteorites are, or are not, representative of the hypothesized source objects.

Vesta poses another problem. Chapman et al (1975) have shown that sampling of objects with albedos as high as that of Vesta is nearly complete down to diameters of 80 km, with significant sampling to 40 km. But Vesta is the only asteroid, among over 100 measured spectrophotometrically, which is known unambiguously to have a surface composition akin to basaltic achondrites. Since basaltic achondrites undoubtedly were formed on a sizeable body, Vesta is the prime candidate parent-body for such meteorites since the moon is now excluded. There are only two alternatives: (1) the original parent-body is highly fragmented, so that the achondrites come from a small asteroid fragment (diameter < 80 km) of largely basaltic surface composition; or (2) the parent-body basaltic surface has been almost entirely (but not completely) eroded away so that the achondrites come from a small basaltic part of some large asteroid of predominantly non-basaltic surface composition.

The simple model that Vesta itself is the source for eucrites, howardites, and diogenites conflicts, however, with Vesta's lack of proximity to the resonances. Thus the original objections to getting asteroidal fragments from the main belt apply. We therefore face the philosophical dilemma of deciding how much pessimism is justified about getting fragments from Vesta (or other main belt asteroids away from resonances) merely because a mechanism has not yet been discovered. We should recall the attitude of Wetherill (1969) who, after demonstrating that "no satisfactory way of perturbing ring asteroids into earth-crossing has been found", concluded that "it does not seem likely that any observed group of asteroids... will serve as satisfactory sources of [meteorites]." Öpik (1965) was still more definite: after demonstrating that "there is no plausible way for the meteoritic fragments of asteroidal collisions to reach us", he concluded that "the idea of asteroidal origin must be renounced completely".

More recently Wetherill himself has been associated with the work demonstrating two independent methods of getting asteroidal fragments to Earth. But once again he is pessimistic about discovering additional methods. Possibly a more realistic attitude is that of Anders; he argued all along, mainly on cosmochemical grounds, for the asteroidal origin of meteorites and always believed that the dynamical difficulties would be solved (Anders, 1964; 1971). He has been partly vindicated by the recent work. Although some implications of resonance effects in the asteroid belt are still unexplored, the understanding of asteroidal dynamics has been improving in recent years (e.g. Williams, 1971). Thus estimates of the implausibility of gravitationally modifying certain asteroidal orbits into meteorite orbits are more firmly grounded than in the past.

One requirement for an asteroidal source mechanism is that the gravitational modification of orbit take place relatively rapidly, on time-scales similar to cosmic ray exposure ages of stony meteorites. Since the lifetime of any object in the source region is short, the volume density of asteroids there must be low. Thus, by analogy with the two mechanisms already proposed, any asteroids close to a sparsely occupied region (in some general dynamical parameter space) are potential sources for fragments knocked into these gaps and then, perhaps, into Earth-crossing orbits. Of course, in the absence of detailed study, one cannot be assured (1) that objects were ever originally formed or placed in these gaps; (2) that the process of removing objects from such gaps is an on-going one, as distinct from one that operated only in the distant past; or (3) that the process removes objects to the required meteorite-like Earth-crossing orbits. But viewed from this perspective, any asteroid such as Vesta that is near a Kirkwood gap is a potential meteorite source. Anders' high-velocity objects are also plausible sources. And of course some comets would be prime candidates if models for their physical nature and environment could be reconciled with the characteristics of meteorites.

IV. DISTRIBUTION OF ASTEROID COMPOSITIONAL TYPES WITH ORBIT

Our sampling of material in the solar system is very non-representative: we have terrestrial and lunar rocks (which are highly altered and fractionated samples from 1 A.U.), meteorites (which, as shown in the previous section, are probably non-representative samples from some asteroids), and the remains of cometary meteors (from unknown, but probably large solar distances); we may someday have planetary rocks from the vicinities of

Mercury, Venus, Mars, Jupiter, and the other planets. However, the asteroids present the potential for sampling less-altered samples of solar nebula condensates throughout the region 1.8 and 4.0 A.U. with some representation from 1 to 5.8 A.U.

The present compositional variability with semi-major axis will fail to reflect early states to the extent that the asteroid orbits have since changed. Since the accretion of asteroids required relative velocities much smaller than the current 5 km/sec., there evidently has been evolution from nearly circular to moderately inclined and eccentric orbits. The combination of processes (e.g. perturbations and collisions) that produced the current spread of eccentricities and inclinations might well have dispersed semi-major axes over several tenths of an A.U. There is little expectation that asteroid orbits have been still more seriously modified with respect to each other, apart from early radial mixing during accretion (e.g. Cameron, 1972) or hypotheses that the overall scale of the solar system changed in the earliest epochs (Alfvén and Arrhenius, 1973).

Early compositional variability through the belt may be masked, as well, if subsequent evolutionary processes have modified asteroid surface compositions. These include differentiation or modification due to collisions, cratering, and the solar wind, all of which may have varied with semi-major axis. In such cases, compositional variability with orbital parameters may tell us more about these evolutionary processes than about early conditions.

Compositional Classes

On the basis of asteroid spectral parameters alone, McCord and Chapman (1975a, 1975b) have identified 34 significantly different spectral types. Some

of these types are very different from the others, both in terms of spectral characteristics and in terms of implied mineralogy. Others are only marginally separable from similar types and imply relatively small compositional differences. Of course, mixtures in different proportions of only a few fundamental components could be responsible for the entire suite of asteroid spectra (McCord and Gaffey, 1974).

For purposes of this paper, I have grouped the 98 observed asteroids into 13 major compositional groups. The correspondence of these groups to the single most important spectral parameter (R/B, a measure of the overall color of the asteroid) is shown in Fig. 4. By direct inference from the spectral reflectance characteristics (e.g. McCord and Gaffey, 1974) and by comparison with meteorites (see Sect. II of this paper), the different spectral types are identified in the legend to Fig. 4 in terms of their probable gross mineralogy, where possible.

The figure shows a gross bimodality in R/B. Chapman et al. (1975) have shown that the bimodality extends, for 90% of the asteroids, to other observational parameters related to composition, including absorption band depth, minimum polarization, and albedo. They call the low R/B group "C-type" (for the "carbonaceous" C2 and C*-types) and most asteroids in the high R/B group "S-type" (for "stony-iron" or "silicaceous" asteroids). About 10% of the asteroids could not be classified C or S, including many of the metallic or E-types, the achondrites, the Trojans (composition unknown), and some of the otherwise silicaceous objects having extreme values for some of the optical parameters (e.g. ordinary chondrites).

Semi-Major Axis Variation*

Fig. 5 shows how the 13 compositional types are distributed as a function of semi-major axis. In examining this graph, the reader should recognize that the sampling favors bright asteroids which biases against the C2-type objects, especially at large semi-major axes; also there is some bias against C*-type and perhaps the E-type objects. Even without correcting for bias, it is apparent that C2-type objects, and especially C*-type objects, predominate in the outer half of the belt. The S-type objects are most numerous in the inner part of the belt, especially those with evident pyroxenes. The non-pyroxene S-type objects are relatively common around 2.4 and 2.9 A.U.; these frequently contain appreciable olivine. The metallic or E-type objects tend to occur in the outer half of the asteroid belt, especially in the sparsely populated portion between 2.8 and 3.05 A.U. where some of the most common compositional types (C- and S-types and pyroxene-metal mixtures) are absent.

One direct interpretation of asteroid composition variability with solar distance would be in terms of solar nebula condensates. Carbonaceous material formed at the largest solar distances where temperatures were lower and ordinary chondrites formed near the inner edge of the belt and inward towards Earth. There has been subsequent mixing over a typical range of 0.3 A.U. accounting for the lack of a 1:1 compositional correspondence with semi-major

* In this Section, I ignore the fine structure associated with the Kirkwood Gaps in the variation of composition with semi-major axis. See Sect. VIII.

axis and for such obvious exceptions as the LL chondrite asteroid 349 Dembowska at 2.9 A.U. Unfortunately, such a model fails to account for the large number of metal-silicate asteroids that apparently are much richer in metallic iron than the most iron-rich ordinary chondrites. It seems clear that the metal-rich material must have resulted from a post-condensation fractionation process since such iron-rich materials in nebular condensates are more appropriate to near-Mercury space than to the asteroid belt. The interpretation also fails to account for the "E-type" asteroids (if they really are of enstatite chondritic composition) since they would have formed at locations sunward of the ordinary chondrites but are actually found in outer parts of the asteroid belt.

In considering the variability with solar distance of nebular condensates, we therefore must exclude all bodies which have been subsequently differentiated, including the achondritic objects (chiefly Vesta), possibly the C* objects (if one considers their surfaces to be basalt), and possibly the E-type objects (if they are really nickel-iron). The S-type asteroids are probably cores of differentiated precursors (see below), so they must also be excluded. The remaining undifferentiated objects, throughout the belt, then, are predominately C2-type objects (and probably C* objects), with a few examples of C3 and ordinary chondrite-like objects mainly (but not exclusively) in the inner belt, and the several E-type objects mainly in the outer belt.

Alternative interpretations, that do not require mixing of asteroids across the width of the belt or from even greater distances, can ascribe the mix of asteroidal surface properties to differing impact or thermal histories

for individual asteroids intially formed in a similar manner throughout the belt. For instance, consider layered models of asteroids, having metallic cores, chondritic mantles, and carbonaceous surface layers. Such objects could have resulted from thermal modification of original carbonaceous= chondritic bodies (e.g. Wood, 1965), and possibly also from inhomogeneous accretion. Then, depending upon the chance encounters with other large objects, some asteroids failed to have been hit at all and remained carbonaceous in surface composition; others were dealt a catastrophic blow, perhaps spalling off the mantles, revealing the stony-iron surfaces of their cores; and a few were fragmented to intermediate degrees, revealing surfaces perhaps composed of ordinary chondrites, achondrites, and enstatite chondrities. Indeed, the overall collisional rate probably is less for asteroids far from the sun, those with high inclinations, and those far from Kirkwood gaps (Wetherill, 1967, Table 3; Wetherill's Table 4 shows an opposite conclusion for variation of collision rate with a, but the observational basis for that table is invalid [Van Houten, 1971]; Chapman et al., 1975.

There are two major model-independent conclusions. First, the asteroid belt is overwhelmingly composed of objects whose surfaces, at least, are of carbonaceous composition. This conclusion tends to support the large temperature gradient of Lewis (1972, 1974), who proposed that carbonaceous chondritic matter resided in the asteroid belt, and differs from the lower gradient of Anders (1971b) who placed the carbonaceous chondrities only in the outer fringe of the belt and beyond. Secondly, a variety of different meteorite types besides carbonaceous ones appear to be represented in the asteroid belt, including equilibrated

LL chondrites, L chondrites, unequilibrated chondrites, basaltic achondrites, stony-irons, enstatite chondrites or irons, and stony-irons. Although we cannot exclude the possibility that these objects were transported to the asteroid belt from other distant locations in the solar system, most celestial dynamical studies imply considerable stability for asteroidal orbits and it would be fruitful to investigate cosmochemical processes that can generate these diverse meteorite types at roughly their present solar distances.

V. SIZE DISTRIBUTION AND PARENT-BODY CORES

Size Distribution

Until very recently, study of the size-distribution of asteroids has been severely hampered by our inability to measure asteroid diameters. Although crude diameters were measured for a few of the largest objects at the turn of the century (see review by Dollfus, 1971), the size distribution has always been derived from the absolute magnitudes of asteroids (apparent brightness reduced to unit distance from the Earth and the sun) by assuming that a geometric albedo, generally ~ 0.2, is applicable to all asteroids. Such diameters are accurate only to the square-root of the ratio of the true albedo to the assumed albedo. The inferred mass distribution has inaccuracies compounded by the necessity to assume a density. Finally, there are selection biases inherent in the first major survey of bright asteroids, the McDonald Survey (Kuiper et al, 1958, hereafter called MDS), and the more recent survey of fainter asteroids, the Palomar-Leiden Survey (van Houten et al, 1970, hereafter called PLS).

However, as mentioned in the Introduction, two new techniques have recently provided indirect estimates of asteroid albedos (and hence diameters).

The polarimetric technique employs an empirical relationship between the variability of polarization with solar phase angle and the albedo of materials; the radiometric technique yields albedos from the ratio of the thermal radiation near 10 μm to that in the visible under the assumption of blackbody thermal equilibrium. Initial calibration difficulties have now been resolved (Chapman et al, 1975) and the resulting diameters for 44 asteroids are probably accurate to 10%. It is apparent that while the S-type asteroids have geometric albedos around 0.15, the much more abundant C-type objects have albedos of only ~ 0.04. Approximate diameters for 52 additional asteroids have been calculated through an approximate empirical relationship between asteroid R/B color and albedo (Chapman et al, 1975). These authors made appropriate corrections for all sampling biases and presented incremental diameter frequency relations for C and S objects; an up-dated version is shown in Fig. 6. Chapman (1974) outlined an interpretation that is elaborated upon in this Section.

Relative to the overall trend of the asteroid size-frequency curve, there is an apparent deficiency of objects with diameters near 300 km, or alternatively, an excess of objects with diameters larger than 400 km. This feature may result in part from the statistics of small numbers since there are only four asteroids with diameters larger than 350 km (the difference between the "C" and "all" lines near 500 km is due solely to Vesta). Hartmann (1968) has argued that these few asteroids may have grown to be unusually large during accretion due to their increased gravitational capture cross-section (see also, Hartmann and Davis, 1975).

A more important characteristic of Fig. 6 is the difference in shape of the relations for C and S objects. While there are nearly equal frequencies at sizes near 150 km, the S objects are lower by nearly an order of magnitude relative to C objects at both large and small diameters; that is, the C frequencies approximately follow a line of slope -3 whereas relative to such a line the S objects show a considerable excess between 100 and 200 km diameter. The reality of these trends is confirmed in Fig. 7 which shows the relations for C objects (dashed lines) and S objects (solid lines) in four different regions of the belt. Although the relative proportions of C and S objects change with semi-major axis, the straightness of the C relation and curvature of the S relation (peaking near 150 km) is evident in all four parts of the belt. It should be emphasized that the bias corrections that have been employed are relatively small for the S objects because they are higher-albedo objects, so there seems to be no doubt of the reality of the curvature of the S relation.

Fig. 6 also shows the best data on the size distribution of asteroids smaller than 60 km. These are from the MDS and PLS magnitude surveys (as reviewed by Dohnanyi, 1972) since actual diameters have not yet been calculated. But I adopt a geometric albedo of 0.06, which gives greatest weight to the albedo of C-type objects since they apparently predominate in the belt. A reported disagreement between the two surveys in the size range of overlap is resolved by Hartmann et al (1975).

Original Accretions?

Nonlinearities or "bumps", in size-frequency distributions of fragments are diagnostic of incomplete fragmentation. It is well-documented (e.g. Marcus, 1965; Hartmann, 1969; Hellyer, 1970; Dohnanyi, 1971) that a population of objects made of the same material subject to mutual collisions, or of craters

formed by the impact of such objects onto a planetary surface, follows a straight line of slope -3 to -3.5 on a log-log incremental size-frequency plot such as Fig. 6.

The first explanation for the "bump" near 150 km was that it consists of a largely intact "original population" of planetesimals incompletely fragmented by subsequent collisions (Kuiper et al, 1958). The theory was developed by Anders (1965) and amplified by Hartmann and Hartmann (1968). Plausibly there was a preferred size in the accretion process and a "Gaussian" distribution of planetesimals (cf. Goldreich and Ward, 1973). Collisional theory shows (e.g. Dohnanyi, 1969) that the longest collisional timescales occur for the largest asteroids, so it seemed plausible that most of the larger asteroids > 50 km diameter are original accretions and that smaller ones constitute a "tail" or collisional fragments.

But this classical interpretation of the "bump" must be re-evaluated in the light of new evidence. The interpretation that virtually no asteroids larger than 100 km diameter were fragmented stretches the limits of most analyses of collisional lifetimes since Piotrowski's (1953) first result. Anders (1965), for instance, deduced that the asteroidal rock had to be especially strong to resist fragmentation to the degree required. But it now seems that most asteroidal material is carbonaceous, with a probable crushing strength about two orders of magnitude less than that calculated for asteroids by Anders. Dohnanyi (1969, 1972) calculated collisional lifetimes for objects the size of Pallas and Vesta of about 4×10^9 years, and only three times shorter for 50 km diameter objects. Even so, he was underestimating the collisional cross-section of asteroids by a factor of 3 because of his

smallest object (of same density) capable of catastrophically fragmenting it upon a collision at velocity v (collisions between objects with larger diameter ratios merely crater the larger object). Asteroid collisions are discussed by Dohnanyi (1969), Hartmann et al (1975), and Chapman et al (1975b). Wetherill (1967) gives values for f of about 1.5 to 2 and $\bar{v}$ is about 5 km/sec (Piotrowski, 1953; Dohnanyi, 1969).

The value of γ is very important inasmuch as a change in γ of a factor of 2 results in a change in the collisional half-life of about a factor of 6 (for b = -3.5). γ depends chiefly on material strength which must be determined experimentally. It is the difference in γ between C-type and S-type asteroids that I suggest yields a highly fragmented C population co-existing with an incompletely fragmented S population and thus the grossly different size-frequency distributions for the two groups of asteroids. Dohnanyi (1969) adopts $\gamma \approx 18$ as applicable to solid basalt, similar to Wetherill's (1967) estimate of $\gamma \approx 10$ to 20 for stony meteorites. Carbonaceous chondrites have crushing strengths about two orders of magnitude less than most stony meteorites; possibly $\gamma \approx 50$ is appropriate. Iron, which is roughly 20 times stronger than stone, has $\gamma \approx 5$ (Wetherill, 1967). In the absence of any experimental data, we do not know how accurately laboratory-scale strengths may be extrapolated to asteroidal scales, but perhaps we can trust estimates of γ to within a factor of 2.

It is well known (cf. Johnson and McGetchin, 1973) that the binding energy for larger asteroids, especially those composed of inherently weak materials, is augmented by the gravitational potential energy. By equating the gravitational potential energy of a large target with the kinetic energy of an impacting projectile (cf. Pollack et al, 1973), the diameter can be determined for which

unrealistically high assumed geometric albedo of 0.2. Chapman and Davis (1975) show that collisions in the belt probably have been more numerous than previously believed by orders of magnitude.

The hypothesis that the asteroids have suffered only occasional collisions, and the concept of two distinct populations of asteroids ("original accretions" and "fragments") clearly requires revision. The fact that the "bump" seems due solely to the asteroids of the S spectral type is the diagnostic clue with important cosmochemical implications.

Iron Cores

A reasonable explanation for the 150 km excess of S-type asteroids invokes a variable crushing-strength or "fragmentability" of asteroids (Chapman, 1974). Given the incremental size-frequency relation for asteroids (number per cubic kilometer per kilometer diameter increment)

$$N = a\, D^b \tag{1}$$

where D is the diameter in kilometers, it can be shown that for an object of diameter D_O, the half-life against catastrophic destruction by collisions is given by

$$t_{cc} = \left[\frac{\pi D_O^2 \bar{v}}{4f} \int_{D_O/\gamma}^{\infty} a\, D^b\, dD \right]^{-1} \qquad \begin{array}{l} \text{provided:} \\ \gamma >> 1 \\ b < -3 \end{array} \tag{2}$$

where $\bar{v}$ is the rms relative velocity of asteroids in the belt, f is the factor by which the true collision frequencies are longer than particle-in-a-box collision frequencies, and γ is the ratio of the target diameter D_O to the diameter of the

gravity begins to dominate over inherent strength. For targets much larger than this limit, it takes an increasingly comparable sized impacting object to fragment it and disperse it against its own gravity.

Evaluation of eq. (2) yields the half-lives for collisional destruction of C and S asteroids shown in Table 1 on the assumption that they have the material properties of carbonaceous and iron meteorites, respectively. Evidently all but the very largest carbonaceous asteroids are fragmented in times short compared with the age of the solar system, consistent with their highly fragmented condition evidenced by the linearity of their diameter-frequency plot (Fig. 6). The S asteroids, on the otherhand, are relatively undepleted by the present asteroid collision rate. Thus the observed diameter distributions of the C and S asteroids appear to be the natural result of the strengths of the materials of which their surfaces are inferred to be composed, on spectrophotometric grounds.

How did the two groups originate? Inasmuch as iron-rich bodies can only be derived from solar nebular condensates by a strongly fractionating process, it is tempting to view the S bodies as iron or stony-iron "cores" of geochemically differentiated asteroids that have had their mantles and crusts stripped away by collisions. The predominant S-asteroid diameters of 100 to 200 km would be appropriate for differentiated bodies of originally chondritic composition with diameters of about 200 to 500 km diameter, in excellent agreement with sizes for the parent-bodies of iron and stony-iron meteorites derived from Widmanstätten pattern cooling curves by Fricker et al (1970) and others. The most likely example of a proto-S body, with crust and mantle intact,

is 4 Vesta, which has a basaltic surface. Indeed, it is the only remaining example, unless the C* asteroids are presumed to be differentiated. Several other asteroids (such as 349 Dembowska) might be partially fragmented proto-S bodies, if their present surface compositions could be reconciled with the presumed mantle compositions of differentiated parent-bodies. Since the outer regions of parent-body cores in most models (e.g. Mason, 1968; Wood, 1968) are of stony-iron composition (such as pallasites; cf. Buseck and Goldstein, 1969), we would expect most cores to be of stony-iron rather than purely metallic surface composition, as observed. The surfaces of these asteroids may also be appropriate environments for forming the highly brecciated mesosiderites (Wasson et al, 1974).

Collisional Evolution of the Asteroids

It is inaccurate to view the present collisional behavior of the asteroids as representative of the past. In particular, extrapolation backwards in time of the present collisional evolution of the belt requires that the belt was somewhat more populous in the past, and probably much more populous, with correspondingly higher collision rates (Chapman and Davis, 1975). Indeed, a vastly larger population of asteroids would collisionally grind itself down to dust at a rate such that the typical collisional-destruction half-life for the larger asteroids is always about equal to the total evolved duration (just as today the half-life for the larger asteroids is roughly the age of the solar system).

Chapman and Davis (1975) have calculated that the asteroid belt was populated with roughly $3 \times 10^{2 \pm 1}$ more asteroids of sub-100 km size than now at the time the differentiated proto-S asteroids solidified and began colliding with other belt asteroids. Their calculation assumes that S-objects are remnant cores

of Vesta-like prototypes and that Vesta is the only remaining prototype. The belt may have contained even more asteroids of smaller sizes or in earlier epochs. Thus the present asteroids may be viewed as a small remnant of a population of planetesimals that may have contained as much as a Martian mass. Since the S objects cannot have been collisionally depleted by more than a factor of 2 or 3 (otherwise they would not show their distinctive diameter-frequency relation), proto-S objects must have formed a tiny minority of the original population of predominantly carbonaceous asteroids. Present-day carbonaceous asteroids are the relatively recent collisional fragments of larger C objects that were lucky enough to avoid destruction during earlier epochs when the collision rates were much higher.

VI. OTHER EVIDENCE ON PARENT-BODY FRAGMENTATION

Other asteroid data bear on their collisional history.

-- Hirayama families are groups of asteroids with similar semi-major axes, proper eccentricities, and proper inclinations. They may be remnants of recent asteroidal collisions. We know the extents of families in a-e-i space, which suggest typical fragment velocities. We know the family size distributions and also physical parameters for some member asteroids.

-- Lightcurves measured as asteroids rotate indicate non-spherical shape, probably of fragmental origin. Amplitudes vary implying shapes ranging from spherical to highly elongated. Rotation periods, perhaps affected by collisions, also vary but average about 9 hours.

-- If differentiated objects are being broken apart, we might expect to see spectral albedos of one type of material on one side, and another on the opposite.

Hirayama Families

Williams (1975) has calculated new lists of Hirayama families from an improved theory. These supplant previous lists by Brouwer (1951) and Arnold (1969) and render obsolete previous reconstructions of the fragments such as attempted by Anders (1965) in his classic paper. From Williams' data we can eventually determine the size-frequency relation, the ratio of the largest object to the fragments, the typical fragment ejecta speeds, and we can compare the compositions and physical properties of family members.

McCord and Chapman (1975b) have shown that while some family pairs are of similar composition, many families show heterogeneity. The compositional sampling is still very incomplete, but ultimately the statistics can provide diagnostic information about asteroid interiors. The heterogeneity of families rules out a simple model of homogeneous precursors. This is because collisional theory shows that most catastrophic collisions occur between objects having a mass-ratio close to the limiting value that would just fragment the larger object, typically $<< 1\%$; therefore, usually all major fragments are from the larger body.

A straightforward interpretation of the heterogeniety was suggested by McCord and Chapman: the presursors were differentiated. If true, then a spectrophotometric survey of all fragments should reveal the compositional structure of the precursor. But there are indications of inconsistencies. Consider Williams' family 140. There is spectrophotometry of the three largest objects (15 Eunomia, 85 Io, and 141 Lumen) which comprise over 99% of the mass. 80% of the volume is contained in Eunomia, an irregularly-shaped

S-type object, indeed the largest S-object in the belt. 141 Lumen, however has about 5% of the volume and is perhaps the best-observed example of a C2-type object; moreover it has been observed for variations in composition on opposite sides and has been found to have none (McCord and Chapman, 1975b). 85 Io, with 15% of the volume, has a slightly peculiar spectrum but is probably also a C2-type. There is no way to construct a plausible parent-body from three objects having these surface compositions, if the compositional inferences of Section II are correct.

Let us assume all asteroids in this family are indeed fragments from a collision (and, for instance, Eunomia is not just a coincidental interloper having a similar orbit to those of true fragments). Then, in the context of the model discussed in the previous Section, there are two possible interpretations: (1) A catastrophic collision fragmented a large differentiated object, spalling off crustal and mantle rocks, leaving a partially intact core as Eunomia. A large subsequent impact flux has further fragmented most mantle material into sub-asteroidal sizes, leaving Lumen and Io as the largest ones. While some parent-body models (e.g. Wood, 1968) leave carbonaceous chondritic matter on the exterior of objects differentiated on the interior, most of the mantle volume is presumably not composed of carbonaceous material. We should at least expect to see non-carbonaceous materials on the opposite sides of Lumen and Io (which we do not, in the case of Lumen) if not whole additional fragments of plausible mantle composition. (2) Another scenario has Eunomia, in more or less its present state, colliding recently with an undifferentiated C-type asteroid. Depending on the subsequent impact flux that would further fragment the carbonaceous fragments, we may or may not have a nearly complete inventory of the fragments,

but in any case Lumen and Io are the largest remaining pieces. Due to its great strength, Eunomia survived the encounter largely intact although its irregular shape may have been caused by the collision and we may find some small fragments of Eunomia among the fainter members of the family.

For a single case, we can always resort to acceptable but atypical scenarios to explain the data. But as exemplified above, with more complete physical data on family members, we can determine if the suite of characteristics among members of a statistically significant sample of Hirayama families is consistent, or not, with models for asteroid compositional structure, given the theoretical collisional probabilities.

Asteroid Shapes

It has long been supposed that planetesimals accrete approximately spherically and that elongated shapes, indicated by large amplitude lightcurves imply fragmentation (cf. McAdoo and Burns, 1973). Given the traditional model of uniform asteroid composition and relatively infrequent collisions, one might expect Hirayama family members to be irregular fragments and at least the larger non-family asteroids to be roughly spherical original accretions. However, available data on lightcurve amplitudes (Hartmann et al., 1975), show no obvious correlation with family membership. The situation is more complex, however, if the model for C- and S-type objects presented in the previous Section is valid.

Substantial non-sphericity cannot be maintained against gravity in the relatively weak C-type objects larger than 100 km diameter (the framework of Johnson and McGetchin (1973) is applied using a crushing strength for

C-type material of several bars). Indeed, the largest lightcurve amplitude among the 12 measured C-objects (all > 100 km diameter) is 0.25 magnitude and the majority are less than 0.15 (see Fig. 8). Highly fragmented C-type objects smaller than 100 km should be quite irregular in shape, but lightcurves have not been measured for such objects.

Among the 28 S-type objects with measured lightcurves, a quarter have amplitudes of 0.3 magnitude or greater and less than a quarter have amplitudes less than 0.15. Assuming nickel-iron compositions, even the largest object could maintain a highly non-spherical shape (Johnson and McGetchin, 1973). Also, S-type objects have all seen at least one collision (otherwise they would be Vesta-type). But they are also expected to be relatively unfragmented and they may have formed as approximately spherical central cores. Hence, the observed non-sphericity of S-objects is consistent with, but not necessarily predicted by, the hypothesis that S-objects are stony-iron cores.

We might expect the fragments of mantle material from differentiated objects to be highly irregular. Indeed 44 Nysa, which has very unusual polarimetric properties, may be just such a fragment: it has one of the largest known lightcurve amplitudes among the brighter asteroids. 349 Dembowska, the large main belt asteroid of probable LL6 composition, also has a very large amplitude. It is the largest member of a Hirayama family and is evidently sufficiently strong to retain its fragmental shape, unlike C-type objects. It may be a Wood-type object only partially fragmented. A priority objective is to measure spectrophotometric parameters for other asteroids in the families of Nysa and Dembowska.

Asteroid Rotation Periods

Many authors have supposed that the rotation periods of asteroids might contain information relevant to asteroid collision history (cf. McAdoo and Burns, 1973). Most asteroids have rotation periods within a factor of two of 9 hours, although a few have very long periods or short periods approaching the limit of instability. If the 9^h period arose naturally from the processes by which the asteroids originally accreted, then those asteroids that have suffered collisions might exhibit different periods. To this end, McAdoo and Burns studied all measured asteroid rotation periods and found marginal evidence that asteroids smaller than 10 km in diameter depart significantly from the constant-period "law".

It is not surprising that large asteroids show little evidence of collisional modification of their rotation periods inasmuch as individual collisions that could change their rotation periods significantly are more than sufficient to shatter them to pieces. But small, multi-generation fragments of large asteroids may be "spun-up" sufficiently by the catastrophic collisions that created them. Also rocky asteroids less than a few km in diameter and iron objects up to 100 km in diameter have sufficient strength to withstand impulses large enough to alter their rotation periods. Indeed, among the larger asteroids, there is some evidence for larger scatter in periods for S objects compared with C objects (Burns, 1975).

Further analysis of asteroid rotation periods may permit independent determination of internal asteroid strengths and collision frequencies. But it remains to be demonstrated that the constant-period law is not itself the end-product of long collisional evolution, in which case there is no evidence concerning collisions retained in the rotation period data.

Compositional Variation Within Individual Asteroids

Given the compositional heterogeneity of Hirayama families and evidence that meteorites sample different layers of geochemically differentiated objects, one might expect individual asteroid fragments to have inhomogeneous surface composition. As such an asteroid rotates, the side that was near the surface of the precursor might be of carbonaceous composition and the other side, nearer the center of the precursor, might be differentiated pyroxene-rich material.

But few asteroids show such evidence for such inhomogeniety. Asteroid lightcurves are dominated by shape variations (Dunlap, 1971; Lacis and Fix, 1971) although residual odd-order terms in the Fourier analysis suggest modest albedo differences on some objects. "Jitter" in asteroid polarization has been noticed, implying either albedo or texture differences, but it is small for all asteroids observed to date (Zellner, 1974, personal communication). Color variability has been reported for a few asteroids (Gehrels, 1967; Chapman et al, 1973a) but such variations have been very small. (19 Fortuna possibly showed grossly different spectra on opposite sides [McCord and Chapman, 1975a], but initial polarimetry of Fortuna [Zellner, 1974, personal communication] shows no major variation with rotational phase.) The reconnaissance observing programs are not designed for efficient detection of rotational variations, but a recent search for spectral variations (McCord and Chapman, 1975b) revealed no examples.

The model of the previous Section, nevertheless, may be consistent with a lack of inhomogeneous asteroids. Even the homogeneous glass targets used by Gault and Wedekind (1969) showed a tendency to spall off their exteriors leaving slightly ellipsoidal "cores". Certainly a layered planetesimal would

tend to spall off layers of differing density so that cross-sections through several layers would be unusual. The spherical zone separating a rocky mantle and a stony-iron core would be an especially likely zone for spallation due to the great discontinuity in material tensile strengths.

Moreover, just the observed dominance of C- and S-type objects and rarity of other types suggests that inhomogeneous bodies would be rare. The C-type objects, after all, are interpreted as fragments of undifferentiated precursors. Chapman and Davis (1975) interpret the preponderance of S-type objects and rarity of Vesta-types as resulting from a large collisional flux which has fragmented and substantially removed most rocky material, leaving very few stony-iron cores with adhering pieces of mantle. The best candidate asteroids for having compositional differences are those few objects not falling into the C and S groupings, such as 349 Dembowska and 44 Nysa. Perhaps S objects showing a relatively high silicate/metal ratio are less thoroughly stripped of their mantles. But near-surface compositional differences may be obscured on some asteroids by regolith formation processes (see next Section).

VII. ASTEROID REGOLITHS AND BRECCIATED METEORITES

Recently there has been much discussion of parent-body regoliths as locations where gas-rich and brecciated meteorites might have formed (e.g. Popeau et al, 1975; Macdougall et al, 1974; Anders, 1975; Pellas, 1972; Rajan, 1974; Wilkening, 1973; and Prinz et al, 1974). These ideas are spurred by the increasing awareness of the number of complex meteorite assemblages (breccias) and their apparent similarities to lunar samples. Yet analysis of regolith-forming processes on asteroids reveals major difficulties

with any hypothesis that envisages many meteorites having been "put together" relatively recently on asteroid surfaces. Below I present a qualitative discussion of asteroid regoliths, based partly on an earlier quantitative theory (Chapman, 1971) as modified by new data on the meteoroid population in the belt (Soberman, et al, 1974), new crater ejecta experiment results (Gault et al, 1975), and criticisms by Anders (personal communication, 1975). I will conclude that most brecciated meteorites must have been formed during early epochs in solar system history when the asteroids were still accreting.

The major trait of asteroids that distinguishes their regolith-forming processes from those of the moon is their low surface gravity. Laboratory impact experiments have been done in the velocity regime relevant for asteroids (5 km sec^{-1}) in both basalt-like targets (Gault et al, 1963) and in unconsolidated sand (cf. Gault et al, 1975). More than half the ejecta created in a single cratering event escapes entirely from rocky asteroids smaller than about 150 km diameter, or from sandy asteroids smaller than 10 km diameter. The critical question is: How deep a layer of regolith can be accumulated on an asteroid surface from the ejecta that fails to escape? Since it can be shown readily that most meteorites must be derived from the largest collisions involving the larger asteroids in the source region, the typical meteorite must sample a depth which is a significant fraction of the parent-body radius -- certainly kilometers deep. Thus if a significant fraction of meteorites are viewed as originating in asteroidal regoliths, such regoliths must be equally deep.

The chief characteristic of the regolith development process, often not appreciated by non-specialists, is that it is self-buffering. For instance,

if a regolith 1 meter deep forms after 1 b.y. of cratering, it does not follow that after 2 b.y., the depth is 2 meters. Rather, the regolith depth is only slightly deeper than 1 meter, since nearly all subsequent impacts serve to redistribute the regolith already present. A good generalization, borne out by direct study of the moon, is that the regolith depth cannot be much greater than the depth of the largest craters that saturate the surface.

This fact alone sets a fundamental limitation on the maximum possible depth of regolith on an intact asteroid. As discussed by Hartmann (1975), the shape of the size-frequency distribution of interplanetary debris is such that if the cumulative cratering flux on the surface of an asteroid were to approach approximately 30 times the post-mare lunar crater accumulation, at which time the regolith depth probably would be only several times the lunar maria regolith depth, then the asteroid would start becoming saturated with large impact craters of all sizes, including impact events sufficient to catastrophically fragment the asteroid!* Thus long before any asteroid has accumulated a regolith approaching 100 meters depth, it will have been shattered. A few asteroids, like Ceres, may exist because they have luckily escaped catastrophic fragmentation; they will have accumulated somewhat deeper regoliths than other asteroids, but still only "skin deep". Anders'(1975) conclusion that moderate-sized asteroids can have regoliths comprising 10% to 20% of the mass of the bodies is, therefore, incorrect.

---

* This argument would be inapplicable to earlier epochs if the population index of asteroids were much steeper than today, as Chapman and Davis (1975) have suggested. But in that case regoliths would be subject to scouring as described below.

The low surface gravities on asteroids further mitigate against retention of regoliths, especially on small asteroids. The population index of interplanetary debris in the size range of millimeters to meters is quite large, so "sand-blasting" by such impacting particles can effectively scour away regolith deposited by earlier generations of larger impacts. The low ejecta velocities indicated by the new cratering experiments in sand imply that large asteroids are largely protected from such scouring. But asteroids smaller than 10 km in diameter** may be expected to retain negligibly thin regoliths; cratering impacts may be expected to erode such small asteroids to considerable depths prior to catastrophic fragmentation.

In general, regoliths on all but the larger asteroids may be expected to be relatively thin and short-lived with less re-working than is characteristic of lunar maria regoliths. They are composed of reasonably fresh asteroidal material. Because of the lack of reworking of asteroidal regoliths and the lower impact velocities in the belt, there should be less impact melting, vitrification, and shock on asteroid surfaces compared with the moon.

If most gas-rich, brecciated meteorites were not formed on asteroid surfaces since the mean impact velocities have been ~ 5 km/sec, then they must have formed during earlier epochs while the asteroids were still accreting. This appears to be the only way to account for regolith-like

---

** This diameter estimate is reduced about a factor of ten from my earlier estimates (Chapman, 1971) due to consideration of the new experiments reported by Gault et al (1975).

properties at the great depths in asteroids sampled by the meteorites that fall today. Others have argued on other grounds that brecciation and solar gas implantation in meteorites must have occurred early in solar system history (Pellas, 1972, suggests 4.0 - 4.3 b.y. ago); such a scenario appears to be the only one compatible with known regolith production processes. Of course, a small fraction of meteorites may have originated from, or have been highly modified in, near-surface regions of modern asteroids; it seems likely that meteorites such as Kapoeta (Papanastassiou, et al, 1974) Kodaikanal (Burnett and Wasserburg, 1967), Lafayette (Podosek and Huneke, 1973), Nakhla (Papanastassiou and Wasserburg, 1974), and St. Mesmin (Schultz and Signer, 1974) may be just such exceptions.

VIII. A SCENARIO

The following scenario for the origin and evolution of the asteroids and the meteorites seems adequate to explain the astronomical data described in earlier Sections. The scenario is not a unique one and doubtless will require modifications to account adequately for meteoritical evidence. But it can serve as a useful paradigm against which to compare additional data. The scenario is underpinned by the interpretation of S and C type asteroids as stony-iron cores and undifferentiated carbonaceous objects, respectively.

Initially, the solar nebula had no density minimum in the asteroidal zone. Planetesimals accreted from the condensates in the central plane, perhaps in the two-stage sequence of gravitational collapses proposed by Goldreich and Ward (1973). Probably full-asteroid-sized planetesimals did not form directly from gravitational instabilities, but accreted from smaller bodies in the more traditional manner from mutual interactions at low relative velocities.

Jupiter became a proto-planet before a sizeable proto-planet had formed in the asteroid zone; possibly it grew first due to sheer chance, due to increased densities of condensates-containing frozen volatiles, or due to other early evolutionary nebular processes: see Safronov (1972). The asteroidal condensates were generally of carbonaceous chondritic composition, although perhaps more like ordinary chondrites near the inner edge of the present belt (Lewis, 1974).

Jupiter's early presence had a major effect on planetary growth in the asteroid zone (and also in the zone of Mars: Weidenschilling, 1975). First, perturbations by Jupiter, especially of planetesimals near the chief Jovian resonances, increased relative velocities, slowing accretion. Secondly, and probably more significantly, planetesimals still closer to Jupiter were perturbed into highly elliptical orbits (Kaula and Bigileisen, 1975). While passing through the asteroid belt, they fragmented the growing asteroids and further enhanced the relative velocities among them. This episode of bombardment probably peaked very early in solar system history. For instance, Lecar and Franklin (1973) showed that the time-scale for the removal of objects between the 3:2 resonance (4 A.U.) and the 4:3 resonance (4.3 A.U.) is only a few thousand years once Jupiter attains its present mass. Asteroids between the 2:1 (3.3 A.U.) and 3:2 resonances were probably similarly depleted but on much longer timescales. By the conclusion of this early bombardment period, the relative velocities of asteroids were approaching

the present value of 5 km/sec* and virtually all asteroidal interactions resulted in fragmentation or net mass loss, rather than accretion.

The process of accretion involved an interplay between aggregation and disintegration of the asteroids. Their growing exteriors were subject to considerable brecciation as well as massive irradiation by the T Tauri solar wind. Many of the gas-rich and brecciated meteorites were created within their parent-bodies during this epoch.

Within the first 10^7 to 10^8 years, some of the larger asteroids were heated to the point of melting and differentiation, others were metamorphosed, while most were thermally unaffected. The cause of melting of such modest sized bodies is a major puzzle. No one has proposed a satisfactory scheme for concentrating potassium, thorium, and uranium in some (but not all) parent-bodies sufficient to melt them. It is now doubted that early heating was accomplished by short-lived radioisotopes (Schramm et al, 1970). Electrical heating during the T Tauri phase of solar evolution (Sonett, 1971; Sonett, 1974) remains a viable possibility, although it is not yet clear why it should prove so efficacious for Vesta and proto-S asteroids, yet leave the majority unaffected. In this regard it is well to realize that the conductivities of meteoritic materials are highly temperature-dependent (see Briggs and Brecher, 1975) so it is possible that minor differences in initial compositions and/or temperatures of different bodies might lead to radically

---

* The conversion of circular co-planar orbits to present asteroid orbits is still not fully understood. Especially puzzling is the high inclination of Pallas (Whipple et al, 1972).

different thermal evolution. The bombardment of asteroids by Jupiter-scattered planetesimals might itself have generated sufficient heat to melt some of the bodies.

Within 2×10^8 years after the origin of the solar system, the processes of differentiation and cooling of somewhat over 100 parent-bodies, chiefly of diameters 200 to 500 km, were complete. (Smaller asteroids subject to similar heating processes radiated the heat too fast to reach melting temperatures.) These objects probably resembled Mason's (1968) model for the parent-bodies of the basaltic achondrites, calcium-poor achondrites, and the pallastic and metallic irons. Vesta is probably the only remaining example of such objects (Fig. 9). It is possible that some of the bodies differentiated only internally and resembled Wood's (1965) meteorite parent-body model, with carbonaceous and ordinary chondrites in the exterior portions of the body. I cannot observationally exclude the possibility that some of the present C* asteroids are examples of such bodies, nor that they have opaque-rich basaltic surfaces, but I prefer to regard Vesta as the sole remaining example of an intact differentiated body.

For each such body there were perhaps 100 undifferentiated carbonaceous asteroids of similar size. At smaller sizes (tens to one-hundred km diameter) there were the order of 300 times as many asteroids as presently exist, all undifferentiated. By this epoch, the asteroids constituted perhaps a lunar mass to several Martian masses, down considerably from the several terrestrial masses or more that may have originally condensed in the zone. Still the volume density was sufficiently high and collisions sufficiently frequent that within a few times 10^8 years the asteroid population was down to within a factor of only ten times the present population (Chapman and Davis, 1975).

Insofar as the rest of the solar system is concerned, the asteroids may have been the most slowly-decaying, and hence longest lived, population of planetesimals to crater the planets. They were, and still are, analogous to the Jupiter-scattered bodies of early epochs, except that Jupiter cannot directly perturb their orbits. Rather, asteroidal collisions cause a gradual random-walk of fragments toward resonances in the belt where they may then be rapidly perturbed into Earth-crossing orbits (see Section III). One major collision about 4.0 b.y. ago involving an asteroid near such a resonance or in a Mars-crossing orbit may have provided the bodies that are hypothesized (Wetherill, 1974b; Wetherill, 1975; Tera et al, 1974; Murray et al, 1975) to have cratered the moon, Mars, and Mercury during a cataclysmic bombardment episode (Chapman and Davis, 1975).

The weak carbonaceous asteroids were rapidly fragmented by inter-asteroidal collisions and the rocky crusts and mantles of differentiated bodies were fragmented away. But the strong stony-iron and iron cores of the differentiated bodies proved highly resistant to catastrophic fragmentation, and roughly half of them have survived to the present. The fragments of those that have been fragmented also remain relatively impervious to destruction, as testified by the long cosmic-ray exposure ages of iron meteorites (an appreciable fraction of the age of the solar system).

Collisional fragmentation proceeded more rapidly in the vicinity of the Kirkwood gaps where Jupiter commensurabilities augmented somewhat the average collision velocities and frequencies. Today the carbonaceous asteroids within 0.05 A.U. of the commensurabilities are depleted, relative to elsewhere in the belt, by at least an order of magnitude. The S-type cores, on the otherhand,

are only slightly depleted in the gaps because of their much reduced susceptibility to fragmentation (Fig. 10 and Table 2). As Chapman and Davis (1975) have argued, the collisional evolution of the two groups of bodies of different strength provides a ready explanation for why the Kirkwood gaps exist and for the observed variation in the C/S ratio as a function of distance from commensurabilities first noted by Chapman et al (1973a).

The scenario I have described is weak in explaining some questions of great interest to meteoriticists. The meteorite types that are rare or not yet observed in the belt include some of the most important: the ordinary chondrites, the enstatite chondrites, and some achondrites. The metallic-colored E-type asteroids predominate in the outer parts of the asteroid belt, which seems at variance with equilibrium condensation models that would place enstatite chondrites interior to the ordinary chondrites, and certainly closer to the sun than the carbonaceous chondrites (e.g. Anders, 1971). Perhaps the idea should be revived (e.g. Ringwood, 1966) that these meteorites were reduced by carbon within a heated C-type body in the outer part of the belt. Alternatively, the E-type bodies may actually be pure nickel-iron cores. The existence of E-type bodies near Kirkwood gaps suggests that they have great strength, suggestive of iron. But enstatite chondrites also are the strongest of the stony meteorites and have relatively long cosmic-ray exposure ages. At least one main belt asteroid (44 Nysa) has been proposed to be of enstatite achondritic composition (Zellner, 1975); these meteorites are often viewed as bearing a genetic relationship to the enstatite chondrites. It is unfortunate that the mineral enstatite lacks a thoroughly diagnostic spectrum, so the relevance of "E-type" asteroids to enstatite meteorites probably cannot be resolved unequivocally from Earth-based studies. But

the only likely alternative -- that they are of nickel-iron composition -- can be tested by radar observations, and a prime example (16 Psyche) is scheduled to be observed by the Goldstone radar later this year (Jurgens, 1975 personal communication).

Ordinary chondrites are quite rare among the asteroids, although preliminary evidence suggests that they may be moderately common at the inner edge of the belt and among Mars-crossing asteroids. Quite surprising, however, is the presence of one large asteroid (349 Dembowska) of probable LL6 composition in the outer part of the belt. It seems difficult to imagine this body being dynamically transported to its present orbit from regions closer to the sun. Possibly LL6 chondrites should also be viewed as originating in the mantle of a highly metamorphosed or differentiated carbonaceous body, somewhat akin to the models of Wood. Then the irregular-shaped Dembowska could be viewed as a parent-body fragmented to a state intermediate between Vesta and the S-type cores.

This tentative, imperfect picture of the relationship between asteroids and meteorites will become clarified as more asteroids are observed and representatives of additional meteorite types (such as H chondrites) are found among the minority of non-S, non-C objects. In the meantime, I encourage meteoriticists to think about how their data may support or refute parts of this scenario.

ACKNOWLEDGEMENTS

I am grateful for discussions on several of these topics with L. Wilkening, E. Anders, and other colleagues. The work was funded in part by NASA Contracts 2522 and 2718.

REFERENCES

Adams, J.B. (1974) Uniqueness of visible and near-infrared diffuse reflectance spectra of pyroxenes and other rock-forming minerals. In Infrared and Raman Spectroscopy of Lunar and Terrestrial Minerals (ed. C. Karr, Jr.), in press. Academic Press.

Adams, J.B., and McCord, T.B. (1972) Electronic spectra of pyroxenes and interpretation of telescopic spectral reflectivity curves of the moon. Geochim. Cosmochim. Acta 36, Suppl. 3, 3021-3035.

Alfvén, H. and Arrhenius, G. (1973) Structure and evolutionary history of the solar system, Part III. Astrophys. Spa. Sci. 21, 117-176.

Allen, D.A. (1970) Infrared diameter of Vesta. Nature 227, 158-159.

Allen, D.A. (1971) The method of determining infrared diameters. In Physical Studies of Minor Planets (ed. T. Gehrels), NASA SP-267, pp. 41-44.

Anders, E. (1964) Origin, age and composition of meteorites. Space Sci. Rev. 3, 583-718.

Anders, E. (1965) Fragmentation history of asteroids. Icarus 4, 399-408.

Anders, E. (1971a) Interrelations of meteorites, asteroids, and comets. In Physical Studies of Minor Planets (ed. T. Gehrels), NASA SP-267, pp. 429-446.

Anders, E. (1971b) Meteorites and the early solar system. Ann. Rev. Astron. Astrophys. 9, 1 - 34.

Anders, E. (1975) Do stony meteorites come from comets? Icarus 24, 363-371.

Arnold, J. R. (1965) The origin of meteorites as small bodies III. General considerations. Astrophys. J. 141, 1548-1556.

Arnold, J. R. (1969) Asteroid families and "jet streams". Astron. J. 74, 1325-1242.

Bowell, E. and Zellner, B. (1974) Polarizations of asteroids and satellites. In Planets, Stars, and Nebulae Studied with Photopolarimetry (ed. T. Gehrels), pp. 381-404. Univ. of Ariz. Press.

Briggs, P. L. and Brecher, A. (1975) Low temperature electrical properties of carbonaceous chondrites. Eos 56, 391 (abstract).

Brouwer, D. (1951) Secular variations of the orbital elements of minor planets. Astron. J. 56, 9-32.

Burnett, D.S. and Wasserburg, G. J. (1967) Evidence for the formation of an iron meteorite at 3.8×10^9 years. Earth Planet. Sci. Lett. 2, 137-147.

Burns, J. A. (1975) The angular momenta of solar system bodies: implications for asteroid strengths. Icarus, in press.

Buseck, P. R. and Goldstein, J. I. (1969) Olivine compositions and cooling rates of pallasitic meteorites. Bull. Geol. Soc. Am. 80, 2141-2158.

Cameron, A.G.W. (1972) Models of the primitive solar nebula. In L'Origine du Systeme Solaire (ed. H. Reeves), pp. 56-70. Centre National de la Recherche Scientifique, Paris.

Chapman, C. R. (1971) Surface properties of asteroids. Doctoral dissertation, Mass. Inst. Technology.

Chapman, C. R. (1973) Mineralogy of the asteroid belt and relationships to meteorites. Bull. Am. Astron. Soc. 5, 388 (abstract).

Chapman, C.R. (1974) Asteroid size distribution: implications for the origin of stony-iron and iron meteorites. Geophys. Res. Lett. 1, 341-344.

Chapman, C.R. and Davis, D. R. (1974) Asteroid collisional evolution: evidence for a much larger early population. Submitted to Science.

Chapman, C.R., Davis, D.R., and Hartmann, W.K. (1975) In preparation.

Chapman, C.R., Johnson, T.V., and McCord, T.B. (1971) A Review of spectrophotometric studies of asteroids. In Physical Studies of Minor Planets (ed. T. Gehrels), NASA SP-267, pp. 51-65.

Chapman, C.R., McCord, T.B., and Johnson, T.V. (1973a) Asteroid spectral reflectivities. Astron. J. 78, 126-140.

Chapman, C.R., McCord, T.B., and Pieters, C. (1973b) Minor planets and related objects. X. Spectrophotometric study of the composition of (1685) Toro. Astron. J. 78, 502-505.

Chapman, C.R., Morrison, D., and Zellner, B. (1975) Surface properties of asteroids: a synthesis of polarimetry, radiometry, and spectrophotometry. Icarus 25, 000 - 000.

Chapman, C.R. and Salisbury, J.W. (1973) Comparison of meteorite and asteroid spectral reflectivities. Icarus 19, 507-522.

Cruikshank, D.P. and Morrison, D. (1973) Radii and albedos of asteroids 1, 2, 3, 4, 6, 15, 51, 433, and 511. Icarus 20, 477-481.

Dohnanyi, J.S. (1969) Collisional model of asteroids and their debris. J. Geophys. Res. 74, 2531-2554.

Dohnanyi, J.S. (1971) Fragmentation and distribution of asteroids. In Physical Studies of Minor Planets (ed. T. Gehrels), NASA SP-267, 263-295.

Dohnanyi, J.S. (1972) Interplanetary objects in review: statistics of their masses and dynamics. Icarus 17, 1-48.

Dollfus, A. (1971) Diameter measurements of asteroids. In Physical Studies of Minor Planets (ed. T. Gehrels), NASA SP-267, 25-31.

Dunlap, J. L. (1971) Laboratory work on the shapes of asteroids. In Physical Studies of Minor Planets (ed. T. Gehrels), NASA SP-267, 147-154.

Egan, W.G., Veverka, J., Noland, M. and Hilgeman, T. (1973) Photometric and polarimetric properties of the Bruderheim chondritic meteorite. Icarus 19, 358-371.

Fricker, P.E., Goldstein, J.I., and Summers, A.L. (1970) Cooling rates and thermal histories of iron and stony-iron meteorites. Geochim. Cosmochim. Acta 34, 475-491.

Gaffey, M.J. (1973) A systematic study of the spectral reflectivity characteristics of the meteorite classes with applications to the interpretation of asteroid spectra for mineralogical and petrological information. Doctoral dissertation, Mass. Inst. of Technology.

Gaffey, M.J. and McCord, T.B. (1975) Spectral reflectance characteristics of the meteorite classes. In preparation.

Gault, D.E., Hörz, F., Brownless, D.E., and Hartung, J.B. (1975) Mixing of the lunar regolith. Proc. Fifth Lunar Sci. Conf. (Supp. 5, Geochim. Cosmochim. Acta) 3, 2365-2386.

Gault, D.E., Shoemaker, E.M., and Moore, H.J. (1963) Spray ejected from the lunar surface by meteoroid impact. NASA TN D-1767.

Gault, D.E. and Wedekind, J.A. (1969) The destruction of tektites by micrometeoroid impact. J. Geophys. Res. 74, 6780-6794.

Gehrels, T. (1967). Minor planets. I. The rotation of Vesta. Astron. J. 72, 929-938.

Goldreich, P. and Ward, W.R. (1973). The formation of planetesimals. Astrophys. J. 183, 1051-1061.

Hansen, O. L. (1975) Radii and albedos of 84 asteroids from simultaneous visual and infrared photometry. Submitted to Astron. J.

Hartmann, W.K. (1968) Growth of asteroids and planetesimals by accretion. Astrophys. J. 152, 337-342.

Hartmann, W. K. (1969) Terrestrial, lunar and interplanetary rock fragmentation. Icarus 10, 201-213.

Hartmann, W.K. (1975) Lunar "cataclysm": a misconception? Icarus 24, 181-187.

Hartmann, W. K., Chapman, C.R., and Williams, J.G. (1975) In preparation for Rev. Geophys.

Hartmann, W. K. and Davis, D. R. (1975) Satellite-sized planetesimals and lunar origin. Icarus 24, 504-515.

Hartmann, W.K. and Hartmann, A.C. (1968) Asteroid collisions and evolution of asteroidal mass distribution and meteoritic flux. Icarus 8, 361-381.

Hellyer, B. (1970) The fragmentation of the asteroids. Mon. Not. R. Astron. Soc. 148, 383-390.

Johnson, T.V. and Fanale, F. P. (1973) Optical properties of carbonaceous chondrites and their relationship to asteroids. J. Geophys. Res. 78, 8507-8518.

Johnson, T.V. and McGetchin, T.R. (1973) Topography on satellite surfaces and the shape of asteroids. Icarus 18, 612-620.

Jurgens, R. and Goldstein, R. (1975) In preparation.

Kaula, W.M. and Bigeleisen, P.E. (1975) Early scattering by Jupiter and its collision effects in the terrestrial zone. Icarus, in press.

Kuiper, G. P., Fugita, Y., Gehrels, T., Groeneveld, I., Kent, J., Van Biesbroeck, G., and Houten, C.J. van (1958) Survey of asteroids. Astrophys. J. Suppl. Ser. 3, 289-428.

Lacis, A.A., and Fix, J.D. (1971) Lightcurve inversion and surface reflectivity. In Physical Studies of Minor Planets (ed. T. Gehrels) NASA SP-267, 141-146.

Larson, H. P. and Fink, U. (1975) Infrared spectral observations of asteroid (4) Vesta. Bull. Am. Astron. Soc., in press (abstract).

Larson, H.P., Fink, U., Treffers, R.T., and Gautier, T.N. (1975) The infrared spectrum of asteroid 433 Eros. In preparation.

Lecar, M. and Franklin, F.A. (1973) On the original distribution of the asteroids. I. Icarus 20, 422-436.

Lewis, J.S. (1972) Metal/silicate fractionation in the solar system. Earth Planet. Sci. Lett. 15, 286-290.

Lewis, J.S. (1974) The temperature gradient in the solar nebula. Science 186, 440-443.

Macdougall, D., Rajan, R.S., and Price, P.B. (1974) Gas-rich meteorites: possible evidence for origin on a regolith. Science 183, 73-74.

Marcus, A. (1965) Positive stable laws and the mass distribution of planetesimals. Icarus 4, 267-272.

Mason, B. (1968) Composition of stony meteorites. In Exterrestrial Matter (ed. C. A. Randall, Jr.) pp. 3-22. Northern Ill. Univ. Press.

Matson, D. L. (1972) Infrared emission from asteroids at wavelengths of 8.5, 10.5, and 11.6 μm. Doctoral dissertation, Calif. Inst. Technology.

McAdoo, D.C. and Burns, J.A. (1973) Further evidence for collisions among asteroids. Icarus 18, 285-293.

McCord, T.B., Adams, J.B. and Johnson, T.V. (1970). Asteroid Vesta: spectral reflectivity and compositional implications. Science 168, 1445-1447.

McCord, T.B. and Chapman, C.R. (1975a) Asteroids: spectral reflectance and color characteristics. Astrophys. J. 195, 553-562.

McCord, T.B. and Chapman, C.R. (1975b) Asteroids: spectral reflectance and color characteristics II. Astrophys. J. 197, 781-790.

McCord, T.B. and Gaffey, M.J. (1974) Asteroids: surface compositions from reflection spectroscopy. Science 186, 352-355.

Morrison, D. (1974) Radiometric diameters and albedos of 40 asteroids. Astrophys. J. 194, 203-212.

Morrison, D. and Chapman, C.R. (1975) Radiometric diameters for an additional 22 asteroids. Submitted to Astrophys. J.

Murray, B.C., Strom, R.G., Trask, N.J. and Gault, D.E. (1975) Surface history of Mercury: implications for terrestrial planets. J. Geophys. Res.; in press.

Nash, D.B. and Conel, J.E. (1974) Spectral reflectance systematics for mixtures of powdered hypersthene, labradorite, and ilmenite. J. Geophys. Res. 79, 1615-1621.

Olbers, W. (1805) Entdeckung eines beweglichen Sterns, den man gleichfalls für einem zwischen Mars und Jupiter sich aufhaltenden planetarischen Körper halten kann, Berliner Astr. Jahrbuch, p. 108.

Öpik, E.J. (1965) The cometary origin of meteorites. Advances in Astron. Astrophys. 4, 301-336.

Papanastassiou, D.A., Ragan, R.S., Huneke, J.C. and Wasserburg, C.J. (1974) Rb-Sr ages and lunar analogs in a basaltic achondrite; implications for early solar system chronologies. In Lunar Science V, 583-585. The Lunar Science Inst.

Papanastassiou, D.A. and Wasserburg, G. J. (1974) Evidence for late formation and young metamorphism in the achondrite Nakhla. Geophys. Res. Lett. 1, 23-26.

Pellas, P. (1972) Irradiation history of grain aggregates in ordinary chondrites. Possible clues to the advanced stages of accretion. In From Plasma to Planet (ed. A. Elvius), pp. 65-92. John Wiley and Sons.

Pieters, C., Gaffey, M. J., McCord, T.B., and Chapman, C.R. (1975) In preparation.

Piotrowski, S. (1953) The collisions of asteroids. Acta Astron. Ser. A 5, 115-138.

Podosek, F.A. and Huneke, J.C. (1973) Argon 40-argon 39 chronology of four calcium-rich achondrites. Geochim.Cosmochim.Acta 37, 667-684.

Pollack, J.B., Veverka, J., Noland, M., Sagan, C., Duxbury, T.C., Acton, C.H Jr., Born, G.H., Hartmann, W.K., and Smith, B.A. (1973) Mariner 9 television observations of Phobos and Deimos, 2. J. Geophys. Res. 78, 4313-4326.

Popeau, G., Kirsten, T., Steinbrunn, F., and Storzer, D.(1974) The records of solar wind and solar flares in aubrites. Earth Planet Sci. Lett. 24, 229-241.

Prinz, M., Fodor, R.V., and Keil, K. (1974) Comparison of lunar rocks and meteorites: implications to histories of the moon and parent meteorite bodies. In Proc. Sov.-Am. Conf. Cosmochem. Moon and Planets., inpress.

Rajan, R.S. (1974) On the irradiation history and origin of gas-rich meteorites. Geochim. Cosmochim.Acta 38, 777-788.

Ringwood, A.E. (1966) Genesis of chondritic meteorites. Rev. Geophys. 4, 113-175.

Ross, H.P., Adler, J.E. M., and Hunt, G.R. (1969) A statistical analysis of the reflectance of igneous rocks from 0.2 to 2.65 microns. Icarus 11, 46.-54.

Safronov, V.S. (1972) Evolution of the Protoplanetary Cloud and Formation of the Earth and the Planets. Israel Program for Scientific Translations, Jerusalem.

Salisbury, J. W. and Hunt, G. R. (1974) Meteorite spectra and weathering. J. Geophys. Res. 79, 4439-4441.

Salisbury, J.W. and Hunt, G.R. (1975) Visible and near infrared spectra of minerals and rocks. Meteorites. Mod. Geol., in press.

Schramm, D.N., Tera, F., and Wasserburg, G.J. (1970) The isotopic abundance of ^{26}Mg and limits on ^{26}Al in the early solar system. Earth Planet Sci. Lett. 10, 44-59.

Schultz, L. and Signer, P. (1974) Rare gases in the St. Mesmin chondrite. Meteoritics 9, 402-403.

Soberman, R.K., Neste, S.L., and Lichtenfeld, K. (1974) Optical measurement of interplanetary particulates from Pioneer 10. J. Geophys. Res. 79, 3685-3694.

Sonett, C.P. (1971) The relationship of meteoritic parent body thermal histories and electromagnetic heating by a pre-main sequence T Tauri sun. in Physical Studies of Minor Planets (ed. T. Gehrels), NASA SP-267, pp. 239-245.

Sonett, C.P. (1974) Evidence of a primordial solar wind. Presented at 3rd Solar Wind Conf., Asilomar, California, March 25-29.

Tera, F., Papanastassiou, D.A., and Wasserburg, G.J. (1974) Isotopic evidence for a terminal lunar cataclysm. Earth Planet Sci. Lett. 22, 1-21.

Van Houten, C.J. (1971) Discussion in Physical Studies of Minor Planets (ed. T. Gehrels) NASA SP-267, pp. 292-295.

Van Houten, C.J., Van Houten-Groeneveld, I., Herget, P. and Gehrels, T. (1970) The Palomar-Leiden survey of faint minor planets. Astr. Astrophys. Suppl. 2, 339-448.

Van Schmus, W. R. and Wood, J.A. (1967) A chemical-petrologic classification for the chondritic meteorites. Geochim. Cosmochim.Acta 31, 747-765.

Veeder, G.L., Johnson, T.V. and Matson, D.L. (1975) Narrowband spectrophotometry of Vesta. Bull Am. Astron. Soc., in press.

Veverka, J. and Noland, M. (1973) Asteroid reflectivities from polarization curves: calibration of the "slope-albedo" relationship. Icarus 19, 230-239.

Wasson, J.T. (1972) Formation of ordinary chondrites. Rev. Geophys. Space Phys. 10, 711-759.

Wasson, J.T., Schaudy, R., Bild, R.W. and Chou C.L.(1974) Mesosiderties== I. Compositions of their metallic portions and possible relationship to other metal-rich meteorite groups. Geochim. Cosmochim.Acta 38, 135-149.

Weidenschilling, S.J. (1975) Mass loss from the region of Mars and the asteroid belt. Icarus, in press.

Wetherill, G.W. (1967) Collisions in the asteroid belt. J. Geophys. Res. 72, 2429-2444.

Wetherill, G.W. (1969) Relationships between orbits and sources of chondritic meteorites. In Meteorite Research (ed. P. M. Millman), pp. 573-589. Springer-Verlag.

Wetherill, G.W. (1974a). Solar system sources of meteorites and large meteoroids. Ann. Rev. Earth Planet. Sci., 2, 303-331.

Wetherill, G.W. (1974b). Pre-mare cratering and early solar system history. Proc. Sov.-Am. Conf. Cosmochem. Moon and Planets (Lunar Science Inst.: Houston) in press.

Wetherill, G.W. (1975). Late heavy bombardment of the moon and terrestrial planets. Presented at 6th Lunar Science Conf., Houston, March 1975 (extended abstract in: Lunar Science VI, 866-868).

Whipple, F.L., Lecar, M., and Franklin, F.A. (1972) The strange case of Pallas. In L'Origine du Systeme Solaire (ed. H. Reeves) pp. 312-319. Centre National de la Recherche Scientifique, Paris.

Wilkening, L.L. (1973) Foreign inclusions in stony meteorites -- I. Carbonaceous chondritic xenoliths in the Kapoeta howardite. Geochim. Cosmochim. Acta 37, 1985-1989.

Williams, J.G. (1971) Proper elements, families, and belt boundaries. In Physical Studies of Minor Planets (ed. T. Gehrels), NASA SP-267, 177-181.

Williams, J.G. (1973) Meteorites from the asteroid belt? Eos 54, 233.

Williams, J.G. (1975) In preparation.

Wood, J.A. (1965) Meteorites and asteroids. Adv. Astronaut Sci. 19, 99-118.

Wood, J.A. (1968) Meteorites and the Origin of Planets. 117 pp. McGraw-Hill.

Zellner, B. (1975) 44 Nysa: an iron-depleted asteroid. Astrophys. J. 198, L45-L47.

Zellner, B., Gehrels, T. and Gradie, J. (1974) Minor planets and related objects. XVI. Polarimetric diameters. Astron. J. 79, 1100-1110.

Zimmerman, P.D. and Wetherill, G.W. (1973) Asteroidal source of meteorites. Science 182, 51-53.

FIGURE CAPTIONS

Fig. 1. Visible and near-infrared spectral reflectance curves for nine meteorites are superimposed on astronomical measurements of nine asteroids.

Fig. 2. Geometric albedo as a function of wavelength for 46 asteroids (condensed from Chapman et al, 1975). Top curve is 4 Vesta. Solid lines are S-types (high albedos) and C2 types (low albedos). Dashed lines are C* types; dotted lines are E-types (see text).

Fig. 3. Mean spectra of major meteorite classes (condensed from Chapman et al, 1975; data mainly due to Gaffey, 1973). Individual meteorites have spectra quite similar in shape but different in albedo by up to a factor of two compared with class means.

Fig. 4. Histogram of asteroid R/B colors, indicating bimodal distribution into C and S groups. Compositional analogs are indicated by the symbols as identified in the legend.

Fig. 5. Proportion of asteroid compositional types as a function of semi-major axis. Symbols are the same as in Fig. 4. The non-uniform sampling is partially compensated in this figure both by non-uniform symbol sizes and by the non-linear semi-major axis scale. Bias in sampling of asteroids is not corrected for; such corrections would greatly enhance the proportion of C2 or C* types, especially at larger semi-major axes.

Fig. 6. Bias-corrected incremental diameter-frequency relations for C, S, and all asteroids. Data for diameters greater than 60 km based on an updated analysis similar to that of Chapman et al (1975). McDonald (MDS) and

Palomar-Leiden (PLS) surveys scaled under the assumption that small asteroids have geometric albedos of 0.06.

Fig. 7. Bias-corrected incremental diameter-frequency relations for C and S asteroids in four zones of semi-major axis (from data of Chapman et al, 1975). Although relative proportions of C and S asteroids vary with semi-major axis, in all cases the C relations are quite linear in such a log-log plot, while S objects are relatively more numerous between diameters of 100 and 200 km.

Fig. 8. Histogram of asteroid R/B colors (as in Fig. 4), showing measured lightcurve amplitudes in magnitudes. Amplitudes > 0.3 mag. suggest markedly non-spherical shapes.

Fig. 9. Mason's (1968) model for an achondrite/stony-iron parent-body is compared with the asteroid Vesta. Size, density, and surface compositions are similar.

Fig. 10. Distribution of S, C, and unclassified (U) asteroids as a function of semi-major axis (dark shading). The lightly-shaded regions are within 0.06 A.U. of the major Jupiter commensurabilities identified at the top; within these zones the C asteroids are strongly depleted, but the other types show little depletion except exactly at the commensurability. The line which backdrops both the S and C distributions is the distribution of all numbered asteroids (not to scale).

TABLE 1

PRESENT COLLISIONAL LIFETIMES ($\times 10^9$ YEARS)
(For optimum input parameters)

Type	Diam.: 10 km	100 km	200 km	500 km	1000 km
"C"	0.2	1.7	3.5	8.6	28.
"S"	24.	21.	22.	40.	266.
proto-S	---	---	4.2	5.0	---

TABLE 2

DISTRIBUTION OF ASTEROID COMPOSITIONAL TYPES WITH RESPECT TO KIRKWOOD GAPS

Asteroid Type	%-tage Within 0.06 AU of Commensurabilities	%-tage Far From Commensurabilities
"C" N = 69	11%	89%
"S" N = 66	36%	64%
"U" N = 13	(31%)	(69%)
Uniform Distribution	43%	57%

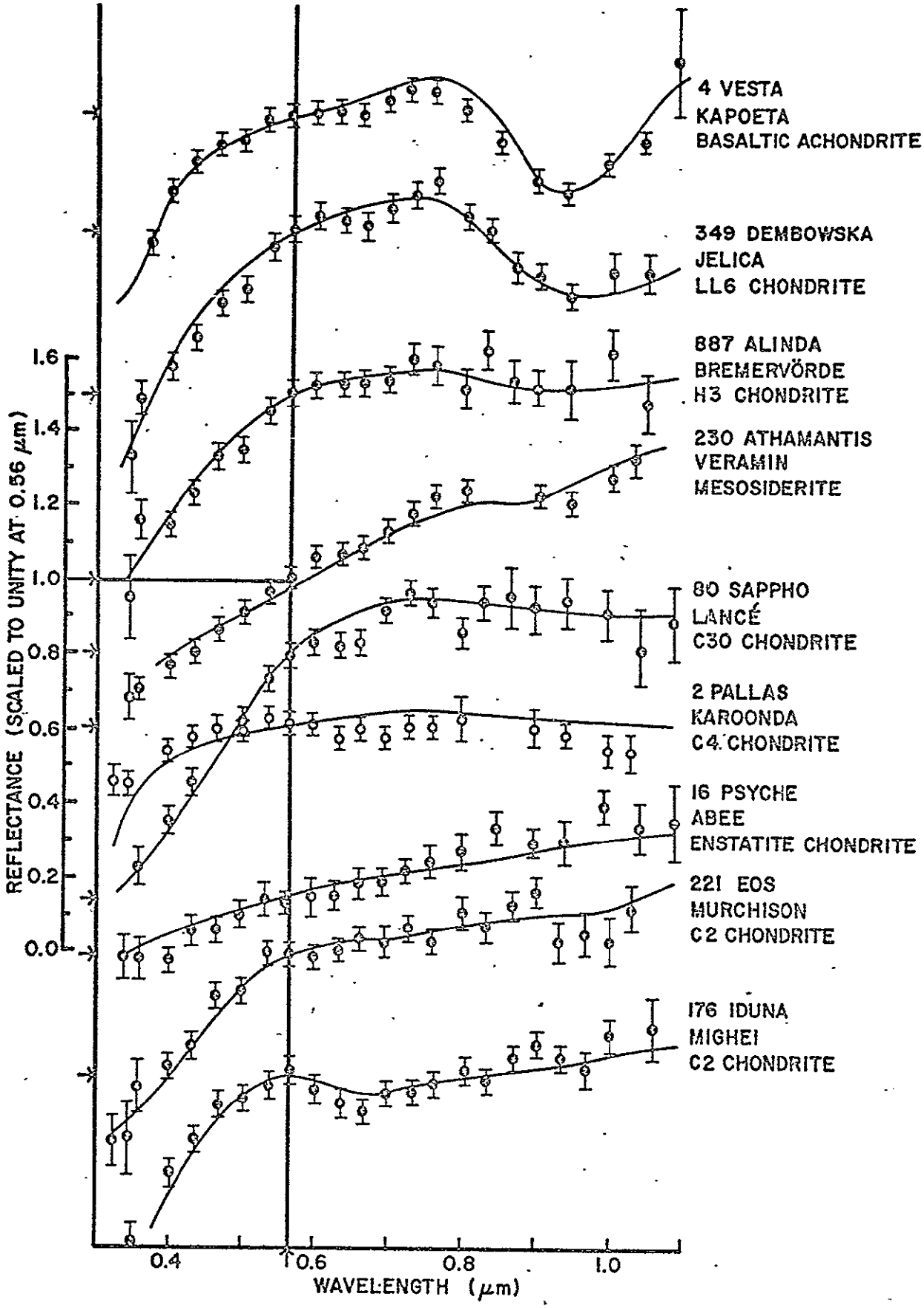

FIGURE 1

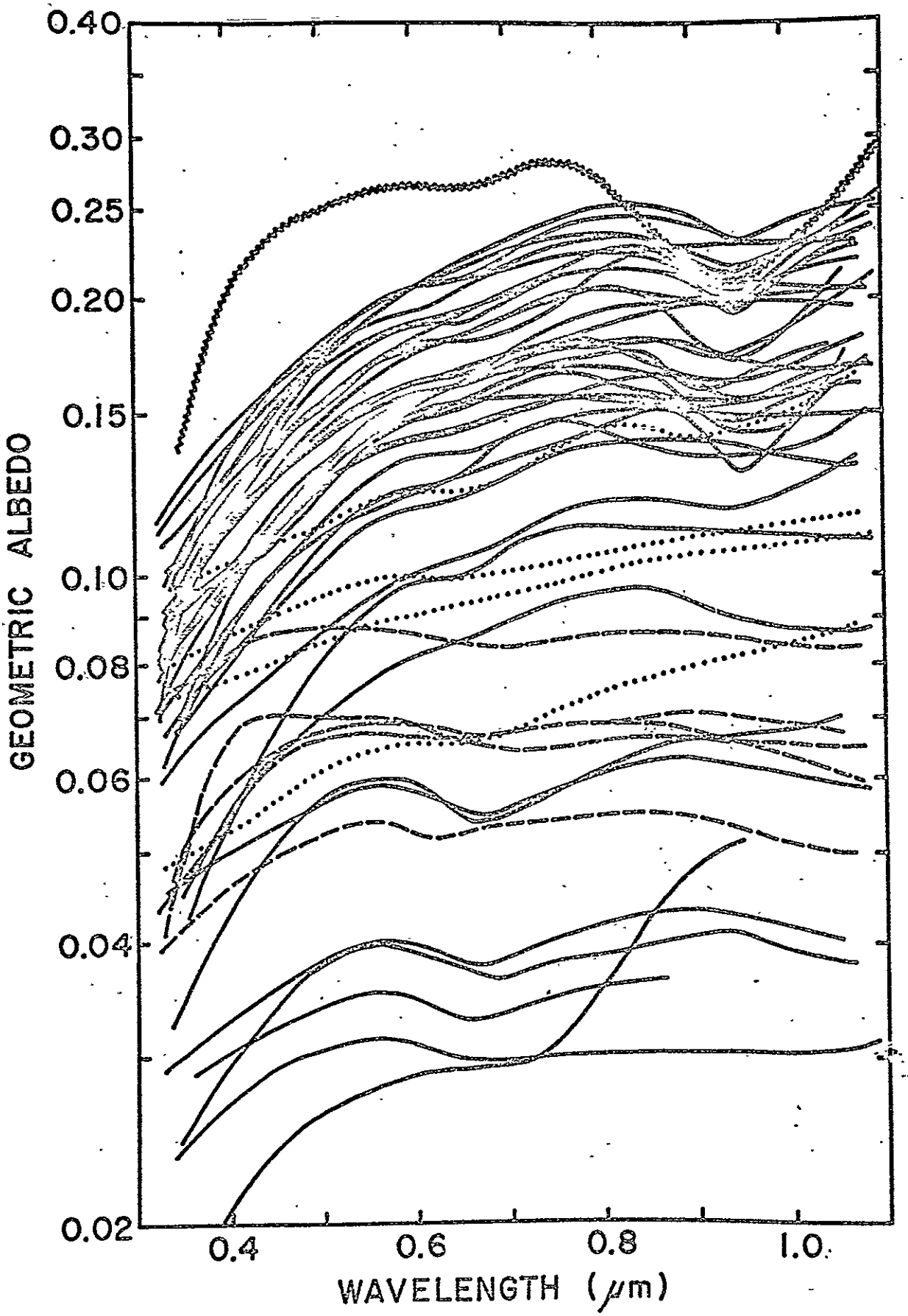
0.40
0.30
0.25
0.20
0.15
0.10
0.08
0.06
0.04
0.02
GEOMETRIC ALBEDO
0.4
0.6
0.8
1.0
WAVELENGTH (μm)

FIGURE 2

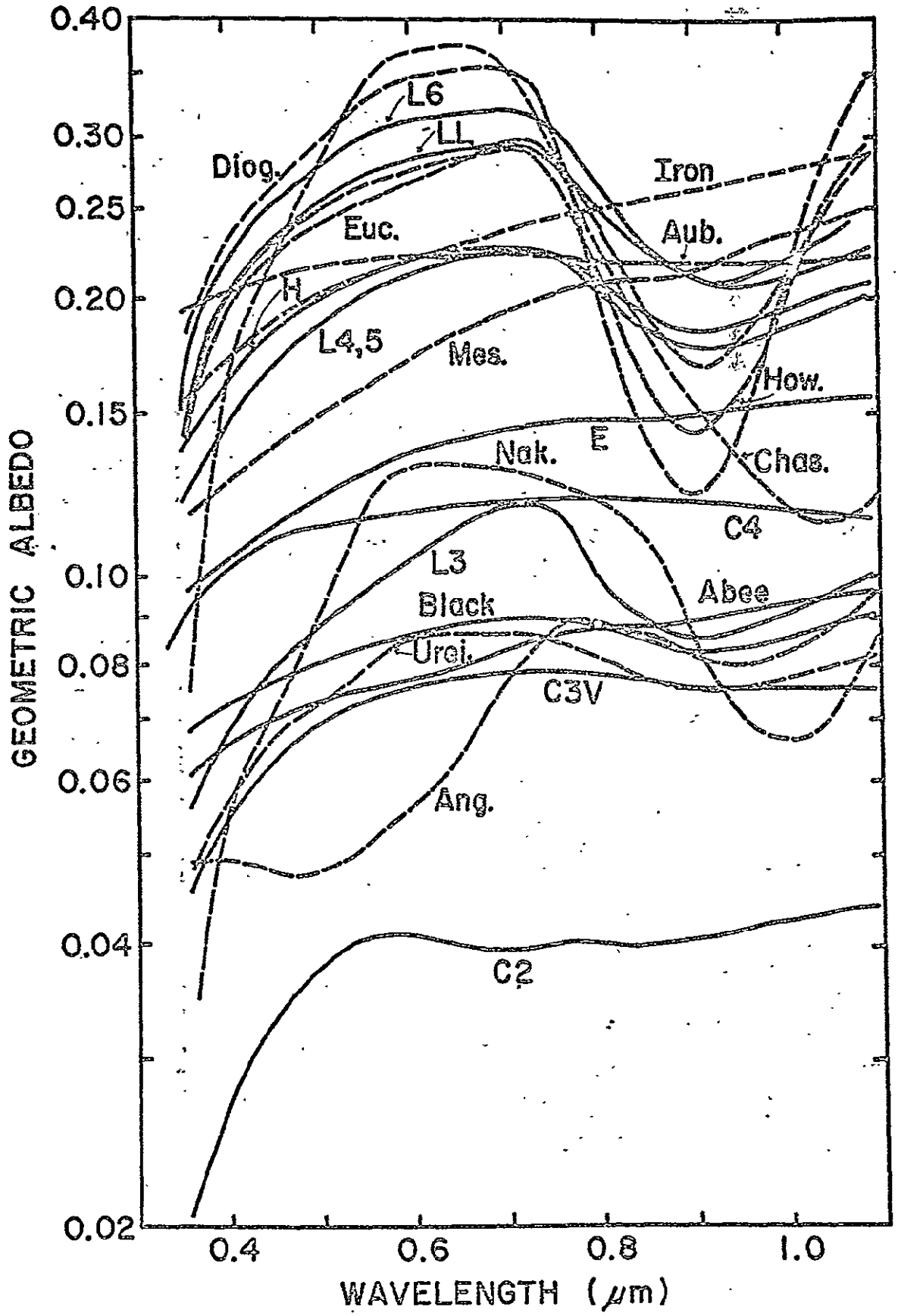
0.40
0.30
0.25
0.20
0.15
0.10
0.08
0.06
0.04
0.02
GEOMETRIC ALBEDO
0.4
0.6
0.8
1.0
WAVELENGTH (μm)
L6
LL
Diog.
Iron
Euc.
Aub.
H
L4,5
Mes.
How.
E
Nak.
Chas.
C4
L3
Abee
Black
Urei.
C3V
Ang.
C2

FIGURE 3

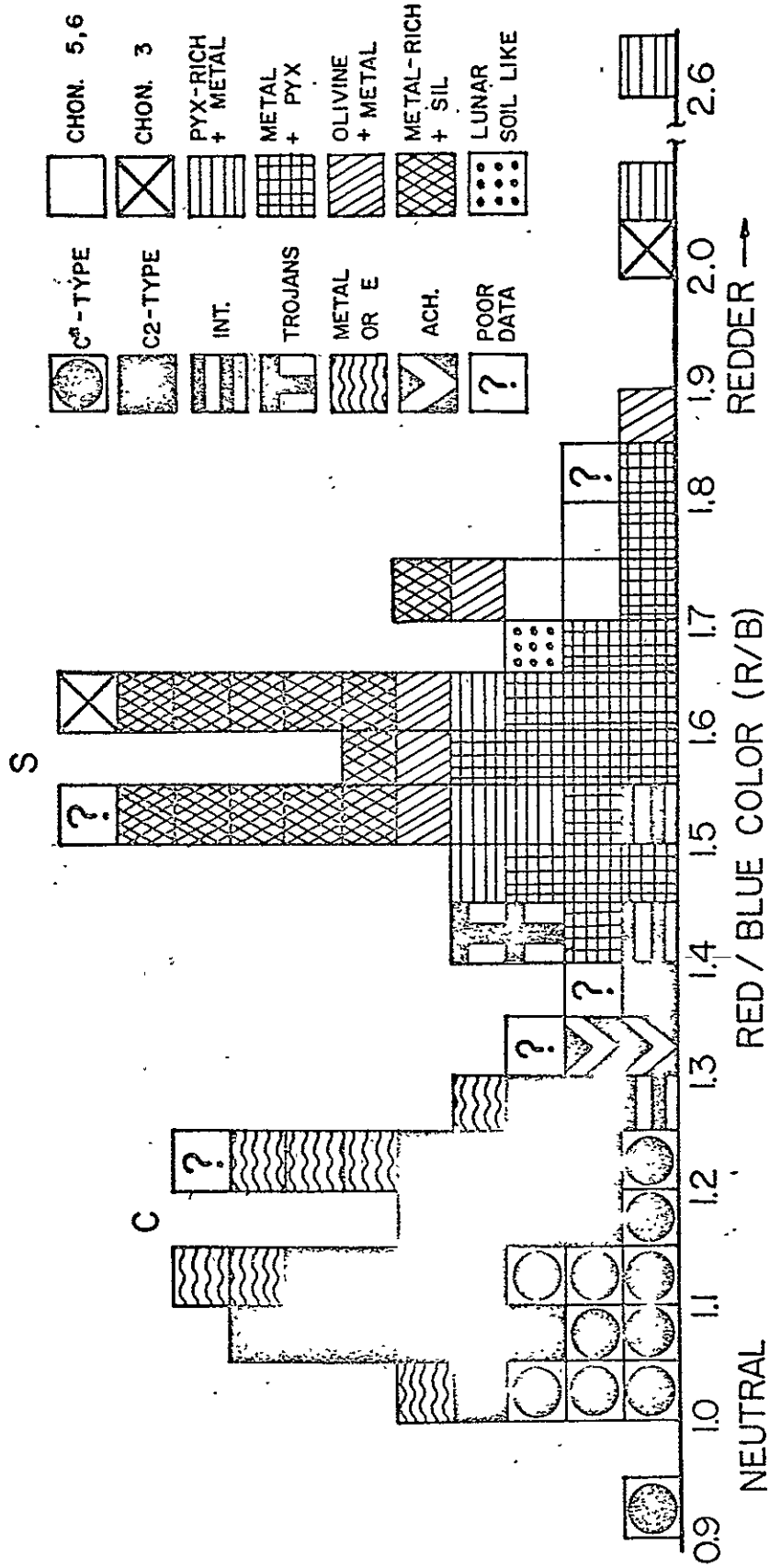

FIGURE 4

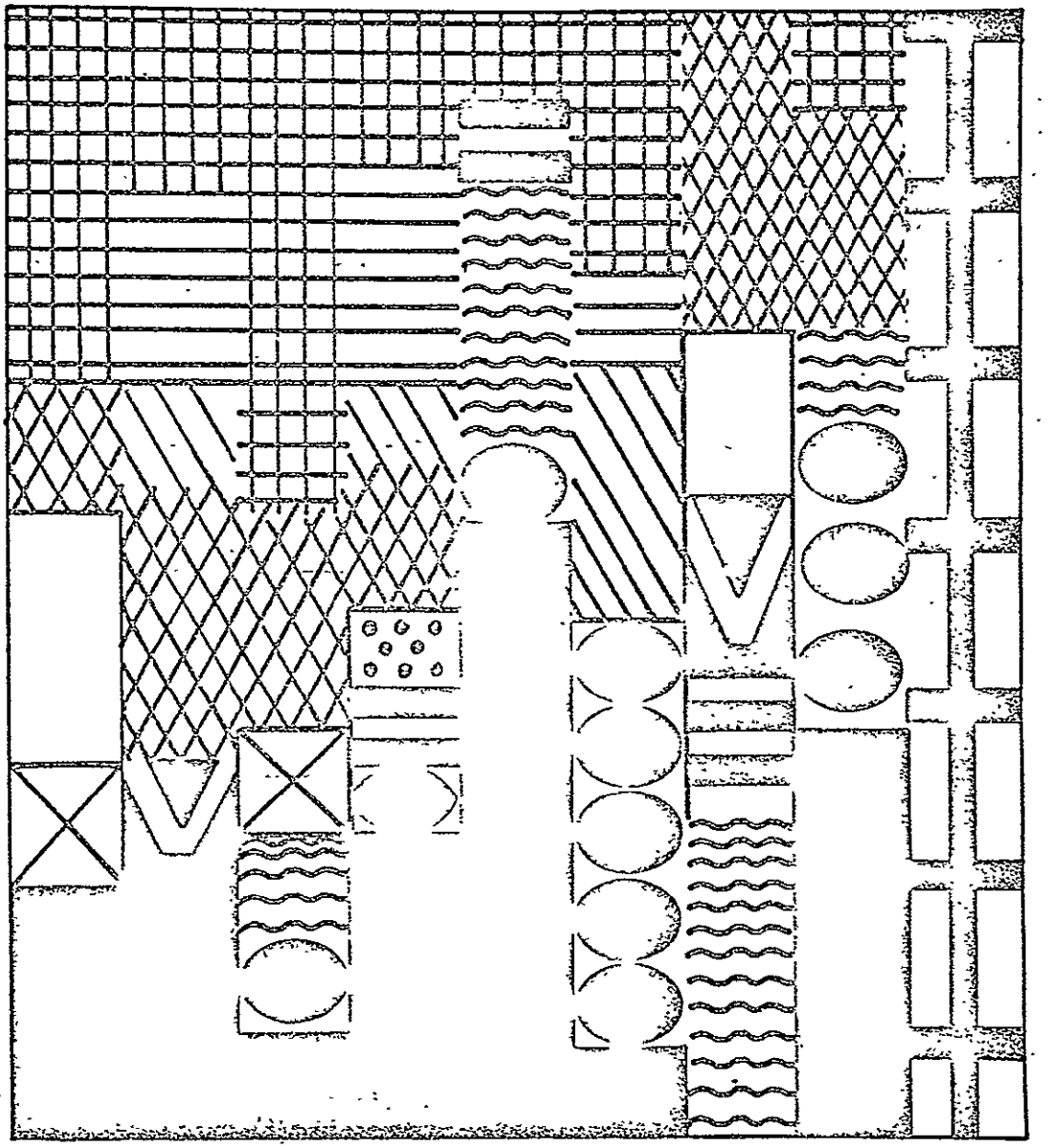

FIGURE 5

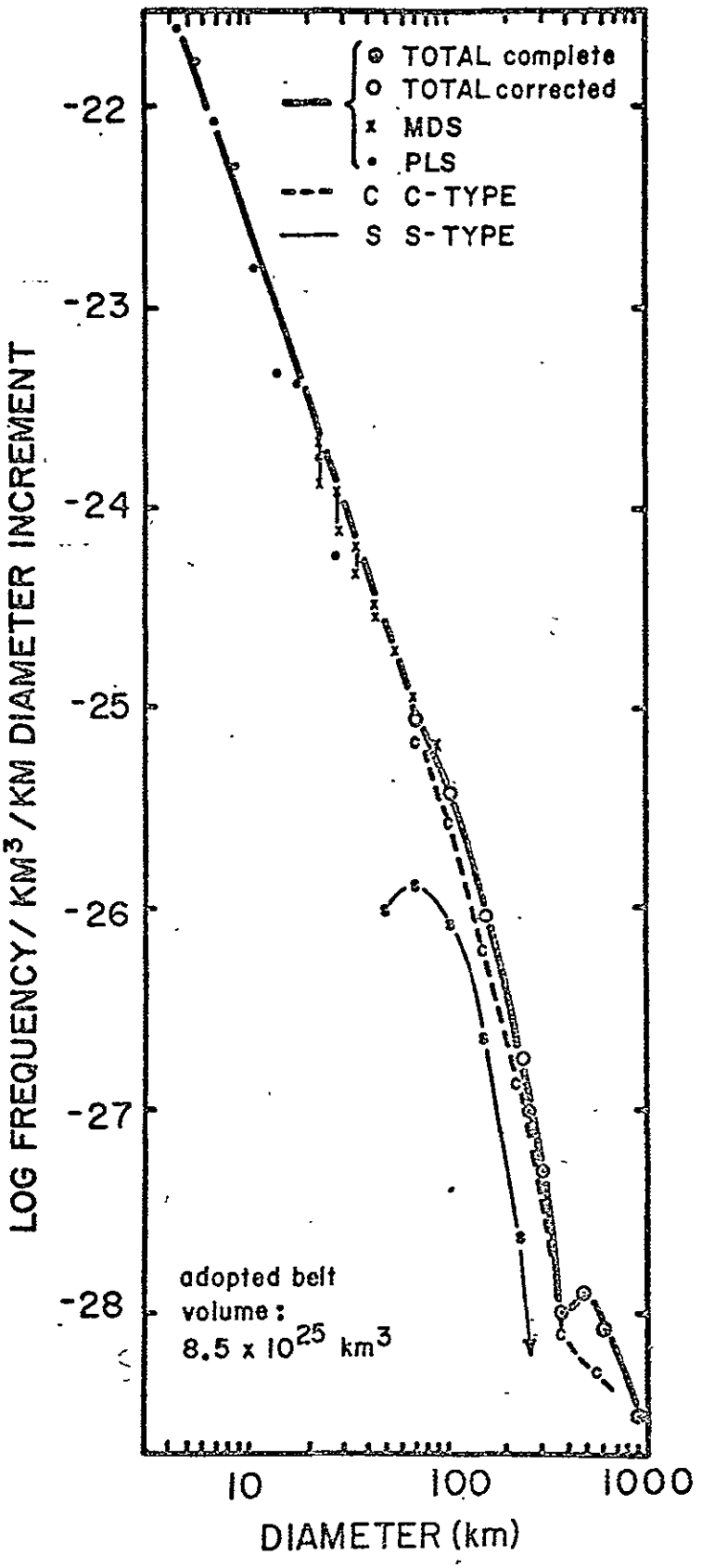

FIGURE 6

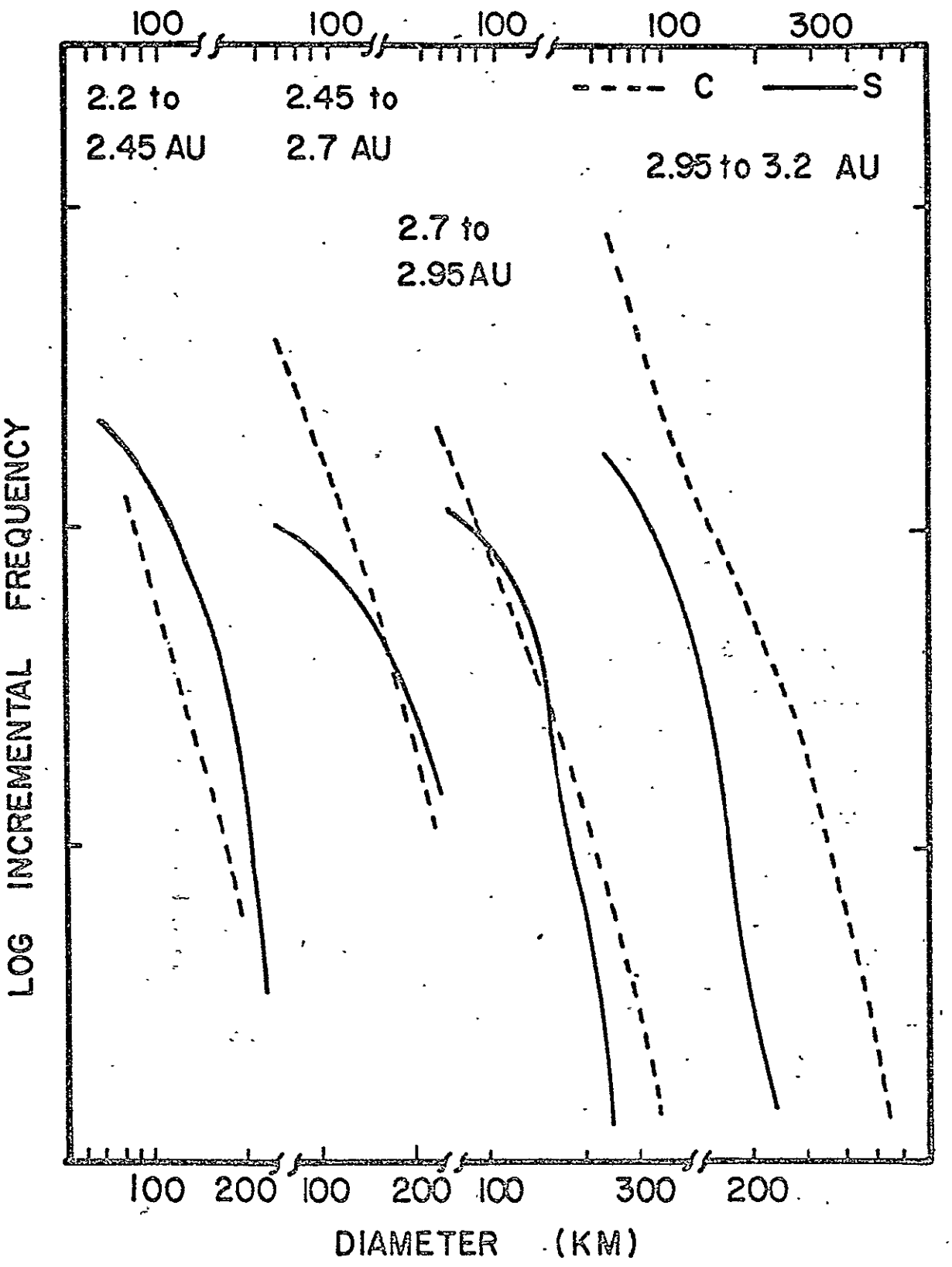
100
100
100
100
300
2.2 to
2.45 AU
2.45 to
2.7 AU
C
S
2.95 to 3.2 AU
2.7 to
2.95 AU
LOG INCREMENTAL FREQUENCY
100
200
100
200
100
300
200
DIAMETER (KM)

FIGURE 7

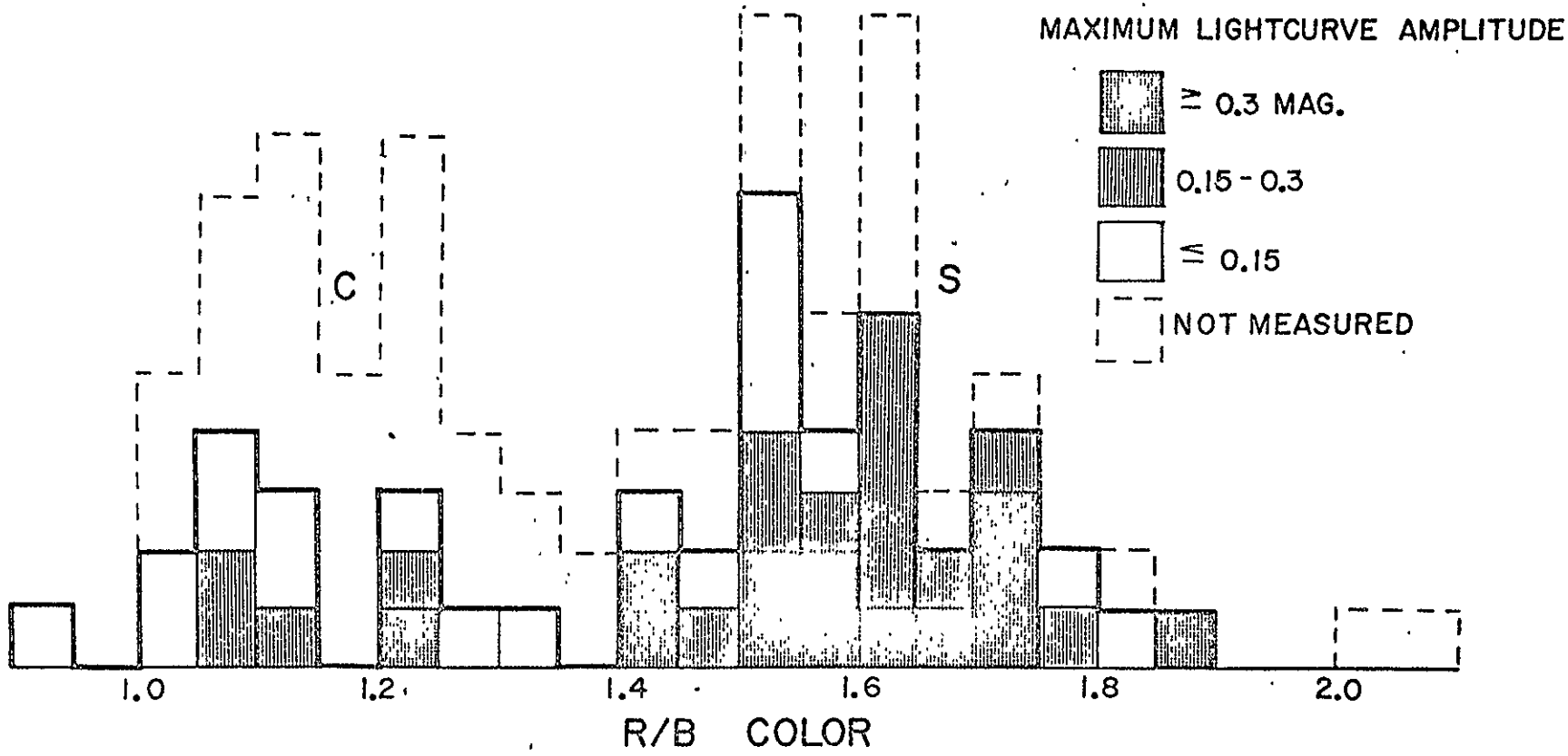
MAXIMUM LIGHTCURVE AMPLITUDE
≥ 0.3 MAG.
0.15 - 0.3
≤ 0.15
NOT MEASURED
C
S
1.0
1.2
1.4
1.6
1.8
2.0
R/B COLOR

FIGURE 8

FIGURE 9

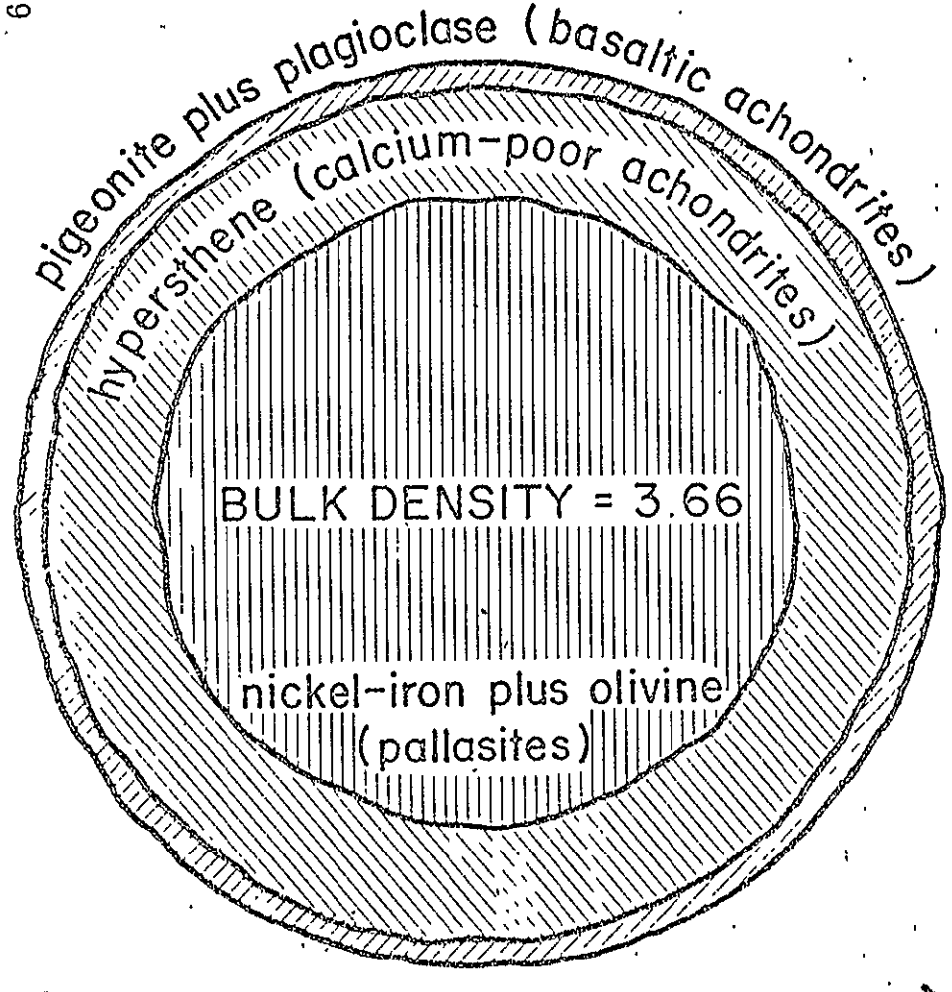

diameter = 600 km

MASON'S PARENT-BODY MODEL

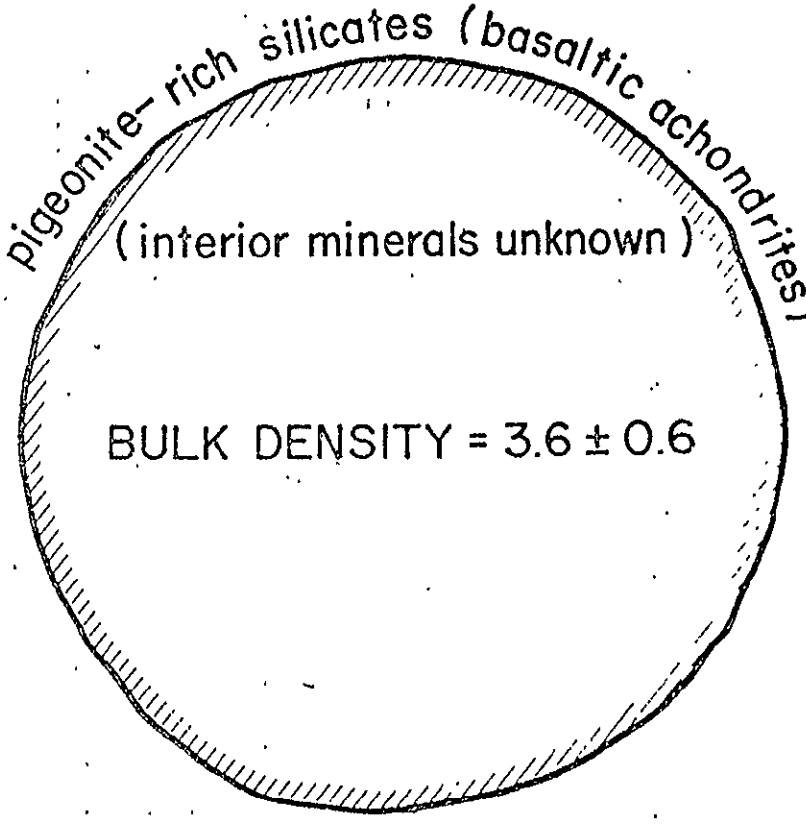

diameter = 500 km

ASTEROID (4) VESTA

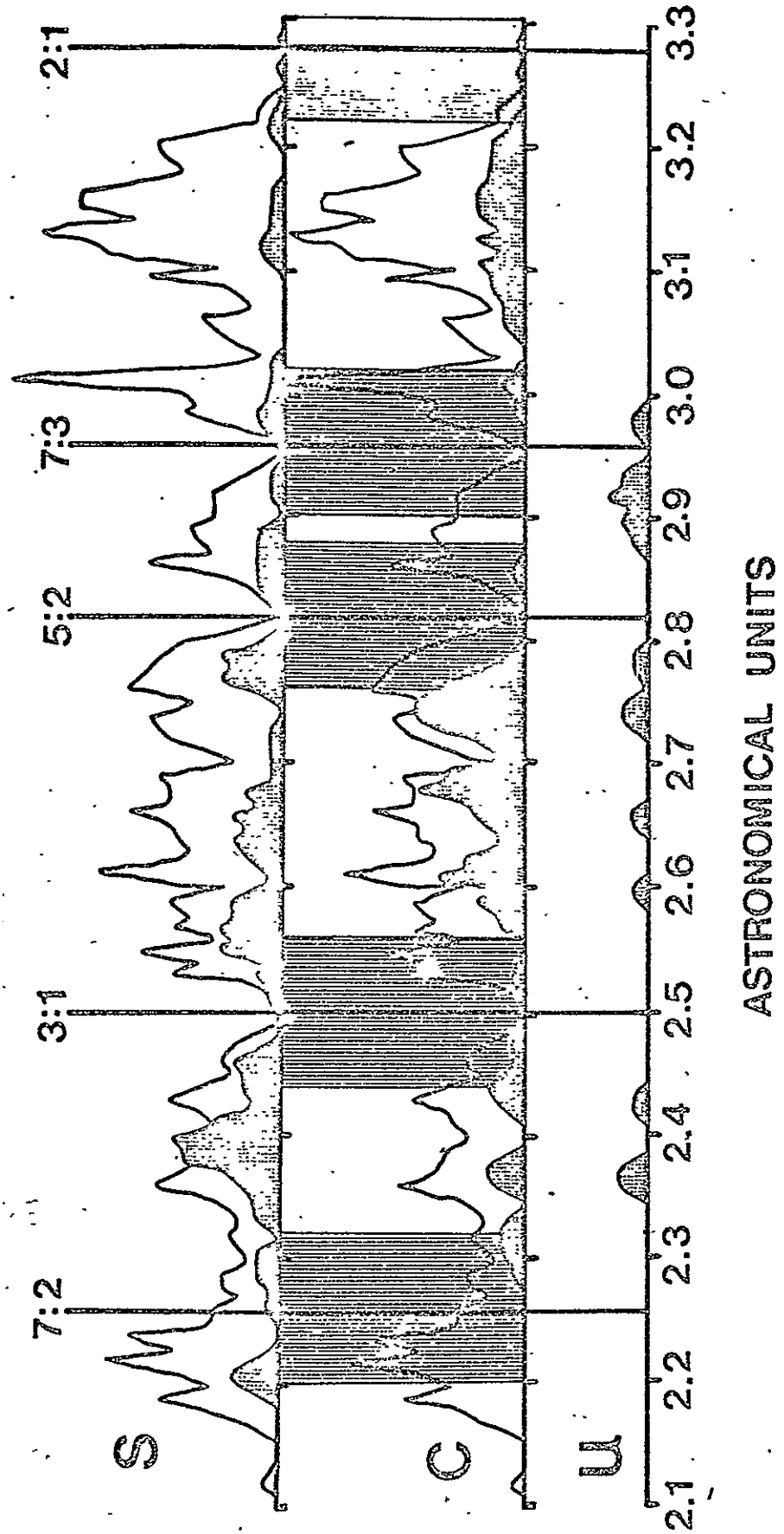

FIGURE 10

APPENDIX D

INFRARED THERMAL MODELS FOR SATURN'S RING

Michael J. Price
Planetary Science Institute
Tucson, Arizona 85704

Received _____

Revised 4 August 75

No. of Copies: 4
No. of MS Pages: 25
No. of Figures: 0
No. of Tables: 5

ABSTRACT

Infrared (10 μm and 20 μm) thermal emission data for Saturn's rings are discussed in terms of isothermal radiative transfer models of finite optical thickness. Interparticle separations are taken to be sufficiently large that mutual shadowing is negligible; the optical scattering phase function corresponds to the far field of a macroscopic sphere. Each particle is assumed to emit radiation isotropically. To investigate the maximum range in thermometric temperature of the ring material, two extreme physical models are used in its definition. The thermometric temperature is taken as characteristic either of an isolated individual particle or of a homogeneous, finite, scattering layer of particles. In both models, the radiative energy balance defines the thermometric temperature. Detailed computations of the penetration of solar radiation, and of the escape of thermal radiation, both utilize the two-stream approximation to describe the local radiation field. Recent brightness temperature measurements, corresponding to essentially maximum ring tilt, have been used to investigate the validity of the optical scattering model. Single scattering albedos less than 0.75 are required to provide sufficient thermal emission. Reconciliation with earlier optical analyses by Price (1974) requires the back-scattering efficiency to be even higher than for a macroscopic sphere. Historical brightness temperature measurements are used to show that no unique isothermal ring model exists. Instead, a temperature gradient perpendicular to the ring plane appears to be present. Particles nearest the sunward face of the ring experience the highest thermometric temperatures. Speculations regarding the thermal inertia of the ring particles are briefly discussed.

1. INTRODUCTION

Valuable information concerning the physical structure of the Saturn ring system can be obtained by analyzing infrared measurements of its thermal emission (Pollack, 1975). But deriving a reliable thermal model requires knowledge of the precise manner in which solar radiation is scattered and absorbed by the rings. Not only must the penetration of sunlight be thoroughly understood, but so must the heating of the particles, together with the subsequent escape of thermal radiation from the system. Choice of the most suitable radiative transfer model is therefore fundamental. Analysis of the optical scattering properties of the ring provides a basis for the selection.

Historically, interpretations of the photometric function have been dominated by the concept of interparticle shadowing, cf: Bobrov (1970). Mutual shadowing has been invoked to explain the pronounced phase effect in which the rings brighten significantly at opposition. Recently, Kawata and Irvine (1973) have published the most elaborate classicial analysis of the optical observations. Their theoretical model of Saturn's rings included both the shadowing effect and realistic anisotropic phase functions for the particles. Effects of multiple scattering and the finite size of the sun, including the penumbra, were rigorously treated. Permissible ranges in the optical thickness, single scattering albedo, volume density, and phase function, were investigated. Anisotropic scattering was necessary to match the observations. The color dependence of the opposition effect was explained in terms of the spectral reflectivity of the ring particles.

Kawata and Irvine (1975) have applied their optical scattering model to the interpretation of infrared thermal emission data for the rings. Their analysis incorporated a particle size-distribution taking the form of a power law relation $dn \propto \rho^{-s}$, where dn is the number of particles with radii between ρ and $\rho + d\rho$. The parameters of the polydisperse model ($s = 2$) could be chosen to satisfy both optical and infrared observations. But, in view of the multiplicity of parameters involved, questions of uniqueness naturally arose. Kawata and Irvine emphasized that further observational testing is needed to verify their model.

Recently, Price (1974) has questioned the validity of the classical approach. In rediscussing the optical scattering properties of the rings, he presented evidence to suggest that primary scattering dominates and that interparticle separations are sufficiently large that mutual shadowing is negligible. The opposition effect was treated as a perturbation to the individual scattering phase function, characteristic of the surface properties of the ring particles. Probable ranges both in the single scattering albedo, and in the general shape of the scattering phase function, were defined using simple anisotropic scattering models. Limits on the corresponding mean perpendicular optical thickness of the ring were also obtained. Results indicated that the individual ring particles are highly efficient back-scatterers of visual radiation. Macroscopic particles were found to account for the general shape of the scattering phase function. On the basis of an infinite optical thickness for the rings, a minimum single scattering albedo ~ 0.75 was found. Use of conservative scattering led to a minimum optical thickness ~ 0.7. The analysis was consistent with the ring particles being centimeter-size pieces of ice.

In this paper, the elementary radiative transfer model introduced by Price (1974) is used to analyze current infrared thermal emission data for Saturn's rings. The analysis has two objectives. First, the validity of the basic optical scattering model is examined. Particular attention is given to the constraints placed on the single scattering albedo, and on the degree of anisotropy in the scattering phase function. Second, conclusions regarding the basic thermal structures of the individual particles, and of the ring itself, are drawn.

II. OBSERVATIONS

Infrared radiometry of Saturn's rings has been reviewed by Pollack (1975) and by Morrison (1975). Spatial and temporal measurements of brightness temperature have been made. Both are quite limited however. Most published data refer to the equilibrium thermal emission of the ansae, rings A and B being measured together. Although brightness temperature measurements have been made separately for rings A and B at large solar elevation angles above the ring plane, the individual components of the system have not in general been resolved. Variations in the brightness temperature of the rings with either phase angle or solar elevation ("tilt") angle are poorly documented. Pollack (1975) has recently hypothesized that the existence of an infrared phase effect, correlated with its optical counterpart, would provide direct support for the concept of mutual shadowing. Unfortunately, no useful data are available to explore the idea.

Variation in the brightness temperature with solar elevation angle is not well defined. But, the brightness temperature does appear to decrease with ring tilt. Table I summarizes the equilibrium infrared brightness temperatures currently available (Murphy, 1974). Adjusted B-ring values correspond to the raw measurements corrected to a constant distance from the sun (9 A.U.); combined A-B system measurements have been modified by the procedure discussed by Murphy (1974). Morrison (1974) noted that the east ansa was brighter than the west ansa by about 10 percent at 20 μm.

In view of the heterogeneous nature of the observations, our analysis will be based primarily on Morrison's (1974) measurements at 10 μm and 20 μm. Constraints imposed on our ring models by Low's (1965, 1966) data will be discussed. Some consideration will also be given to the eclipse cooling of the ring particles. Morrison (1974) found that the 20 μm temperature 5 arc sec outside the shadow after eclipse was $2.0 \pm 0.5^{\circ}$K lower than at the equivalent position before eclipse.

III. THEORY

Predicting brightness temperatures for the ring requires a detailed knowledge of the variation of its thermal source function with optical depth. Four basic questions are involved. But solving the problem is difficult. Not only are its individual aspects strongly coupled, but the coupling itself is imperfectly understood.

First, solar radiation is the principal source of heating. Its penetration of, and absorption by, the ring must be reliably computed. Determining the local

TABLE I

INFRARED BRIGHTNESS TEMPERATURES, T_B

Based on Summary by Murphy (1974)

Observation Year	Observers	$\lambda(\mu)$	Position	$T_B(^oK)$		Solar Elevation Angle
				Raw	Adjusted B-Ring	
1964	Low (1965)	10	Ansa	<80	<85	9^o
1965	Low (1966)	20	Ansa	<60	<64	5^o
1969	Allen & Murdock(1971)	12	Ansa	83 ± 3	86 ± 3	17^o
1971	Murphy et al (1972)	20	Peak at Ansa	89 ± 3	90 ± 3	25^o
1972	Murphy (1973)	20	B Ring at Ansa	94 ± 2	94 ± 2	26^o
1972	Murphy (1973)	20	A Ring at Ansa	89 ± 3	N/A	26^o
1973	Morrison (1974)	11	B Ring at Ansa	90 ± 3*	90 ± 3	26^o
1973	Morrison (1974)	20	B Ring at Ansa	96 ± 3*	96 ± 3	26^o
1973	Nolt et al (1974)	35	Ansa	90-95	92-97	26^o

* Temperature Difference $T_{20} - T_{11}$ Accurate to $\pm 2^oK$

solar radiation field requires the solution of a non-grey optical radiative transfer problem. Three parameters are always involved, the single scattering albedo, the shape of the scattering phase function, and the optical thickness. Their selection depends on the distributions in the size, shape, and surface characteristics of the ring particles. Choosing the correct approach to the solution of the radiative transfer problem depends on the volume density of the ring. Specifically, the degree of mutual shadowing must be decided (Price, 1974).

Second, the thermal structure of the individual ring particles must be modelled. Whether or not a ring particle emits radiation uniformly over its surface depends on its basic composition, its size, its shape, and its internal structure. Unless its thermal conductivity is infinite, each particle will not be at a uniform thermometric temperature. Uneven emission of thermal radiation from its surface will likely occur.

Third, the dynamical histories of the ring particles must be considered. Particles which have spent the most time, most recently, near the sunward face of the ring will be at the highest temperatures. Rotation of the ring particles is important. Rapid rotation will minimize non-uniformity in their thermal structures; slow (e.g. synchronous) rotation will maximize non-uniformity. In a collisionless system, each particle would make a completely unrestricted excursion between opposite faces of the ring during its orbital period. The degree to which collisions do in fact occur will greatly affect the local distributions of thermometric temperatures both within and among the individual particles.

Fourth, the manner in which thermal radiation escapes from the ring must be considered. Once again solution of a non-grey radiative transfer problem is required. Note that the basic radiative transfer parameters at infrared wavelengths could bear no resemblance to their optical counterparts. Specifically, the single scattering albedo may be very different. Mutual heating of the ring particles will certainly occur. Optical distance from each ring face is, therefore, a major factor in determining the local thermometric temperature of the ring material.

Knowledge of the ring structure is still too rudimentary to consider attempting the complete solution of the problem. Even so, significant progress can still be made by considering its various aspects individually. Fundamental information can be derived on the basis of elementary considerations. Two extreme physical models will be used to define the thermometric temperature of the ring particles. Besides encompassing a very broad spectrum of possible situations, the pair can be used to sidestep the issue of solving the coupled physical, radiative, and dynamical problem. In both cases, the ring system is assumed to be an homogeneous, isothermal, finite, plane-parallel layer.

Model I may be called the isolated particle model. It consists of two variants. In Model Ia, the surface temperature of every ring particle is taken as characteristic of an isolated flat plate oriented to receive solar radiation at normal incidence. The surface temperature is determined by the albedo at optical wavelengths (A), and by the emissivity at infrared wavelengths (ϵ).

Grey absorption and grey emission are assumed. The thermometric temperature, T, is given by

$$T = \left(\frac{1 - A}{\epsilon}\right)^{1/4} \cdot \left(\frac{F}{\sigma}\right)^{1/4} \qquad (1)$$

where σ is the Stefan-Boltzmann constant, and F is the solar flux at Saturn. In Model Ib, the surface temperature of each particle is taken as characteristic of our isolated, perfectly conducting, sphere. Solar energy absorbed by one hemisphere will be radiated uniformly from the entire surface of the particle. Compared to Model Ia, the thermometric temperature is reduced by a factor $\sqrt{2}$. The mean surface temperature of a real isolated particle should lie somewhere between the predictions of Models Ia and Ib.

Model II may be called the isothermal slab model. Heating of the individual ring particles is not considered explicitly. Instead, the thermometric temperature of the ring material is determined by the energy balance of the entire system. To obtain the total absorption and emission of radiation, the relevant radiative transfer equations must be solved; grey absorption and grey emission are assumed. The thermometric temperature is obtained by an iterative technique. At both optical and infrared wavelengths, the ring particles are treated as macroscopic spheres, their individual scattering phase functions being described by the far-field approximation(Price, 1974). Solutions of the radiative transfer problems at optical and infrared wavelengths are discussed in Appendix I.

TABLE II

THERMOMETRIC TEMPERATURES: MORRISON (1974) GEOMETRY

MODEL / $\tilde{\omega}$	Ia	Ib	II*	
			$\tau = .1$	$\tau = 1$
0	131.1	92.7	92.1	88.7
0.75	92.7	65.5	66.2	70.8

*MAXIMUM THERMOMETRIC TEMPERATURE($\tau = \infty$) is 90.0 ^{o}K

Note: The Sun-Saturn distance is taken as 9.015 A.U. (i.e., at opposition) with the solar elevation angle at 26.4 degrees. Cosines of the angles of incidence (μ_0) and emergence (μ) with respect to the outward normal are taken equal at 0.4446.

TABLE III

11μ/20μ BRIGHTNESS TEMPERATURES cf: MORRISON (1974)

MODEL / $\tilde{\omega}$	Ia		Ib		II	
	τ = .1	τ = 1	τ = .1	τ = 1	τ = .1	τ = 1
0	113.0/101.5	129.7/128.5	83.3/76.8	92.0/91.4	82.8/76.4	88.0/87.5
0.75	83.3/ 76.8	92.0/ 91.4	60.6/57.2	65.1/64.8	61.2/57.7	70.4/70.0

Note: The Sun-Saturn distance is taken as 9.015 A.U. (i.e., at opposition) with the solar elevation angle at 26.4 degrees. Cosines of the angles of incidence (μ_0) and emergence (μ) with respect to the outward normal are taken equal at 0.4446.

TABLE IV

$10\mu/20\mu$ BRIGHTNESS TEMPERATURES cf: LOW (1965, 1966)

MODEL / $\tilde{\omega}$	Ia		Ib		II.	
	$\tau = .1$	$\tau = 1$	$\tau = .1$	$\tau = 1$	$\tau = .1$	$\tau = 1$
0	118.0/118.5	125.8/126.5	85.1/85.4	89.0/89.5	80.8/77.0	67.4/58.6
0.75	85.1/ 85.4	89.0/ 89.5	60.9/61.2	62.9/63.3	58.7/56.0	53.5/46.3

Note: The $10\mu/20\mu$ Sun-Saturn distances are taken as 9.784 A.U./9.677 A.U. (i.e., at opposition) with the solar elevation angles at $9^{o}/5^{o}$. Cosines of the angles of incidence (μ_0) and emergence (μ) with respect to the outward normal are taken equal at 0.1564 (10μ) and 0.0872 (20μ).

IV. ANALYSIS

Fundamental in our analysis of infrared brightness temperatures is the assumption that each ring particle emits thermal radiation like a black-body. For ice, the candidate ring material, evidence that the infrared emissivity at 10 μm and 20 μm is not far from unity comes from Bezverkhniy, Bramson, and Moiseyeva (1970) and from Irvine and Pollack (1968). For unit emissivity, each particle will emit the maximum amount of thermal energy relevant to its thermometric temperature. Solar energy absorbed at optical wavelengths throughout the ring will be converted with optimum efficiency into infrared thermal radiation. Thermal emission will, therefore, be maximized for each choosen set of optical scattering parameters. Unit emissivity greatly simplifies our basic theory cf. Appendix I. For Model I, the thermometric temperature of each particle depends only on the effective optical scattering albedo. For Model II, the infrared source function corresponds to the Planck function at the relevant thermometric temperature.

Model predictions of the brightness temperature of the rings are listed in Tables III and IV. Table III is relevant to the interpretation of the 11 μ/20 μ measurements made by Morrison (1974) at large solar elevation angles; Table II lists the corresponding thermometric temperatures. Table IV is relevant to the 10 μ/20 μ measurements made by Low (1965, 1966) at small solar elevation angles. Computations were made for the individual geometrical circumstances.

For Model II, the thermometric temperatures (T_p) depend both on the optical single scattering albedo ($\tilde{\omega}$) and on the optical thickness (τ). For constant τ, the thermometric temperature decreases as the ring particles become less absorbed. For τ tending to zero, the T_p value naturally

approaches the Model Ib figure. For τ tending to infinity, the ring absorbs like a flat plate inclined to the incident solar flux. For constant $\tilde{\omega}$, T_p depends on τ. If $\tilde{\omega}$ is large, T_p increases with τ; more energy is then absorbed by the ring. If $\tilde{\omega}$ is small, T_p tends to decrease with increasing opacity; spreading the energy over a larger quantity of ring material compensates to some extent for the increased optical thickness.

For large τ, the accuracy of the Model II computational technique can be estimated by comparing T_p predictions for τ equal to unity and infinity, with $\tilde{\omega}$ set equal to zero. Taking into account ring tilt, the finite ring model will then be almost totally opaque; the T_p predictions should be essentially identical. In the usual rotation, the maximum energy absorbed per unit area of the slab will be $\mu_0 F$. Since Model II always emits one-half of the absorbed energy from each ring force, the black-body flux emitted per unit area of the ring will be $1/2\ \mu_0 F$. The corresponding maximum thermometric temperature is $90^{\circ}K$. Comparing the relevant T_p predictions in Table II indicates a $1.3^{\circ}K$ difference, which illustrates the level of uncertainty in the Model II calculations.

Table III may be compared directly with Morrison's (1974) $11\,\mu/20\,\mu$ brightness temperature measurements of $90^{\circ}K/96^{\circ}K$. Only Model Ia explains the observations without difficulty. Even so, the Model requires $\tilde{\omega} < 0.75$. Table II indicates that the observed $20\,\mu$ brightness temperature cannot be explained by higher single scattering albedos, even if the optical thickness is infinite, with unit emissivity. Models Ib and II can explain only the $11\,\mu$

observations. Even so, it is difficult; $\tilde{\omega}$ must be very close to zero. The $20\,\mu$ measurement cannot be explained even with $\tilde{\omega}$ equal to zero, unit emissivity, and a completely free choice of optical thickness ($0 \leq \tau \leq \infty$). For an isothermal ring, the optimum thermometric temperature model would appear to be an intermediate Model Ia/b; Model II appears to be completely ruled out. Moreover, the effective single scattering albedo at optical wavelengths must be less than 0.75. By comparison, Morrison (1974) estimated $\tilde{\omega} < 0.6$ using basic physical arguments.

Table IV may be compared with Low's (1965, 1966) $10\,\mu/20\,\mu$ upper limits to the brightness temperature of $80^{\circ}K/60^{\circ}K$. Neither measurement can be explained by using Model I to define the thermometric temperature of the ring material unless $\tilde{\omega} > 0.75$ or there exists a vertical temperature gradient perpendicular to the ring plane. Particles deep within the ring may well be colder than those near the sunward face. Penetration by solar radiation becomes progressively inhibited with decreasing ring tilt. No useful conclusions can be drawn concerning Model II. Although the $10\,\mu/20\,\mu$ measurements are readily explainable for $\tau \sim 1$, no reliable limits can be placed on $\tilde{\omega}$. More stringent observational upper limits to the brightness temperature would be required.

V. TOWARDS A REALISTIC RING MODEL

Analysis of the meagre brightness temperature measurements suggests that the most relevant thermometric temperature model for the ring material has characteristics of an intermediate Model Ia/b. An effective optical single scattering (Bond) albedo less than 0.75 is essential. Moreover, a vertical temperature gradient perpendicular to the ring plane may be present. Our

tentative conclusions may be placed on a firmer footing by considering independent estimates for the thermometric temperature of the ring.

Be making use of the temperature dependence of the water-ice feature near 1.65 microns, Fink and Larson (1975a,b) have empirically derived thermometric temperatures for the ring at two solar elevation angles. Spectral data were obtained in 1969 near Saturn opposition, and on 1975 March 2. The corresponding thermometric temperatures were $80\pm5^{o}K$ and $90\pm5^{o}K$, respectively.

Thermometric temperatures obtained from the Fink and Larson technique will necessarily be a weighted mean for the ring, taking into account contributions from all optical depths. If the actual thermometric temperature decreases with optical depth, the observed value will necessarily be smaller than for an individual particle closest to the sunward face of the ring. If the ring is non-isothermal, lower single scattering albedos are required to reproduce the weighted thermometric temperature which corresponds to the isothermal situation.

Predictions from our thermometric temperature models are listed in Table V. Model Ia can be reconciled with the observations only if $\tilde{\omega} > 0.75$ or the ring is non-isothermal. Models Ib and II are both reconcilable with the measurements, but only if $\tilde{\omega} < 0.75$. If the results obtained from the thermometric and brightness temperature analyses are evaluated together, several conclusions appear to be inescapable. First, the single scattering (Bond) albedo is virtually certain to be less than 0.75. Second, a vertical temperature gradient perpendicular to the ring plane most likely exists. Third, the

TABLE V

THERMOMETRIC TEMPERATURES cf: FINK AND LARSON (1975a, b)

MODEL / DATE	I		I		II *			
					τ = .1		τ = 1	
	ϖ = 0	ϖ = 0.75	ϖ = 0	ϖ = 0.75	ϖ = 0	ϖ = 0.75	ϖ = 0	ϖ = 0.75
1969 Oct 29	129.5	91.6	91.6	64.8	89.9	64.6	81.0	64.5
1975 Mar 2	131.0	92.6	92.6	65.5	91.9	66.0	87.3	69.7

* MAXIMUM THERMOMETRIC TEMPERATURE ($\tau = \infty$): 1969 Oct 29 80.7 ^{o}K

1975 Mar 2 88.2 ^{o}K

Note: For the 1969 measurement, the Sun-Saturn distance was taken as 9.23 A.U., corresponding to the date of opposition (October 29); the solar elevation angle was 17.5 degrees (μ_0 = 0.3007). For the 1975 measurement the Sun-Saturn distance was taken as 9.03 A.U.; the solar elevation angle was 24.2 degrees (μ_0 = 0.4099). Unit emissivity was assumed.

thermometric temperature appears to be characteristic of an intermediate Model Ia/b.

Since the Bond albedo and the optical single scattering albedo (λ5500Å) are essentially identical (Appendix II), our upper limit for $\tilde{\omega}$ has an important consequence. Price (1974) found that the optical single scattering albedo must be greater than 0.75 unless the ring particles back-scatter radiation even more efficiently than for the case of a macroscopic sphere. Higher optical back-scattering efficiency is demanded by the infrared analysis. Greater anisotropy in the scattering phase function will further inhibit the penetration of the ring by solar radiation. Conclusions regarding the inadequacy of Model II, and presence of a vertical temperature gradient, are reinforced.

Several interesting speculations may be made. First, since the heating model appears to be an intermediate Model Ia/b, the interiors of the ring particles cannot be at a uniform temperature. Second, the apparent presence of a temperature gradient perpendicular to the ring plane suggests that the particles have a rapid thermal response to changes in the amount of solar illumination; optical distance from the sunward face of the ring is continually changing for each particle throughout its orbital resolution around Saturn. Eclipse observations are consistent with the idea.

ACKNOWLEDGEMENTS

Support for this research was provided by the National Aeronautices and Space Administration under contract NASW-2718.

REFERENCES

Allen, C. W. (1963) "Astrophysical Quantities," (Athlone; London).

Allen, D. A. and Murdock, T. L. (1971) "Infrared Photometry of Saturn, Titan and the Rings," Icarus 14, 1.

Bezverkhniy, Sh.A., Bramson, M.A., and Moiseyeva, E.V. (1970) "Emissivity and Reflectivity of Ice in the Infrared Region of the Spectrum," Atmospheric and Oceanic Physics 6, 314.

Bobrov, M.S. (1970) in "Surface and Interiors of Planets and Satellites," edited by A. Dollfus (Academic: London, 1970).

Chandrasekhar, S. (1950) "Radiative Transfer" (Oxford U.P., Oxford, England, 1950).

Fink, U. and Larson, H.P. (1975a) "Temperature Dependence of the Water Ice Spectrum between 1 and 4 microns: Application to Europa, Ganymede and Saturn's Rings", Icarus 24, 411.

Fink, U. and Larson, H.P. (1975b) Private Communication.

Irvine, W.M. and Pollack, J.B. (1968) "Infrared Optical Properties of Water and Ice Spheres", Icarus 8, 324.

Kawata, Y. and Irvine, W.M. (1973) "Models of Saturn's Rings Which Satisfy the Optical Observations", in Exploration of the Planetary System (Woszcyk and Iwaniszewska, Eds.) I.A.U. Symposium No. 65.

Kawata, Y. and Irvine, W.M. (1975) "Thermal Emission from a Multiple Scattering Model of Saturn's Rings", Icarus 24, 472.

Kuo-Nan Liou (1973) "A Numerical Experiment on Chandrasekhar's Discrete-Ordinate Method for Radiative Transfer: Application to Cloudy and Hazy Atmospheres", J. Atmos. Sciences 30, 1303.

Kuo-Nan Liou (1974) "Analytic Two-Stream and Four-Stream Solutions for Radiative Transfer", J. Atmos. Sciences 31, 1473.

Lebofsky, L.A., Johnson, T.V. and McCord, T.B. (1970) "Saturn's Rings, Spectral Reflectivity and Compositional Implications", Icarus 13, 226.

Low, F.J. (1965) "Planetary Radiation at Infrared and Millimeter Wavelengths", Lowell Observatory Bull. 5, 184.

Low, F.J. (1966) "Observations of Venus, Jupiter, and Saturn at $\lambda 20\mu$", Astron. J. 71, 391.

Morrison, D. (1974) "Infrared Radiometry of the Rings of Saturn", Icarus 22, 57.

Morrison, D.(1975) "Radiometry of Satellites and the Rings of Saturn" in I.A.U. Colloquium No. 28 "Planetary Satellites".

Murphy, R.E. (1973) "Temperatures of Saturn's Rings", Astrophys. J. 181, L87.

Murphy, R.E. (1974) "Variations in the Infrared Brightness Temperature of Saturn's Rings" in "The Rings of Saturn" (Ed. F.D. Palluconi) NASA SP-343, p. 65.

Murphy, R.E., Cruikshank, D.P., and Morrison, D. (1972) "Limb-darkening of Saturn and Thermal Properties of the Rings from 10 and 20 Micron Radiometry", Bull. Amer. Astron. Soc. 4, 358.

Nolt, J.G., Radostitz, J.V., Donnelly, R.J., Murphy, R.E., and Ford, H.C. (1974) "Thermal Emission from Saturn's Rings and Disk at 34 μm", Nature 248, 659.

Pollack, J.B. (1975) "The Rings of Saturn", Space Sci. Review (in press).

Price, M.J. (1974) "Optical Scattering Properties of Saturn's Ring, II.", Icarus 23, 388.

APPENDIX I: RADIATIVE TRANSFER

Our radiative transfer model consists of a plane-parallel, isothermal, particulate layer of finite optical thickness, τ_R. In order to derive the brightness temperature, T_B, corresponding to a particular geometrical aspect and wavelength, the variation of the thermal source function with optical depth and direction must be known. Specifically, we have

$$B_\lambda (T_B) = \frac{1}{\mu} \int_0^{\tau_R} S_\lambda (\tau, \mu)\ e^{-\tau/\mu} d\tau$$

where $B_\lambda (T)$ is the Planck function corresponding to a temperature, T, and wavelength, λ; $S_\lambda (\tau, \mu)$ is the source function corresponding to an optical depth τ; μ is the cosine of the angle of emergence with respect to the outward normal to the ring plane. Computing $S_\lambda (\tau, \mu)$ requires the solution of the radiative transfer equation in the infrared.

By analogy with the stellar atmosphere case, the thermal radiation field is axially symmetric with respect to the outward normal to the ring plane since each particle is assumed to emit radiation uniformly from its surface. The equation of transfer can be written

$$\mu \frac{dI_\lambda}{d\tau_\lambda} (\tau, \mu) = I_\lambda (\tau, \mu) - \frac{1}{2} \int_{-1}^{+1} I_\lambda (\tau, \mu')\ p_\lambda (\mu, \mu') d\mu' - \epsilon_\lambda B_\lambda (T_p)$$

where I_λ denotes the specific intensity as a function of direction and optical depth; ϵ_λ is the emissivity of the particles; T_p is the thermometric temperature

of their surfaces. The function, $p_\lambda(\mu,\mu')$, corresponding to the axially symmetrical phase function, is given by

$$p_\lambda(\mu,\mu') = \frac{1}{2\pi}\int_0^{2\pi} p(\mu,\varphi;\mu',\varphi')\, d\omega'$$

where

$$p_\lambda(\mu,\varphi;\mu',\varphi') \equiv p_\lambda(\cos \textcircled{H}) \equiv \tilde{\omega}_\lambda (1 + x\cos \textcircled{H}) \quad .$$

The single scattering albedo is denoted $\tilde{\omega}_\lambda$. The scattering angle, $\textcircled{H}$, can be directly related through spherical trigonometry to the cosine of the zenith angles, μ and μ', and the azimuth angles, ω and ω'. The anisotropy parameter, x, is taken equal to -1 (Price, 1974). Equation (A.2) can be re-written as

$$\mu \frac{dI_\lambda}{d\tau_\lambda}(\tau,\mu) = I_\lambda(\tau,\mu) - \frac{1}{2} \cdot \tilde{\omega}_\lambda \int_{-1}^{+1} I_\lambda(\mu',\tau)(1+x\mu\mu')\, d\mu' - \epsilon_\lambda B_\lambda(T_p) \; .$$

By definition, the thermal source function can be written as

$$S_\lambda(\tau,\mu) = \epsilon_\lambda B_\lambda(T_p) + \frac{1}{2} \cdot \tilde{\omega}_\lambda \int_{-1}^{+1} I_\lambda(\tau,\mu')\,(1+x\mu\mu')\, d\mu' \; .$$

Given T_p, $\tilde{\omega}_\lambda$, x and ϵ_λ, solving equation (A.5) for the local radiation field will lead to determination of the thermal source function. Brightness temperatures can then be calculated from equation (A.1).

In the grey approximation, the radiative transfer equation at optical wavelengths may be written

$$\mu \frac{dI}{d\tau} (\tau, \mu, \varphi) = I(\tau, \mu, \varphi) - \frac{1}{4\pi} \int_0^{2\pi} \int_{-1}^{+1} p(\mu, \varphi; \mu', \varphi') I(\tau, \mu', \varphi') \, d\mu' \, dp'$$

$$- \frac{1}{4} F \, p(\mu, \varphi; \mu_0, \varphi_0) \exp(-\tau/\mu_0)$$

where I denotes the total specific intensity. At infrared wavelengths, the radiative transfer equation takes a form identical to the non-grey case. But the Planck function is then given by $\sigma T_p^4 \pi$, where σ is the Stefan-Boltzmann constant. With the calculation of T_p, the monochromatic infrared radiative transfer equation can be solved for the local radiation field. Evaluation of the source function, and brightness temperature, follow directly.

Solving the solar and thermal radiation transport problems within Saturn's ring requires a fast, convenient, yet reliable approach. Recently, Kuo-Nan Liou (1973, 1974) has developed the discrete-ordinate method originally introduced by Chandrasekhar (1950) into a useful tool for studying the transfer of optical and thermal radiation within cloudy and hazy planetary atmospheres. With minor modifications, the formulation developed is directly applicable to the Saturn ring problem. Our approach will utilize the two-stream approximation to describe the local radiation field. Flux errors are limited to ~ 3 - 10 percent for moderate optical thicknesses and moderate anisotropy in the scattering phase function (Liou, 1973). Since current absolute measurements of infrared fluxes are accurate to no better than 10-15 percent (Morrison, 1974), the computational accuracy achieved by the two-stream approximation is wholly adequate for our investigation.

APPENDIX II: THE BOND AND OPTICAL SINGLE SCATTERING ALBEDOS

The optical single scattering albedo inferred by Price (1974) from an analysis of the scattering properties of the rings at visual (λ5500Å) wavelengths is readily related to the Bond albedo.

Lebofsky, Johnson, and McCord (1970) have measured the spectral reflectivity of ring B throughout the range 0.3 - 1.05μ. Their tabulated values were normalized to unity at λ5640Å. For λ5500Å, the spectral reflectivity is $\sim$ 0.99. If the spectral distribution of solar radiation is known, the effective reflectivity of the rings integrated over wavelength can be readily computed. Solar radiation can be taken to correspond to a black-body at 5770°K (Allen, 1963). On the assumption that the spectral reflectivity outside the range measured remains constant at either the upper or lower limit value, the effective reflectivity is 1.00. Neglecting the contribution below 0.3μ has a negligible effect on the result ($\sim$ 0.01). Introducing ice-band absorption in the range 1μ - 4μ reduces the effective reflectivity by $\sim$ 0.10. Evidently, the visual single scattering albedo and the Bond albedo are essentially identical.

APPENDIX E

MARS: GEOGRAPHIC CONTROL OF CLOUDS, 1907-73

William K. Hartmann
Planetary Science Institute
Tucson, Arizona 85704

ABSTRACT

Mariner 9 high resolution and topographic information has been used to analyze "blue" and "red" clouds reported over many decades. Comparisons are made with photographic data in the Lowell Collection, covering a 66-year period from 1907 to 1973. A sample of 77 "blue" clouds lay preferentially at the highest Martian elevations; 60% of them centered precisely on the seven major volcanic mountain peaks; another 16% of them lay on noticeable slopes or contacts between great cratered terrain and lower plains. Over half of 131 sporadic yellowish or red clouds, identified with filter photography, associated with blue clouds or volcanoes, and thus probably did not represent dust storm phenomena, contrary to a commonly held belief. Rejecting these, a sample of 61 "possible dust clouds" revealed that 34% associated with basin rims, basin floors, or the Valles Marineris complex. Others preferentially occur at borders between light and dark areas, perhaps sites of current depositional or denudational activity. Major dust storms begin in 3 or 4 core areas associated with major basins and (in a puzzling case) the Solis Planum plain of Solis Lacus. Basins are probably mobile dust reservoirs. A histogram of elevation frequencies (hypsometric diagram) was derived for the study and is discussed.

I. INTRODUCTION

Through the years, many researchers have tabulated the behavior of clouds and other variable features on Mars (Martin and Baum, 1969; Capen, 1974; Martin, 1974) and even attempted to infer physical processes and topographical characteristics from such studies (Wells, 1966; Arvidson, 1972; Schlosser and Haupt, 1973). However, only with the combination of synthesized global topographic information -- not available in relatively final form until 1975 -- and high-resolution Mariner 9 global photography, could variable feature behavior be reliably correlated with Martian topography and geology.

The purpose of this study was to seek systematics of Martian clouds as a function of topography and probable cause. The study was particularly designed to utilize archives of observations that stretch back nearly 70 years, thus providing a more general survey than detailed studies of recent phenomena, made possible by the world-wide planetary patrol photography of recent years (Capen, 1974; Martin, 1974). This approach was made possible only through the excellent archival collection at the Planetary Research Center of Lowell Observatory, and through the knowledge of that collection on the part of W. A. Baum, C.F. Capen, and L.J. Martin, who made much unpublished material available to the writer. This is believed to be the first such long-term survey with reliable global topographic information.

II. MARTIAN TOPOGRAPHY AND GEOGRAPHY

During this study, a major synthesis of topographic information (occultation, radar, pressure surfaces) was being completed by the U.S. Geological Survey. Two versions, August 1974 and June 1975, were consulted, and the conclusions of this study were not affected by the modest changes between these versions in the non-polar regions studied here. The final tabulations and analyses of data were made with the 1:25,000,000 topographic map (M 25M 3RMC; June 1975). It includes topographic contours, structural features in shaded relief, and albedo markings based on earth-based and Mariner 9 imagery. The reference elevation (zero km) is defined as the 6.1 mb pressure level.

Elevation distributions on Mars were studied in order to compare with the distributions of variable features such as blue clouds and red clouds. Mars was divided into 720 equal-area blocks, from which mean elevations and a histogram of elevation frequency were obtained, following the technique used in an earlier study (Hartmann, 1973). This histogram, or hyposometric diagram, is compared with the elevation distribution of other features in Figure 1.

As shown in Figure 1, the current hypsometric diagram shows clearly a bimodal distribution of elevations, confirming a conclusion (based on less clear evidence) in the earlier study. Both the August 1974 and June 1975 syntheses show this result , as illustrated in Figure 1 by dots representing the earlier data. That the crust of Mars can be divided into two types of units, low-standing and high-standing has important ramifications for early crustal evolution of planets, discussed in more detail by Hartmann (1973). The lower crust, lying

at about -0.4 km consists mostly of sparsely cratered plains, mostly in the northern hemisphere, and bounded by marked slopes that rise toward the upper unit. The upper unit, lying near +3.4 km, consists mostly of ancient cratered plains. The well-known Tharsis dome is represented on the histogram by a long tail at elevations exceeding +5 km.

It is significant that the most ancient cratered crust -- the earliest known surface -- defines a prominent lobe on the hypsometric diagram, lying at about +3 to +4.5 km. Younger surfaces are either depressed plains (the well-defined lower lobe, -1.5 to +1.5 km) or elevated volcanic units. The depressing or elevating processes are planetologically important and poorly understood. The earlier study cited evidence that the volcanic domes are not mere inert piles, but were uplifted. This conclusion is based on their structure and on terrestrial rifted volcanic domes of similar dimension.

A median elevation for the entire surface of Mars was found to be +2.4 km; this will be compared with median elevations for other classes of features.

III. BLUE CLOUDS

The primary source of information for this study was an unpublished Lowell Observatory report by Martin and Baum (1969). The authors reported a search of 5,000 Mars plates or any groups-of-plates on which discrete clouds were observed over a period of a few days. The purpose of that search was to measure rates of motion of clouds, and so there was a selectional bias toward discrete clouds whose motions could be traced. This tended to restrict the study to

well-defined bright clouds, a selection which appears useful for the present study. Martin and Baum reported 95 cloud histories ranging from 1907 through 1958. The vast majority of these clouds were photographed on blue sensitive or yellow=green sensitive plates and are believed to be blue clouds or bluish-white clouds. Martian and Baum described cloud histories against a background of traditional pre-Mariner maps of albedo features, and some interpretation was required. For example in May, 1937, a bright cloud was seen in successively north-eastern positions in apparent motion across the Maria Tyrrhnum region. Between the fourth and fifth day the cloud jumped some 240 km to a new position over Elysium. Martin and Baum noted that this might imply a new Elysium cloud rather than a continuation of the earlier cloud, but listed the whole group as a single cloud history.

The present author, noting that the final cloud position precisely overlapped the Elysium volcano, chose to plot it as a separate cloud position and defined other clouds similarly. The author also deleted 11 clouds observed primarily on red sensitive plates and several other clouds of ambiguous color, observed with different filters. In this way the Martin-Baum list was altered to 77 blue cloud positions. Positions plotted were essentially the initial positions or area of origin of the blue cloud, as the purpose was to study geographic conditions at sites where clouds originate.

It was found that 46 clouds or 60% occurred directly over the flanks or summits of seven major volcanic mountains on Mars. These were: Olympus Mons, Ascreaus Mons, Pavonis Mons, Arsia Mons, Tharsis Tholus, Alba Mons, and Elysium Mons. In addition another 16% occurred on noticeable

slopes (defined by considerably higher than average contour line density -- typically slopes averaging ≥ 2 km rise over 500 km, or ≥ .004%), contacts between higher cratered areas and lower featureless plains, or basin rims.

The very strong correlation with seven volcanic mountains standing about 2 to 16 km above their surroundings, whose existences were unknown at the time the blue clouds were mapped, strongly supports the explanation of these clouds as products of condensation of water ice due to orographic uplift, convection, and possible local degassing. The latter interpretation was developed for similar clouds in the same positions, observed independently by Mariner 9 (Leovy, Briggs, and Smith, 1973), and the cloud composition was determined spectroscopically to be water ice. The importance of orographic uplift for blue clouds is similarly supported by the association of the additional 16% with slopes and contacts between structural units at different altitudes. Thus three-fourths of all blue clouds can be described as associated with volcanoes or sloping contacts.

The median elevation of the 77 blue clouds was found to be 4.5 km, significantly higher than the global median of 2.4 km. This again indicates the association of blue clouds with high-altitude air masses, and confirms the conclusion of Schlosser and Haupt (1973) who found that evening and morning terminator clouds correlate with high radar-determined elevations in the equatorial regions.

IV. YELLOW CLOUDS

Yellow clouds are commonly pictured as a phenomenon distinct from the blue clouds. Indeed, the clouds prominent in yellow light are frequently thought

of as "dust clouds," in contrast to blue clouds that are orographic. This is incorrect. For example, the tabulation by Martin and Baum (1969) and the original plots of clouds from 1907 to 1958, prepared by Martin for that report, show that clouds detected in yellow light are frequently found to be identical with clouds shown in blue light, if blue plates are available for the date in question. Martin kindly made his original plots from the 1907-58 survey available, and the author identified and mapped 131 red and yellow clouds (clouds detected in red or yellow light), noting initial positions of such clouds when motion was detected. Of these, 52 clouds (39%) could be identified with major blue clouds or blue cloud complexes! Another 18 (14%) were found to lie on the summits of major volcanoes, and were assumed to identify with the blue clouds.

To obtain a sample that might be more accurately identified with dust storms, these 70 clouds (54% of sample) were rejected, leaving a sample of 61 red or yellow clouds that will be called "possible dust clouds." No prominent simple relation was seen to Martian topography or structure, although 21 clouds (34%) overlapped the floors and rims of basins or the Vallis Marineris=Labyrinthus complex. The elevation distribution of these 61 "possible dust clouds" is shown in Figure 1. The median elevation is +1.9 km, falling below the globe-wide median.

This coarse survey of yellow clouds from 1904-58 leads to the suggestion that dust clouds tend to originate at low elevations, where higher air pressure favors dust transport, and near basins or valleys that may be reservoirs of dust. But the behavior of Martian dust clouds is not so simple, as shown by detailed studies of recent major dust storms.

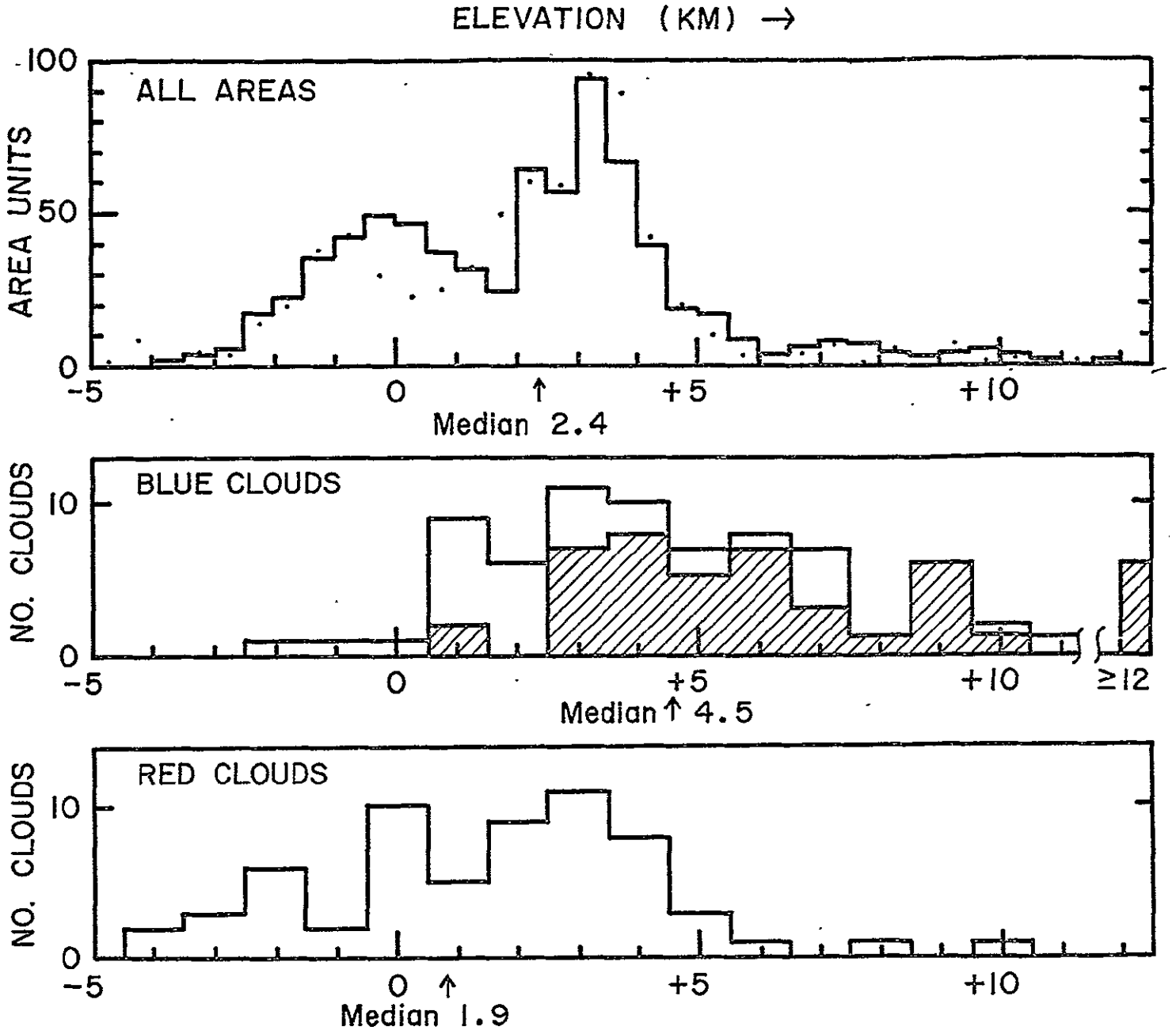

Fig. 1. Altitude distributions of general Martian surface (top), locations of blue clouds (middle), and locations of red clouds (bottom). Shaded blocks represent blue clouds over volcanic mountains.

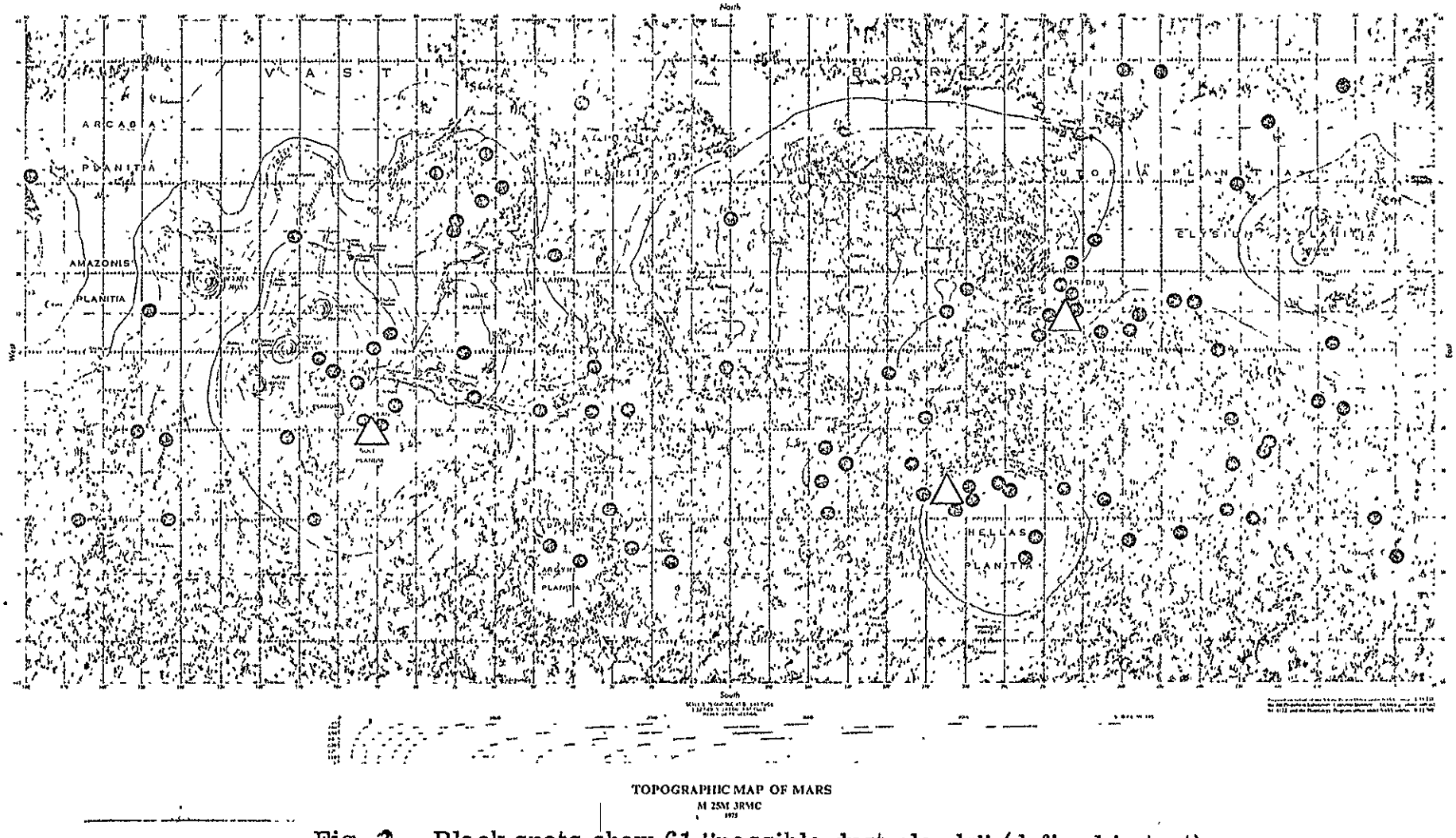

Fig. 2. Black spots show 61 "possible dust clouds" (defined in text) plus 27 other red clouds from selected sources. Triangles show "core areas" where major dust storms have formed. Dust storms appear associated with basins (dust reservoirs?) and borders of dark areas.

REFERENCES

Arvidson, R.E. (1972). Aeolian Processes on Mars: Erosive Velocities, Settling Velocities, and Yellow Clouds, G.S.A. Bull., 83, 1503.

Capen, C.F. (1974). A Martian Yellow Cloud - July 1971, Icarus 22, 345.

Hartmann, W.K. (1973). Martian Surface and Crust: Review and Synthesis, Icarus 19, 550.

Leovy, C., G. Briggs, B. Smith (1973). Mars Atmosphere During the Mariner 9 Extended Mission: Television Results, JGR 78, 4252.

Martian, L.J. (1974) The Major Martian Yellow Storm of 1971, Icarus 22, 175.

Martin, L.J. and W. A. Baum (1969). A Study of Cloud Motions on Mars, Lowell Observatory Report, August.

Schlosser, W. and W. Haupt (1973). Large Scale Surface Structure of Mars, Astron. and Astrophys. 23, 471.

Wells, R. A. (1966). An Analysis of Yellow Clouds and Their Topographical Relations, Europe. Space. Res. Organ., SN-54.